UNIVERSITÀ DEGLI STUDI DI MILANO

Ph.D. SCHOOL IN FOOD SYSTEMS

Department of Food, Environmental and Nutritional Sciences

XXIX Cycle

The late blowing defect in Grana Padano cheese: the mechanisms of milk healing through natural creaming and the effects of cheese making conditions in inducing *Clostridium* spore germination

Scientific field – AGR/15

PAOLO D'INCECCO
(R10608)

Tutor: prof.ssa Luisa Pellegrino
Co-tutor: prof. Franco Faoro

Ph.D. Dean: Prof. Francesco Bonomi

2016/2017

INDEX

ABSTRACT

This thesis project was designed to explore the technological, chemical and microbiological factors involved in the late blowing defect (LBD) of Grana Padano (GP) with the aim of setting up every possible precaution to overcome this economically important flaw. LBD is a cheese defect caused by some *Clostridium* species, mostly *Clostridium tyrobutyricum*, and characterized by holes, cracks as well as an unpleasant flavour. Natural creaming of milk is the first and most critical step in GP making, during which *C. tyrobutyricum* spores are risen to the top of milk together with fat globules, thus being eliminated from partially skimmed milk. This step has been thoroughly investigated with particular reference to the interaction type between spores and fat globules. Transmission Electron Microscopy (TEM) revealed an electron-dense material sticking bacteria to fat globules. This material has been identified as immunoglobulins, mainly IgA and to a lesser extend IgM, by immunogold labelling. Many IgA molecules, but not IgM and IgG, were localized on *C. tyrobutyricum* cell wall suggesting the presence of anti-IgA receptors on it. Following this finding, immunoglobulins were purified from colostrum and their ability to enhance bacteria rising during natural creaming of milk investigated. Indeed, the addition of immunoglobulins led to a significant increase in spore rising with respect to untreated control. Specific natural creaming trials were also carried out to study the effect of creaming temperature on fat microstructure. Fat supramolecular organization, the unwanted fat globule structural rearrangement, was observed when creaming was carried out at 22 and 40 °C, as well as in sample tempered at 37 °C prior to the normal creaming at 8 °C. This suggests that the often-adopted thermal treatment before creaming is deleterious for fat microstructure.

The behaviour of *C. tyrobutyricum* throughout the further steps of GP making and ripening was also investigated by an innovative approach. Vegetative bacteria cells and spores, independently sealed within dialysis tubes, were kept in the vat for the entire cheese making and then into the cheese over 6-month ripening. They were sampled and counted at milk renneting, curd cooking, curd extraction, in-mould acidification, brine salting, 3- and 6-month ripening. Furthermore, their morphological changes were monitored by TEM and the free amino acid utilization evaluated. Vegetative bacteria cells died during curd cooking up to 54 °C and then were no longer cultivable. However, 2 x 10^2 CFU/mL of these cells were sporulated in the curd at extraction and a higher number of spores was found at the end of 6-month ripening. Few spores germinated during curd acidification, when lactate was available. *C. tyrobutyricum* proved to convert arginine to citrulline and then to ornithine throughout the

cheese ripening. This capability was confirmed in both milk and cheese model systems, indicating the vitality and metabolic activity of bacterial cells and, possibly, their ability of modifying GP sensorial properties.

Lysozyme (LZ) is used in GP as well as in other cheese varieties to prevent the LBD. Thus, it has been considered important to verify its effects on lactic acid bacteria population and cheese free amino acid pattern. This study was carried out in 16 raw-milk hard cheeses produced in eight parallel cheese makings conducted at four different dairies using the same milk with (LZ+) or without (LZ-) addition. LZ- cheeses were characterized by higher numbers of cultivable microbial population and lower amount of DNA arising from lysed bacterial cells with respect to LZ+ cheeses. At both 9 and 16 months of ripening, *Lactobacillus delbrueckii* and *L. fermentum* proved to be the species mostly affected by LZ. The total content of free amino acids indicated that the proteolysis extent is characteristic of each dairy, regardless to the presence of LZ. Instead, in LZ+ cheeses, microbial degradation of arginine into citrulline and ornithine was always promoted. As, the amount of ornithine was quantitatively lower than citrulline it is likely that the arginine-deiminase pathway was only partially adopted.

Working with *C. tyrobutyricum* spores gave rise to the need of a practical and effective staining method that could both facilitate spore detection and easily discriminate spore from vegetative bacterial cells. A fast and robust protocol for fluorescent staining of spores and vegetative cells of *C. tyrobutyricum* was set up, by using Hoechst 34580 and Propidium Iodide (HO/PI) stains that allowed to distinguish viable, dead and sporulated cells of *C. tyrobutyricum*. The HO/PI staining protocol proved to be suitable for other three Clostridia that can cause LBD: *C. butyricum*, *C. sporogenes* and *C. beijerinkii*. Furthermore, Hoechst 34580 dye was successfully used, together with Nile Red and Fast Green, to observe spores into the cheese matrix. In this case, spores were experimentally added to milk during cheese making and the triple staining was performed on slices of cheese after a month ripening.

Finally, during the investigations related to this thesis project, it was possible to shed light on other inclusions present in GP matrix during and after ripening, such as specks, spots and microcrystals. Light microscopy revealed that the small, hard specks had the structure of crystalline tyrosine, as confirmed by amino acid analysis. Spots showed a complex structure, including several curd granules, cavities, and microcrystals, and were surrounded by a dense protein layer. Spots contained significantly less moisture and ash than the adjacent cheese area, and were significantly richer in protein, including significantly higher levels of valine,

methionine, isoleucine, leucine, tyrosine and phenylalanine. Microcrystals were observed by light and electron microscopy and analysed by confocal micro Raman. Among others, calcium phosphate crystals appeared to consist of a central star-shaped structure immersed in a matrix of free fatty acids besides leucine and phenylalanine, in free form or in small peptides. A hypothetical mechanism for the formation of these structures was also formulated.

RIASSUNTO

In questo progetto di dottorato sono stati studiati i fattori tecnologici, biochimici e microbiologici coinvolti nel difetto del gonfiore tardivo del formaggio Grana Padano (GP) allo scopo di individuare operazioni utili a prevenirne l'insorgenza ed evitare le elevate perdite economiche che ne conseguono. Il gonfiore tardivo è causato da alcune specie di microrganismi appartenenti al genere *Clostridium*, principalmente *C. tyrobutyricum*, ed è caratterizzato da una fermentazione del lattato altamente gasogena, che causa la comparsa di occhiature e fessurazioni nella pasta del formaggio accompagnati da odore sgradevole. La prima operazione tecnologica nella lavorazione a GP è la scrematura del latte per affioramento naturale, durante la quale in realtà i globuli di grasso affiorano insieme cellule batteriche, spore e cellule somatiche. Pertanto la loro concentrazione nello strato di crema superficiale ne permette la rimozione, determinando un sostanziale effetto di risanamento del latte scremato destinato alla caseificazione. Per questa ragione l'affioramento naturale del latte è stato studiato approfonditamente. La microscopia elettronica a trasmissione ha rivelato la presenza di materiale electron-denso all'interfaccia dei globuli di grasso con cellule e spore batteriche nella crema. Attraverso la marcatura con oro colloidale questo materiale ha mostrato contenere due immunoglobuline (Ig), principalmente IgA e marginalmente IgM. Siti antigenici per le IgA sono stati localizzati anche sulla parete cellulare di *C. tyrobutyricum* IN15b. In considerazione di questi risultati, la frazione delle Ig è stata isolata da colostro e addizionata a latte microfiltrato o a tampone fosfato per testarne la capacità di aumentare la risalita di cellule e spore batteriche durante l'affioramento del grasso. I risultati hanno mostrato un significativo aumento di spore affiorate nel campione addizionato di Ig rispetto al controllo.

Prove sperimentali sono state realizzate per studiare l'effetto della temperatura di affioramento sulla microstruttura del grasso. L'effetto negativo di temperature elevate (22 o 40 °C), rispetto all'affioramento a 8 °C, si è mostrato con diversi gradi di riorganizzazione sopra molecolare dei globuli di grasso. Lo stesso effetto è stato determinato da un trattamento del latte a 37 °C prima dell'affioramento a 8 °C, spesso adottato nella lavorazione a GP per la "riattivazione" del latte raffreddato.

Il comportamento di cellule e spore di *C. tyrobutyricum* è stato studiato durante le fasi di caseificazione a GP e successiva stagionatura mediante un approccio sperimentale innovativo. Cellule e spore sono state separatamente inserite in tubi da dialisi e tenute immerse nel latte durante la lavorazione in caldaia e quindi nel formaggio fino a sei mesi di

stagionatura. Coppie dei rispettivi tubi sono state prelevate alle fasi di: latte in caldaia, cottura della cagliata, estrazione della cagliata, acidificazione della cagliata, salatura, formaggio stagionato 3 e 6 mesi. Ad ogni campionamento sono state effettuate le conte in piastra e monitorati sia i cambiamenti morfologici, mediante microscopia elettronica a trasmissione, sia i consumi in termini di amminoacidi liberi (AAL) mediante analizzatore a scambio ionico. Le cellule vegetative non sono sopravvissute alla cottura della cagliata (54 °C), tuttavia alcune ($2*10^2$ ufc/mL) sono sporificate nella cagliata all'estrazione e un più alto numero di spore fu ritrovato nel formaggio a sei mesi di stagionatura. Alcune spore sono germinate durante l'acidificazione della cagliata, quando il lattato si rende disponibile. L'analisi degli AAL ha messo in evidenza la capacità del *C. tyrobutyricum* di convertire l'arginina in citrullina ed ornitina. Questa capacità è stata confermata in latte e formaggio mediante prove *in vitro* indicando un metabolismo specifico finora non riportato per questo microrganismo.

Il lisozima (LZ) è usato in GP, così come in altri formaggi, per prevenire il difetto del gonfiore tardivo, pertanto si è ritenuto importante verificarne l'effetto sulla composizione della microflora lattica e sulla conseguente composizione in AAL del formaggio. Utilizzando la tecnologia del GP e presso 4 caseifici consortili diversi, sono state prodotte 8 coppie di formaggi, ognuna a partire dallo stesso latte con (LZ+) o senza (LZ-) lisozima. I batteri lattici del latte e dello starter non sono risultati essere quantitativamente influenzati dalla presenza di lisozima, diversamente la degradazione dell'arginina è risultata maggiore nei formaggi LZ+. La quantità totale di AAL e quindi l'entità della proteolisi dipendevano dal caseificio di produzione del formaggio indipendentemente dalla presenza di LZ.

La necessità di valutare cellule e spore di *C. tyrobutyricum* in matrici diverse mediante microscopia in fluorescenza ha reso necessario mettere a punto un protocollo rapido e robusto per la loro colorazione differenziale. L'utilizzo dei coloranti Hoechst 34580 e Propidium Iodide ha permesso la necessaria distinzione tra cellule vive, morte e sporificate. Inoltre Propidium Iodide, in opportuno abbinamento ai coloranti Nile Red e Fast Green, consente di osservare le spore immerse nella matrice del formaggio, anch'essa fluorescente.

Nell'ambito degli studi ultrastrutturali sul GP è stata anche studiata la formazione di inclusioni cristalline nella matrice del formaggio. Cristalli, microcristalli e "spots" sono stati caratterizzati a livello micro ed ultrastrutturale cosi come a livello chimico. I cristalli derivano dall'accumulo di tirosina libera, mentre concentrazioni significativamente più elevate degli amminoacidi idrofobici (valina, metionina, isoleucina, leucina, tirosina, fenilalanina) sono state rilevate negli "spot", rispetto al formaggio circostante, in conseguenza di fenomeni di disidratazione localizzati. Mediante la microscopia confocale

Raman i microcristalli sono stati classificati come cristalli di fosfato di calcio e la loro organizzazione in tre strutture concentriche è stata messa in evidenza.

INTRODUCTION

Traditionally, Italian cow's milk is mostly processed into typical cheeses bearing the Protected Designation of Origin (PDO) (European Union Regulation, 2012) such as the long-ripened Grana Padano and Parmigiano-Reggiano cheeses. Grana Padano is the most important PDO cheese, being 2.6 million tons milk (23% of the 2015 Italian production) destined to its manufacturing. This gives rise to 4.8 million cheese loaves, about one third of them exported (CLAL, 2016).

Grana Padano cheese is characterized by a 9-month minimum ripening period that is necessary for the development of the typical structure and taste. However, a variety of defects may also develop during this period. Among them, the "late blowing defect" (LBD) caused by *Clostridium tyrobutyricum* is certainly the most serious (Avila et al., 2016; D'Incecco et al., 2015; Morandi et al., 2015). Considering that approximately 2% of cheese loaves are affected by LBD, the economic loss due to this defect is about 22 million Euro per year.

In light of the above, the possibility to avoid LBD is of primary importance and, at the same time, very difficult to achieve because the potential technological strategies that may be adopted at this purpose must necessarily respect the restrictions imposed by the product specification in the European Regulation (European Union Regulation, 2011a). Nowadays, the addition of hen's egg white lysozyme (EC 3.2.1.17) (LZ) to milk is the only tool authorized to prevent the LBD in Grana Padano (Brasca et al, 2013; Jiménez-Saiz et al., 2013). However, new basic knowledge on LBD mechanisms could reduce the economic loss due to this defect and, possibly, pave the way for new technological strategies leading to highly desirable lysozyme-free Grana Padano cheese.

RATIONALE AND AIMS

This project was planned to investigate the development of the late blowing defect (LBD) throughout the whole Grana Padano cheese making, from the milk preparation step to a cheese ripening period lasting up to 20 months. Consequently, due to the number of the involved phenomena, including technological, microbiological, chemical and biochemical aspects, and the complexity of their interactions, the thesis structure is organized in five chapters with their own goals. An additional (sixth) chapter is dedicated to the study conducted on side structural defects sometimes observed in long-ripened extra-hard cheeses. The list of aims for each chapter follows.

- **Chapter 1** aimed to clarify the interactions occurring among fat globules, bacteria and spores of *C. tyrobutyricum* in cream raised during natural creaming of milk and to evaluate the effect of creaming temperature on cream microstructure.

- **Chapter 2** aimed to identify the role of milk immunoglobulins both in fat globule clustering and in agglutination of *C. tyrobutyricum* to fat globules during natural creaming of milk.

- **Chapter 3** aimed to study morphological, physiological and metabolic changes of both cells and spores of *C. tyrobutyricum* along an industrial sized Grana Padano cheese making. Both chemical compounds and technological factors playing a key role in the *C. tyrobutyricum* life cycle were the targets.

- **Chapter 4** aimed to investigate the side effects of lysozyme (LZ) in Grana Padano cheese with respect to both the microbial populations and proteolysis pathways responsible for cheese ripening.

- **Chapter 5** was aimed at developing a fluorescence staining protocol suitable for advanced microscopy techniques and able to show morphological details of four species of *Clostridium*.

- **Chapter 6** was aimed at shedding light on features, composition and origin of crystalline micro and macro-structures observed in long ripened Grana Padano cheese.

1. Chapter 1: Mechanisms of *Clostridium tyrobutyricum* removal from milk through natural creaming

1.1 INTRODUCTION

The consolidated manufacturing process of Grana Padano and Parmigiano Reggiano cheeses involves technological treatments that give the finished product a regular quality and the specific features. Natural (static) creaming process or gravity separation, performed in the preparation of cheese milk, is one the most effective among these treatments. Besides allowing to decrease fat content to 2.2-2.4%, and thus the standardization of the fat-to-casein ratio, which is relevant for the development of the unique grainy cheese texture, this process determines a substantial sanitization of milk. In fact, during the 8-10 hours creaming, most of bacteria, somatic cells and spores rise to the top of the milk together with the fat globules and are removed with cream (Bottazzi, 1971; Abo et al., 1981). This cleaning effect is mostly relevant with respect to spores. Spores of some *Clostridium* species could determine the late blowing defect (LBD) in the derived hard and semi-hard cheeses, characterized by openings and holes, sometimes accompanied by cracks, and also an undesirable flavour. In fact, the outgrowth of clostridial spores leads to the butyric acid fermentation producing mainly butyric acid, carbon dioxide and hydrogen (Bergère and Lenoir, 2000). *Clostridium tyrobutyricum* is the main spoilage agent responsible for LBD in Grana Padano and Parmigiano-Reggiano (Bottazzi and Dellaglio, 1970; Bosi et al., 1984; Bassi et al., 2009), while other species, including *C. sporogenes*, *C. beijerinckii* and *C. butyricum*, have been shown to contribute to development of the defect in other hard and semi-hard cheeses as well (Le Bourhis et al., 2007; Cremonesi et al., 2012). Although LBD is a dated issue, very well known by cheese manufacturers, its eradication is a difficult task since *Clostridium* spores are ubiquitous. Several tools have been proposed to prevent LBD, including i) use of additives like nitrate and lysozyme, ii) milk bactofugation or microfiltration, iii) addition of inhibiting strains of lactic acid bacteria (Lodi, 1990; Stadhouders, 1990a; Stadhouders, 1990b; van den Berg et al., 2004). However, according to product specification, most of those tools are not allowed or explicitly renounced in PDO cheese manufacturing. This situation suggests the technological relevance of maximizing the efficiency of the natural creaming step in spore removal. Accurate studies were conducted in the past on natural creaming of milk and the involved phenomena. Some of these studies suggested that native bovine immunoglobulins might mediate the interactions between fat globules and bacteria occurring in milk upon

gravity separation and leading to bacteria entrapment into the cream (Stadhouders and Hup, 1970; Bottazzi and Zacconi, 1980; Euber and Brunner, 1984; Frenyo et al., 1986; Pharman, 2009). Recently, Caplan et al. (2013) and Geer and Barbano (2014a) confirmed that immunoglobulins are at least one of the factors necessary for the removal of somatic cells and bacterial spores from milk during gravity separation of fat. However, direct evidence of a role for immunoglobulins in this process is still lacking. The complex structure of milk fat globule membrane (MFGM) has been investigated in numerous studies and both light and confocal microscopy observations allowed to evidence its great heterogeneity (Evers, 2008; Evers et al., 2008; Lopez et al., 2010; Lopez et al., 2011). Transmission electron microscopy (TEM) was also used as a tool to study the MFGM in different dairy products (Resmini et al., 1984; Schmidt and Buchheim, 1992; Zamora et al., 2012). Nevertheless, no ultrastructural studies have been carried out so far to investigate interactions between fat globules and bacterial cells or spores in milk or cream, possibly because the high water content of these matrices represents a difficult task for electron microscopy (Silva et al., 2015).

In this work we experimented different microscopy techniques, including TEM, to study the interactions occurring among fat globules, bacteria and spores upon natural creaming. The idea behind this study was to understand whether bacteria and spores in the cream establish specific interactions with fat globules or mostly remain in the cream due to the physical entrapment into fat globule clusters. To reach this goal, a suitable procedure was firstly set up to prepare experimental samples. Raw milk was intentionally contaminated with spores of *C. tyrobutyricum* and submitted to gravity separation of fat.

The effect of temperature on the microstructure of the cream layer and on the clustering and coalescence phenomena involving the fat globules were studied. The clustering occurs when at least two fat globules are in close contact for a substantial time thank to an attractive force (van der Waals) that is stronger than the repulsive one (electrostatic). Instead, coalescence, in addition to the contact, implies the break of the membrane, so that two globules fuse (coalesce) to form one larger globule. This is due to the Laplace pressure that moves the free fat from a globule to another where the pressure is lower (Fredrick et al., 2010).

Part of the work described in this chapter is already published as a research article (D'Incecco et al., 2015).

1.2. MATERIAL AND METHODS

1.2.1 Chemicals

Fluorescent probe $DilC_{18}(3)$-DS (1,1'-dioctadecyl-3,3,3',3'-tetramethylindocarbocyanine-5,5'-disulfonic acid) was purchased from Molecular Probes (Eugene, OR, USA). Glutaraldehyde, paraformaldehyde, cacodylate buffer, and osmium tetroxide were purchased from Agar Scientific (UK). Green malachite and calcofluor were purchased from Sigma-Aldrich (USA). Microbiological analyses were performed using the following chemicals: Ringer and Reinforced Clostridial Medium (RCM) from Scharlau Microbiology (Spain), skimmed milk powder, Anaerocult A and sodium lactate and sodium acetate from VWR (Belgium), yeast extract from Formedium (UK), cysteine from Sigma Aldrich (USA), and paraffin/vaseline mixture from Sacco (Italy). Water purified using Milli-Q system (Millipore Corporation, Bedford, MA, USA) was used.

1.2.2 Samples of raw milk

All samples were prepared from raw bulk milk collected at a local farm of 120 Holstein dairy cows immediately after the morning milking. Aliquots of 500 mL of milk were taken before refrigeration and brought to the laboratory within one hour from milking.

1.2.3 Bacterial strains and spore suspension production

Clostridium tyrobutyricum DSMZ 2637 provided by the Deutsche Sammlungvon Mikroorganismen und Zellkulturen, Braunschweig (Germany), was used for all experiments. The strain was routinely cultured in RCM broth and incubated at 37°C in anaerobic jars equipped with Anaerocult A. Spores suspensions were obtained by adapting the protocol described by Bassi et al. (2009). Spores were prepared inoculating 1% of 24h-grown *C. tyrobutyricum* culture in a bottle holding 400 mL of RCM broth. The culture was maintained anaerobically for four days at 37°C and for further 15 days at room temperature. Then spores were harvested, centrifuged (8,000 g at 4°C for 10 min), washed (three times with sterile water) and finally stored in water at 4°C until use. The presence of spores was inspected by phase contrast microscopy and quantified by Burker's chamber and was equal to 3.0-3.2 × 10^6 cfu/mL.

1.2.4 Preparation of intentionally contaminated cream samples

Aliquots of 25 mL of raw milk were transferred into 30-mL screw-cap tubes, each added with 1 mL of spore suspension, prepared as above described, and carefully mixed by gentle inversions. In some cases, spores were previously stained (as below indicated) with green malachite or calcofluor to be easily recognizable by light or fluorescence microscopy. The tubes were kept at 8°C overnight and the cream layer raised on top of milk was gently removed by a pipette. By this procedure, two different samples were obtained: the cream taken at the top of the test tube and the skim milk below the cream.

1.2.5 Evaluation of anaerobic spore count in cream and skim milk

Spores of anaerobic clostridia were determined by the most probable number (MPN) technique in cream and skim milk samples. Aliquots (1 mL) from serial dilutions of samples prepared using sterile Ringer solution were inoculated into five tubes containing 5 mL of reconstituted (10% wt/vol) skimmed milk that was sterilized and supplemented with yeast extract (1.0% wt/vol), sodium lactate (3.36% wt/vol), sodium acetate (1% wt/vol) and cysteine (0.2% wt/vol) and sterilized. Each tube was overlaid with 1.5 mL of sterile melted paraffin/vaseline mixture (1:1, wt/wt) and heated at 80°C for 10 min to kill vegetative cells. Incubation was carried out at 37°C for 7 days and daily inspected for gas production. MPN counts were expressed as spore/mL. Two trials were performed using three and five dilutions respectively. Five tubes were used for all of the dilution series.

1.2.6 Light and fluorescence microscopy

For light microscopy, spores were stained with malachite green (adapted from Shaeffer and Fulton, 1933). An aliquot of 1 mL of spore's suspension was added with 200 µL of malachite green solution (5% in water, wt/vol) and mixed. The mixture was heated by immersion in boiling water bath for 2 min and washed five times with distilled water by centrifugation.
Cream samples contaminated with previously stained spores were layered on microscope slides and examined with an Olympus BX optical microscope equipped with Nomarski interference contrast and QImaging RetigaTM camera. For fluorescence microscopy of fat globules, an aqueous solution of the lipophilic probe DilC_{18}(3)-DS (1 mg/mL) was added to raw milk at the final probe concentration of 10 µg/mL. Milk was kept at either 40° C for 4.5 or 8°C overnight and the obtained cream samples were examined by UV light (λ excitation =

570 nm - λ emission= 590 nm) with the same microscope described above. The emission wavelength of the probe was 570 nm. When calcofluor stained spores were added to the raw milk, the derived cream samples were examined by UV light at λ excitation = 400 nm and λ emission= 420 nm to detect both spore and fat globule fluorescence.

To stain the spores, 100 µL of calcofluor (1 g/L in water) were added to 1 mL of spore suspension and, after 5 min of incubation, the spores were washed three times with distilled water by centrifugation.

1.2.7 Transmission Electron Microscopy (TEM)

To investigate spore-fat globule interactions at ultrastructural level, both freeze-fractured replicas and ultrathin sections of cream contaminated with spores were observed by TEM.

For freeze-fracturing samples, cream was first cryoprotected by mixing 1 mL of sample with 1 mL of glycerol (60%, wt/wt), then cryofixed by immersion of small droplets into melting Freon 22 (- 160°C). Specimens were freeze-fractured at -120°C with a BAL-TEC BAF 400 unit (Balzers, Liechtenstein). Freeze-fractured specimens were replicated by layering Pt/C and C by electron-gun evaporation. The replicas were cleaned in concentrated sodium hypochlorite and in acetone with repeated intermediate rinses in distilled water. Specimen replicas were examined with FEI Tecnai 10 (Eindhoven, Netherlands) TEM operating at 80 kV.

For the preparation of ultrathin sections, 1.5 mL of fixative solution (glutaraldehyde 1%, paraformaldehyde 4% in cacodylate buffer, wt/vol) was added to 0.5-mL aliquot of cream and the mixture kept for 2 h at room temperature, then mixed with 2 mL of warm melted (35-40°C) 2% in water low-temperature gelling agarose. Before gelling the suspension was layered onto a microscope slide, allowed to set, and then cut into 1 mm^3 cubes. Cubes were further fixed in the same fixative solution as above for 30 min at 4°C, then washed with cacodylate buffer for 1 h and post-fixed in osmium tetroxide (1% in water) for 2 h. Dehydration was carried out in an ethanol series, then samples were embedded in Spurr resin and cured at 60°C for 24 h. Ultrathin sections, 50-60 nm thick, were stained with uranyl acetate and lead citrate and examined with a Philips E208 transmission electron microscope.

1.2.8 Confocal Laser Scanning Microscopy (CLSM) of cream samples

The cream samples were prepared for CLSM by staining with either Nile Red (Sigma-Aldrich, St Louis, USA) or fast green FCF (Sigma-Aldrich) to observe the triacylglycerol core of fat globules or the protein respectively. The Nile red and Fast green solutions (1 mg mL^{-1}) were prepared in dimethyl sulfoxide (DMSO, Chem Supply, Gillman, Australia) and in milliQ water respectively. The cream samples were diluted 1:5 in water, then 1 mL of sample was mixed with 10 µL of Nile red solution and 10 µL of Fast green solution and then incubated for 15 minutes at room temperature. An inverted confocal laser scanning microscopy from Leica Microsystem (Heidelberg, Germany) was used adopting the conditions described by (Ong *et al.*, 2010). Nile red was excited at 488 nm using an argon laser and the emission filter was set at 520-590 nm. Fast green was excited at 633 nm and the emission filter was set at 660-790 nm.

1.2.9 Image analysis

Three dimensional (3D) CLSM images of cream samples were reconstructed using Imaris image analysis software (Bitplane, South Windsor, CT, USA). The 3D image consists of 40 layers of 512 x 512 pixels that are stacked together with the distance between layers set at 0.25 µm. The volume of the fat globules in ~~of~~ the cream was calculated using ImageJ software (Research Services Branch, National Institute of Health and Medicine, USA). Microsoft Excel was used for calculating the volume distribution of fat globules.

1.3 RESULTS

1.3.1 Natural creaming of intentionally contaminated milk samples

The conditions adopted at the laboratory scale to obtain cream samples for our study were chosen in order to keep the native properties of fat globules unchanged. In fact, raw milk was processed within a few hours from milking, thus avoiding milk cooling and addition of preservatives. Furthermore, conditions similar to those adopted in real cheese manufacturing process of Grana Padano and Parmigiano-Reggiano were considered. We used 25-mL cylinders in order to have 18-20 cm height of milk (Dellaglio et al., 1969).

The MPN method was used to confirm the concentration of the spores in the cream layer obtained by gravity separation in our experimental system. Samples of cream and skimmed milk were taken from the test tubes of two independent experiments and analysed for clostridial spores. In both trials *Clostridium* spp. spores count was higher in the cream sample (table 1.1). The cream of trial 1 contained 99.4% of the total spores detected and 99.5% were present in the cream of trial 2. The fat content of raw milk destined to manufacturing of Grana Padano and Parmigiano-Reggiano PDO cheeses must be lowered by natural creaming according to the product specification of these cheeses (European Union Regulation, 2011a; European Union Regulation, 2011b). This process, which lasts for 8-12 hours at a temperature between 8 and 20 °C, also allows the removal of the majority of microorganisms, spores and somatic cells with the cream. Bottazzi and Zacconi (1980) reported that the debacterization obtained by natural creaming is quantitatively equivalent but qualitatively better than that obtained with the pasteurization, especially due to the removal of *Clostridium* spp. spores. It is commonly assumed that even very few spores remaining in the cheese curd may cause the late blowing defect (LBD). Thus, when the initial count of *Clostridium* spp. spores in milk is high, their removal by natural creaming can be insufficient to avoid the development of LBD in cheese loaf. The experimental procedure we adopted correctly reproduced the natural creaming phenomenon with high efficiency in spores and bacteria removal (>90%) after an overnight fat separation at 8°C. A better understanding of the mechanisms causing spores and bacteria to rise with milk fat globules was the major aim of the present work since it may provide the basic knowledge to maximize the efficiency of spore removal.

Table 1.1 - Most probable number (MPN) counts of *Clostridium* spp. spores in milk after natural creaming

Sample	Trial 1		Trial 2	
	MPN/mL	**MPN log_{10}**	**MPN/mL**	**MPN log_{10}**
Cream	1,700	3.23	1,300	3.11
Skim milk	11	1	6	0.8

1.3.2 Milk fat globule membrane (MFGM) and fat globules interactions

The MFGM was evidenced by staining with the lipophilic probe DilC_{18}(3)-DS. As suggested by Evers (2008), we used the aqueous solution of the probe because ethanol might perturb the membrane structure by denaturing constitutive proteins. However, differently from what reported by this author, we found DilC_{18}(3)-DS to fully dissolve in water at the concentration of 1 mg mL^{-1}. Two staining conditions were tested: 40 °C for 4.5 h and 8 °C overnight, both in the darkness. Overnight staining gave the best results, showing that DilC_{18}(3)-DS was located exclusively in the MFGM as expected (Evers, 2008; Lopez et al., 2010) (Figure 1.1). MFGM fluorescence was often heterogeneous, characterized by areas that were almost non-fluorescent and others densely stained (Figure 1.1, arrows).

To test the stability of the interactions among fat globules, the cream was progressively diluted with skimmed milk and observed over time by Nomarski interference microscopy. Two types of interactions were recorded: (ì) a transient one, in which fat globules seemed to interact weakly for a limited time, then separated, and (ìì) a persistent interaction where globules remained steady attached each other. In the latter case, MFGM was not visible in the contact area of the involved fat globules, suggesting their partial coalescence (Figures 1.1 c and d, arrows). Fat globule clusters were still present in the cream after 12 times dilution with skimmed milk and in some cases they derived from the aggregation of 5-6 globules at least (Figure 1.1 c). The accuracy of adopted conditions in keeping the surface of fat globule intact was assessed by DilC_{18}(3)-DS fluorescent staining. MFGMs were brightly, but heterogeneously stained and the absence of fluorescence in some portions could be regarded as either a lack of a lipid bilayer (Evers et al., 2008) or the presence of co-existing fluid and gel phases which impair membrane staining. More recently, Lopez et al. (2011) suggested the local differences in the thickness of the MFGM to be due to the liquid-ordered domains of sphingomyelin with long-chain saturated fatty acids. Such a heterogeneous composition and

complex structure of the MFGM are likely to have an impact on both the persistent interactions among fat globules and the coalescence phenomena we have sometimes observed by light fluorescence microscopy (Figures 1.1 c, d).

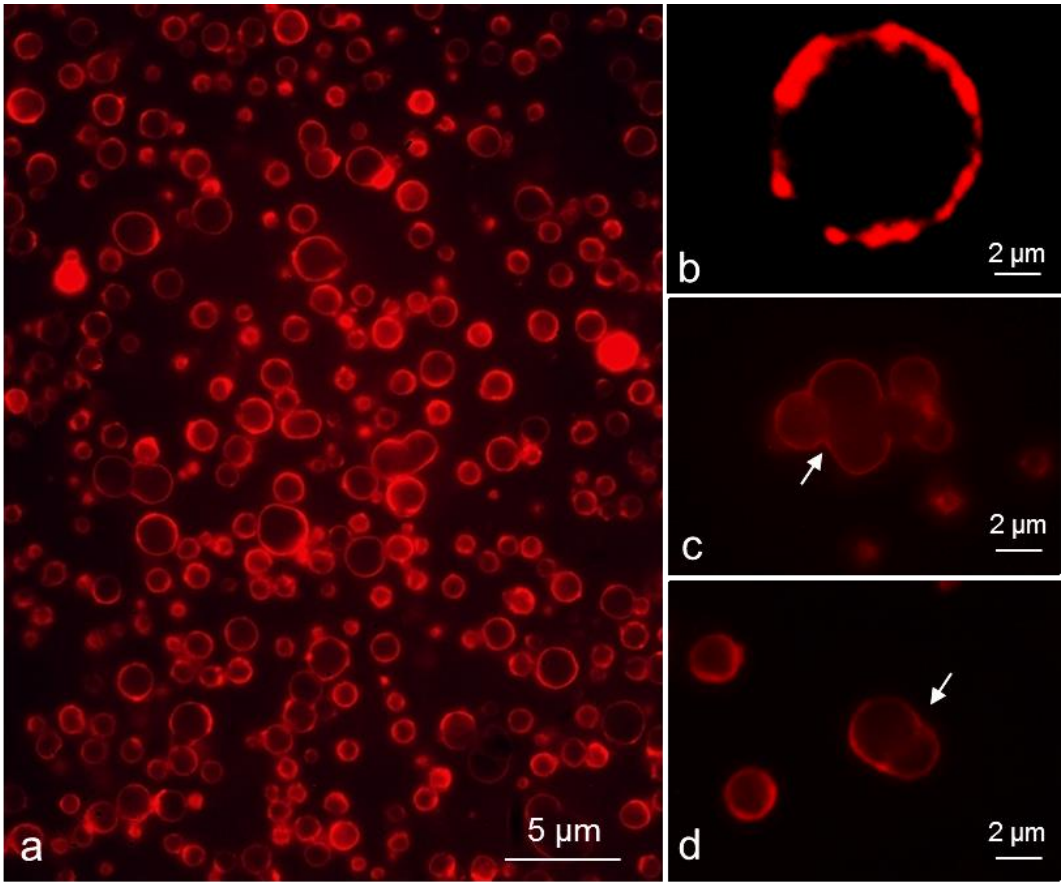

Figure 1.1. Fluorescent microscopy of DilC$_{18}$(3)-DS stained milk fat globules. The lipophilic probe is localized exclusively in the milk fat globule membrane (MFGM) which appears in bright red. a) Cream obtained after overnight gravity separation of fat at 8°C. b) MFGM is heterogeneously stained, possibly due to different lipid composition and/or thickness. c-d) Persistent interaction among fat globules after cream dilution with skim milk (1:12)**:** MFGMs are often not visible in the contact area (arrows).

1.3.3 Interactions of bacteria and spores with fat globules

As concentration of fat globules in whole cream was too high to be observed directly by light microscope, cream samples were diluted five times with skim milk. The dilution of the cream also allowed to see bacterial cells and spores of *C. tyrobutyricum* (Figure 1.2 a), stained with malachite green before addition to milk. Most of bacteria adhered to the surface of fat

globules (arrows) but it was very difficult to discriminate spores from bacterial cells, even at the highest magnification. Interestingly, bacterial adhesion occurred preferably to single fat globules and not to globule clusters, though no information were gained on the nature of these interactions. Calcofluor staining of bacteria gave similar results, allowing to show adhesion of both bacterial cells and spores to fat globules. Calcofluor stained spores appeared bright also when inside the cell (Figure 1.2 b). Some attempts were also made to stain fat globules with DilC$_{18}$(3)-DS in cream samples contaminated with calcofluor-stained spores, to verify if spore adhesion occurred in the fluorescent area of MFGM or in the non-fluorescent one. However, due to the difficult separation of emission wavelengths of the two fluorochromes it was impossible to address this question.

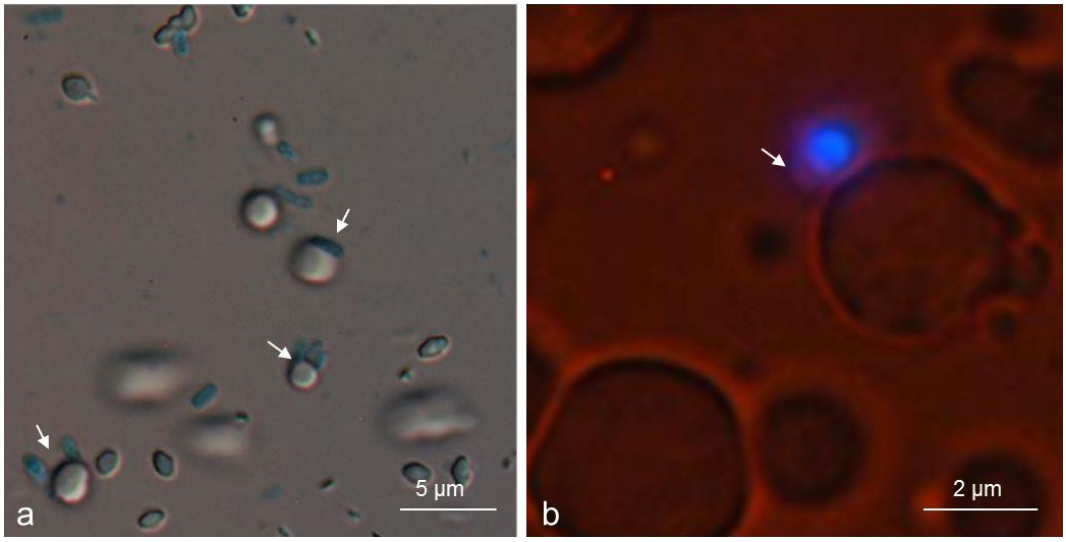

Figure 1.2. Cream obtained from natural creaming of milk contaminated with stained *C. tyrobutyricum* spore suspension. a) Light interference microscopy showing that most of the bacteria stained with malachite green are tightly stuck to fat globules (arrows). b) Fluorescent microscopy of a spore stained with calcofluor (in bright blue) adhering to a fat globule stained with the lipophilic probe DilC$_{18}$(3)-DS: the halo (arrow) around the spore is due to the bacterium containing it.

TEM examination of replicas from freeze fractured cream samples again allowed to observe adhesion of spores to fat globules (Fig. 1.3). Since this technique of sample treatment is highly conservative, the strength of the interaction established between these two particles was confirmed, however without adding further details concerning its nature.

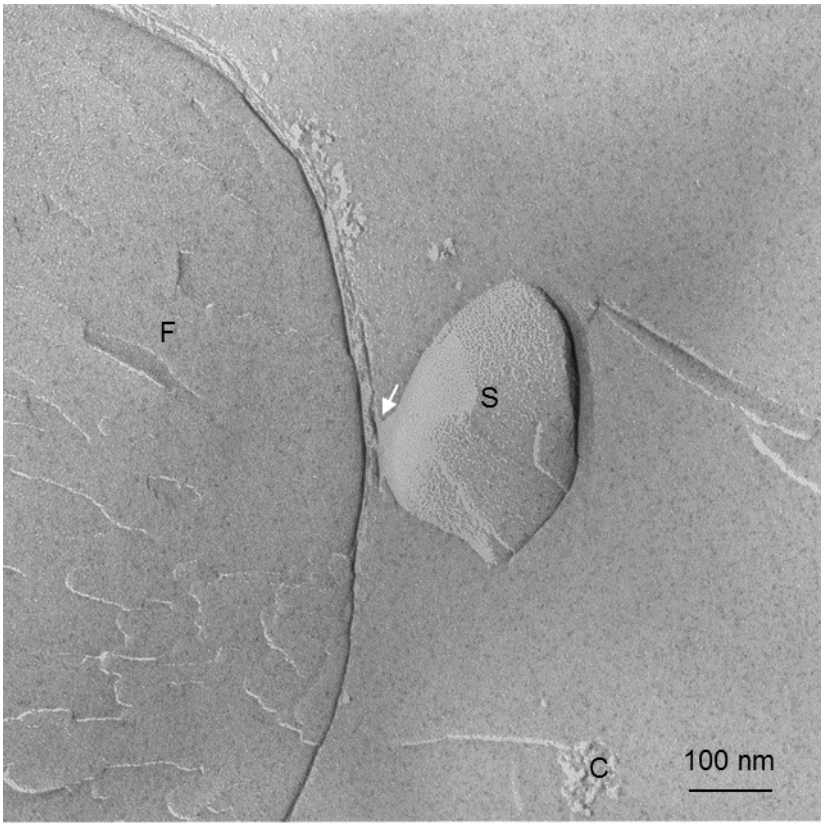

Figure 1.3. TEM micrograph of freeze-fractured cream from natural creaming of milk contaminated with *C. tyrobutyricum* spore suspension. Spore (S) adhering to a fat globule (F) membrane, possibly through a sticking material (arrow); casein micelles (C) seem not to be involved in the interaction

To gain information, ultrathin sections were cut from resin-embedded contaminated cream samples and examined by TEM. The observation of numerous serial sections obtained from resin embedded cream samples from three independent creaming experiments showed that in most of the cases bacteria adhesion to fat globules was mediated by an amorphous, slightly electron-opaque material, sometimes granular in appearance (Figure 1.4, arrows). Adhesion was observed to the thicker part of MFGM layers (Figures 1.4), corresponding to the bright fluorescent areas after staining with $DilC_{18}(3)$-DS. However, in some instance bacteria were stuck to the thinner MFGM layers, or where layers were not visible at all (Figure 1.4 b). The irregular thickness of MFGM is a well know feature of fat globules, already reported by other authors with different microscopy techniques (Buccheim, 1986; Evers, 2004; Robenek et al., 2006; Evers et al. 2008; Lopez et al. 2011).

Interestingly, bacteria cells at different stages of development, as well as endospores and free spores can be put in evidence by this technique. This situation is confirmed by literature data

(Bergère, 1970) showing that sporulation in *C. tyrobutyricum* is a very slow multi-stage process. In some cases bacteria adhered to single fat globules linking them together (Figure 1.4 a) and suggesting that adhesion was strong enough to maintain a stable contact between them. From ultrathin sections of cream samples, it was also possible to see that, in some cases, adhesion of fat globules each other's implies a fusion of their MFGM (Figure 1.4 b) that may correspond to a kind of persistent interaction like those observed by light fluorescence microscopy (Figure 1.1 c and d). Numerous casein micelles were typically stuck to MFGM (Zamora et al., 2012), though they did not appear involved in bacteria adhesion (Figures 1.4 a-c).

As regards the supposed stable interaction between bacteria and fat globules in cream, light microscopy clearly showed that this interaction does exist. In fact, most of the time both spores and bacterial cells appeared firmly adherent to fat globules, even in presence of sample streaming on the microscope slide (Figure 1.4 a). However, the staining procedures for both light and fluorescence microscopy did not give any information on the nature of this binding. The close adhesion of either bacteria or spores to fat globules was confirmed by TEM examination of replicas of cryofixed cream. By this technique bacteria seem to stick to MFGM (Figure 1.3) but, despite the high resolution, no molecules possibly involved in this mechanism could be visualized. Much more details on adhesion mechanism came from the examination of ultrathin sections by TEM. An electron-opaque amorphous material apparently sticking bacteria to MFGM, but not fat globules among themselves, seems to be responsible for adhesion and hence for bacteria rising during creaming (Figure 1.4). Thus, the rising would not be merely due to physical entrapment of bacteria in the fat clusters, as suggested by Rossi (1964), but to a more complex mechanism. Indeed, the involvement of milk immunoglobulins in the interactions among fat globules was proposed since a long time, as suggested by the pioneering experiments of Bottazzi et al. (1972). At this regard, Bottazzi and Zacconi (1980) isolated from cream a proteinaceous material they called "active fraction" able to agglutinate each other either fat globules or bacteria. This fraction proved to contain part of milk IgM however the contribution of other molecules was stated (Zacconi and Bottazzi, 1982). Beta-lactoglobulin and proteins from MFGM, like Muc1 and peripheral proteins PAS 6/7 were reported to contribute to this phenomenon (Evers, 2008; Sando, 2009) but their role was only indirectly demonstrated because the fat globule aggregation was not observed in heat treated milk. Honkanen-Buzalskiand Sandholm (1981) showed that IgA and IgM were present on the surface of the MFGM, while Euber and Brunner (1984) demonstrated that in absence of IgM, removed by a specific antiserum, gravity separation of

fat did not occur. More recently, other indirect evidences of the involvement of immunoglobulins in bacteria adhesion to fat globules have come out from the research work by Barbano and collaborators (Ma and Barbano, 2000; Caplan et al., 2013; Geer and Barbano, 2014a; Geer and Barbano, 2014b). They found that different levels of bacteria in milk influence the degree of gravity separation of fat but not of somatic cells (Caplan et al., 2013), suggesting that bacteria may compete for interaction with the immunoglobulins involved in gravity separation of the fat. As a consequence, high bacteria counts in milk may reduce the extent of creaming. However, the story of immunoglobulin involvement in creaming has turned out more complicated than expected. Very recently, Geer and Barbano (2014b) found that the immunoglobulins themselves were not able to cause the rising of fat globules, bacteria and spores in milk but the presence of somatic cells was also necessary. However, in our microscopy studies, we have never seen somatic cells in contact with the fat globules, nor with bacteria, thus it is possible that the contribution of these cells to creaming is not necessarily a consequence of direct interactions but other factors could be involved.

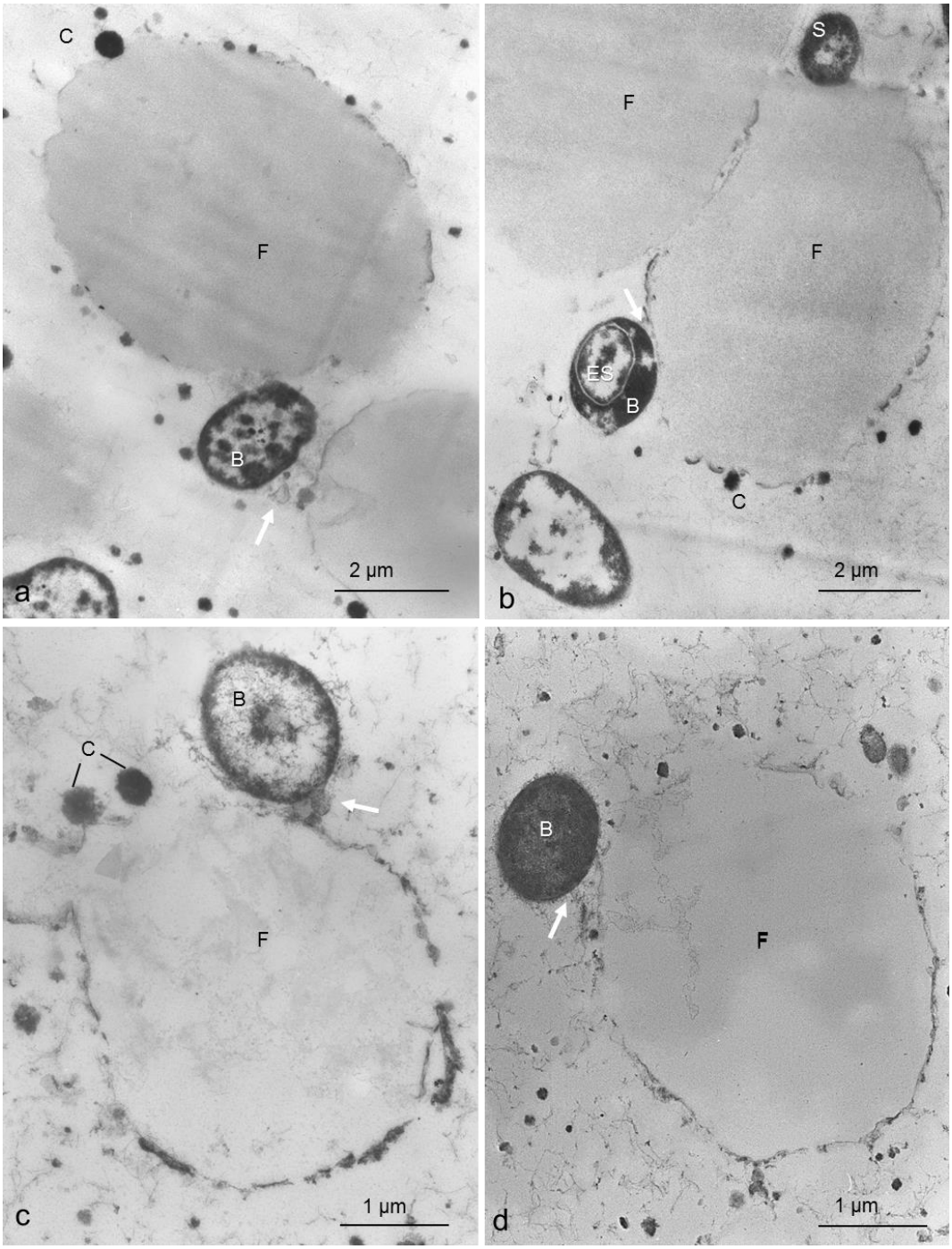

Figure 1.4. TEM micrographs of ultrathin sections of cream from natural creaming of milk contaminated with a *C. tyrobutyricum* spore suspension. a-d) Bacteria (B) are stuck to fat globules (F) by an amorphous, slightly electron-opaque material (arrows). In some instances (a) bacteria (B) link fat globules (F) together. (b) *C. tyrobutyricum* may adhere to fat globules, either as a spore (S) or cell with or without the endospore (ES).

1.3.4 Effect of creaming temperature on the chemical and physical properties, and the microstructure of the cream layer.

Natural creaming trials were carried out at laboratory scale. Raw milk (50 mL) was kept in graduated cylinders at 4, 8, 22 and 40 °C for 24 hours and the volume, the fat content and the microstructure of creams were studied. Preheating of milk at 37 °C for 5 minutes prior to creaming at 8 °C was also considered since it is a common treatment for milk intended for Grana Padano cheese making.

The creaming rate was faster at higher temperature (Fig. 1.5). A cream layer was observed in samples at 8 °C preheated at 37 °C, 22 and 40 °C after 0.5 hour of creaming whereas in samples creamed at 4 and 8 °C it appeared only after three hours.

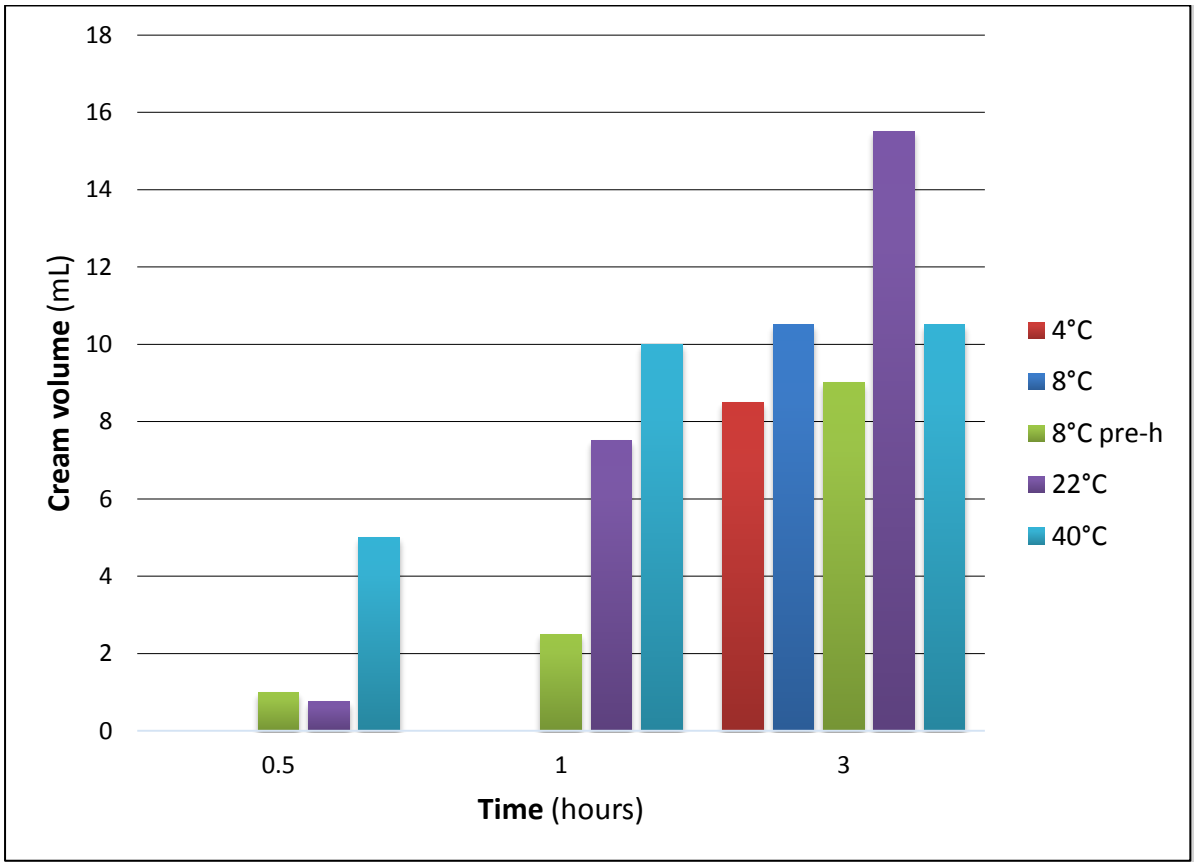

Figure 1.5. Cream volume (mL) raised at various temperatures during the first three hours of natural creaming of 50 mL raw milk. Data are the average of two separate creaming trials.

Cream layers looked different after 24 hours of creaming at the selected temperatures. The volume (mL) of the cream layer decreased and the fat content (% w/w) increased as the temperature of creaming increased (Fig.1.6). A larger cream volume and a lower fat content

(% w/w) were observed in the sample preheated at 37 °C prior to creaming at 8 °C with respect to the sample where no preheating was applied.

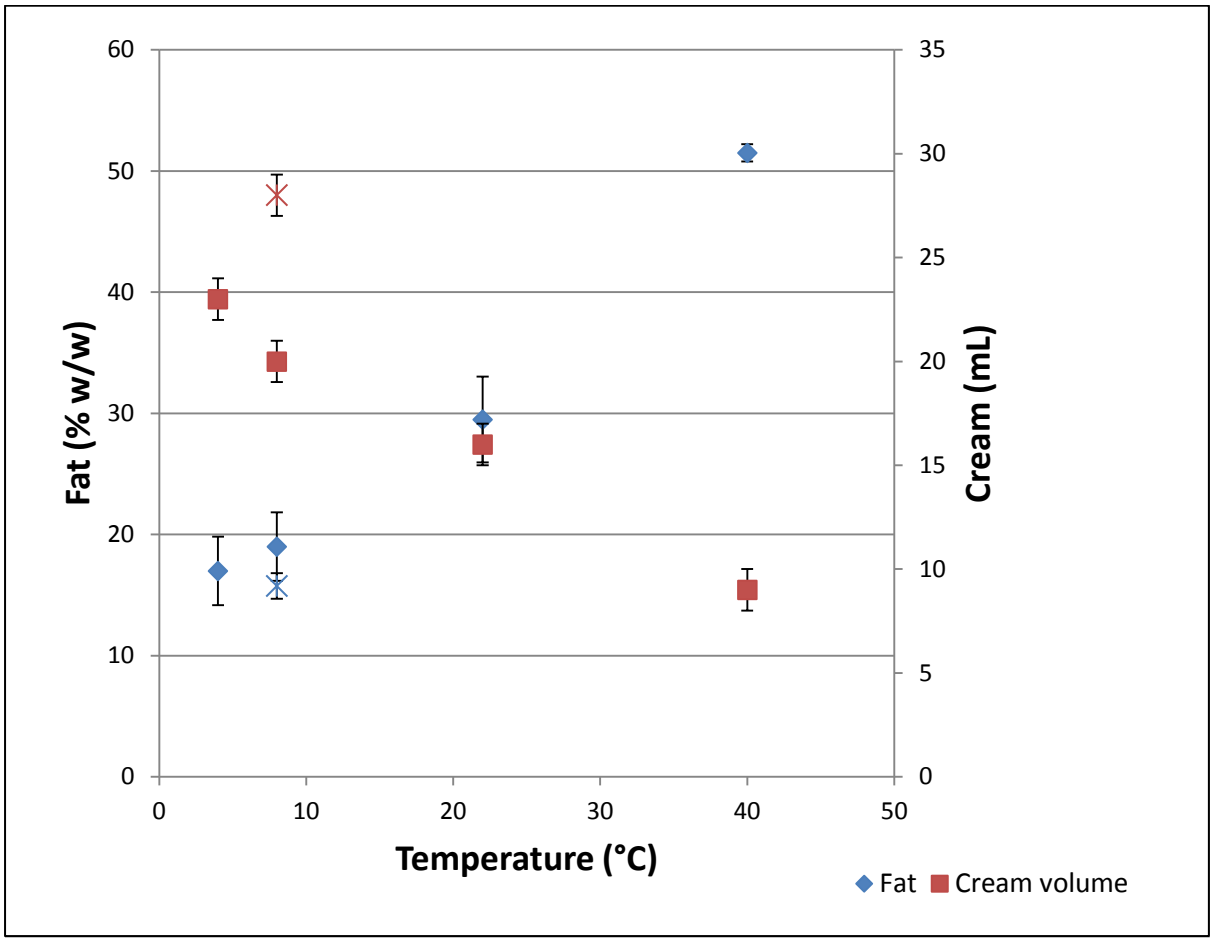

Figure 1.6. Volume and fat content of the cream layers obtained by natural creaming of 250 mL of raw milk kept at different temperatures for 24 hours. Each data point is the mean value of two separate trials. The error bars are the standard deviation of the mean.

Microstructure of cream samples was investigated by CLSM and image analysis was performed on the related z-stacks. The information obtained by CLSM analysis was consistent with that of cream characterization. Fat globules are more concentrated in cream obtained at higher temperature (Fig. 1.7). In addition, CLSM images showed fat coalescence phenomena in samples obtained at 8 °C preheated, at 22 and 40 °C. In particular, fat coalescence increased with increasing temperature, with the exception of the sample preheated at 37 °C that showed a coalescence more extensive than the sample creamed at 22 °C. This means that the preheating treatment at 37 °C for 5 minutes is more destructive for fat matrix then the creaming at 22 °C for 24 hours.

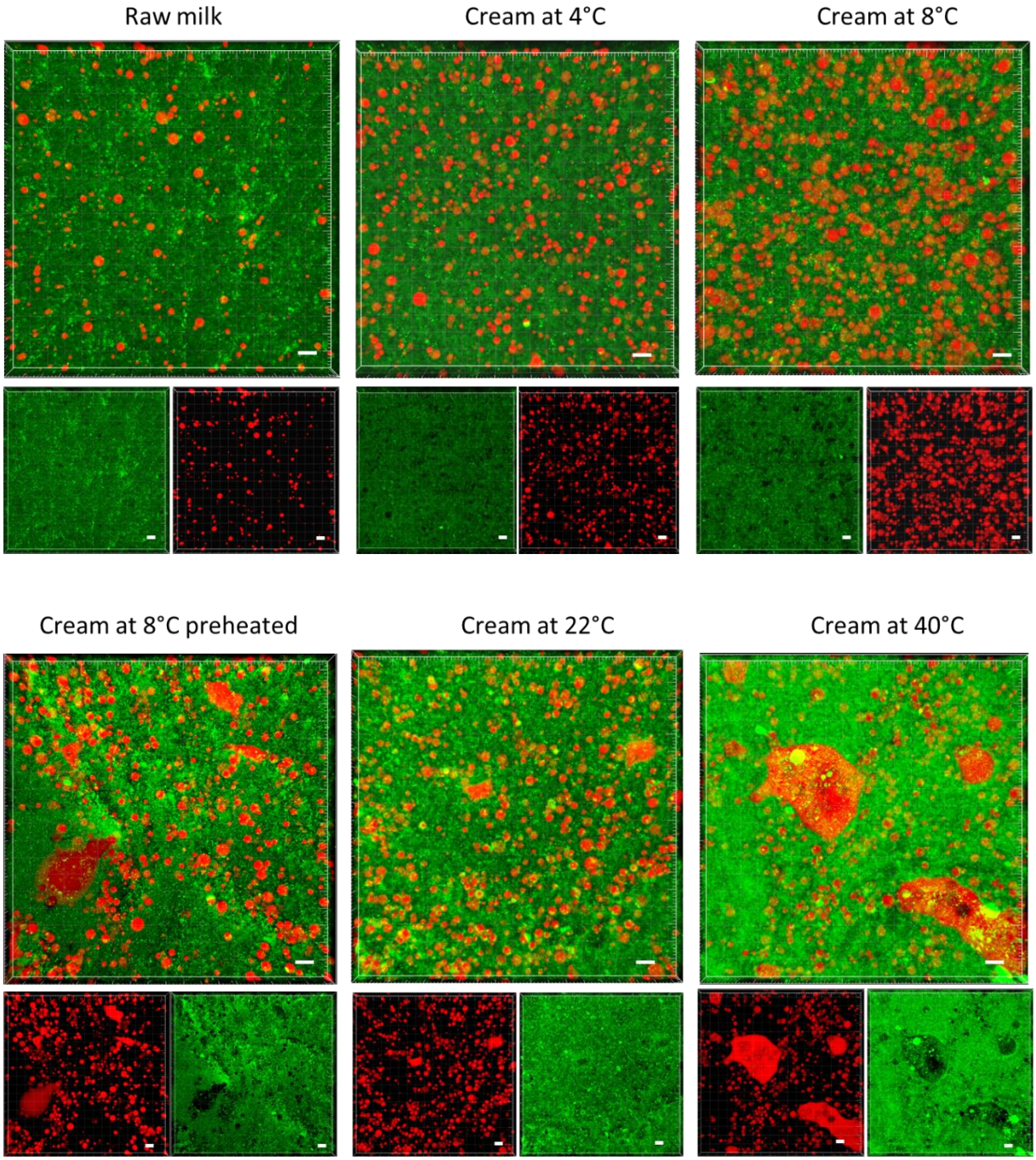

Figure 1.7. Microstructure of cream raised from raw milk at various temperatures. The Nile red stained triglyceride core appears red. Fast green stained protein appears green. The scale bars are 10 µm in length.

Image analysis was performed on fat component by means of 3D image reconstruction and fat volume rendering (Fig. 1.8). These post processed pictures clearly showed fat coalescence to be more extensive in creams raised at 8 °C with preheating and at 40 °C with respect to all of the others. The coalesced fat globules look like large free-fat droplets with irregular shape and where entrapped globules can be observed.

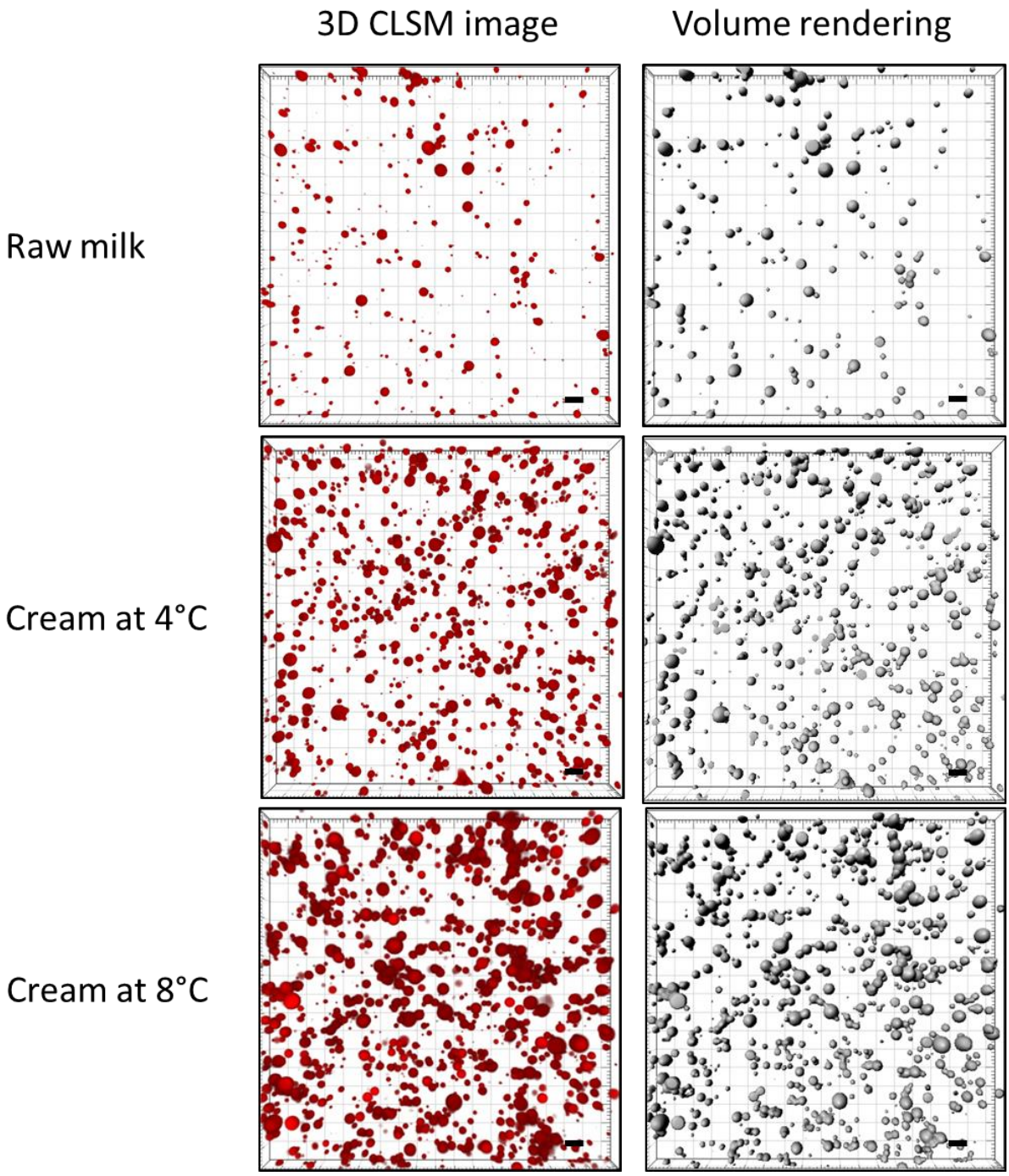

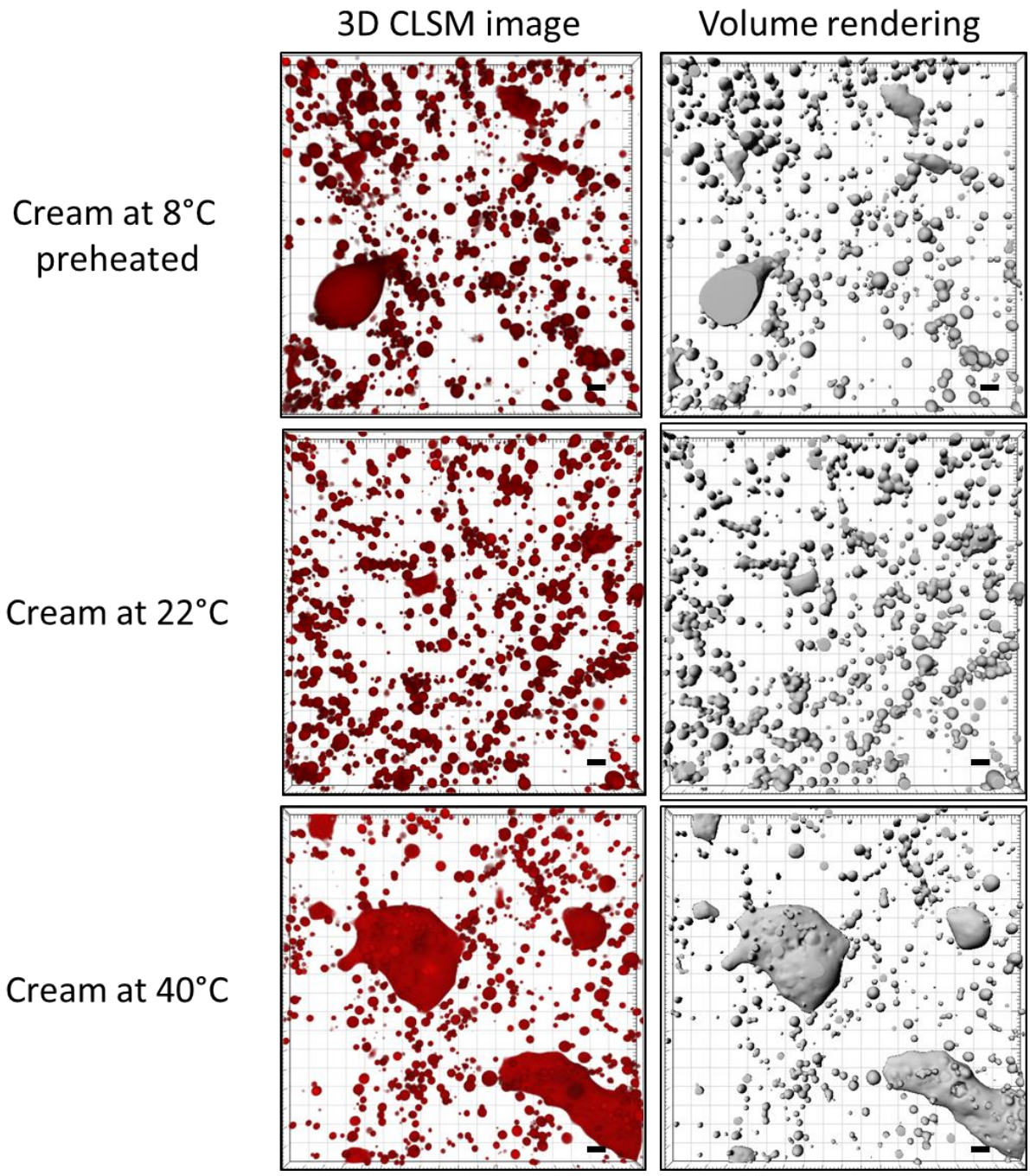

Figure 1.8. Fat microstructure in creams at various temperatures. 3D CLSM images of Nile Red stained fat globules are red and the rendered volume of the fat is grey. The scale bars are 10 µm in length. The microstructure is representative of two separate trials.

Image analysis was performed on rendering image (Fig.1.8) and % volume distribution of fat in creams raised at different temperatures is reported in Figure 1.9. Data were obtained by analysing ~1000 fat globules per sample. Fat globule size progressively increased with increasing temperatures due to coalescence phenomena, as shown by CLSM, while the large

population of native fat globules of raw milk disappeared. A new population of fat droplets with ~30 µm average size was observed in creams raised at both 8 °C after preheating and 40 °C. This population represented 20 and 39% of the total fat volume in the former and the latter samples, respectively. In cream at 40 °C, 10% fat volume was represented by fat droplets ~17 µm in size.

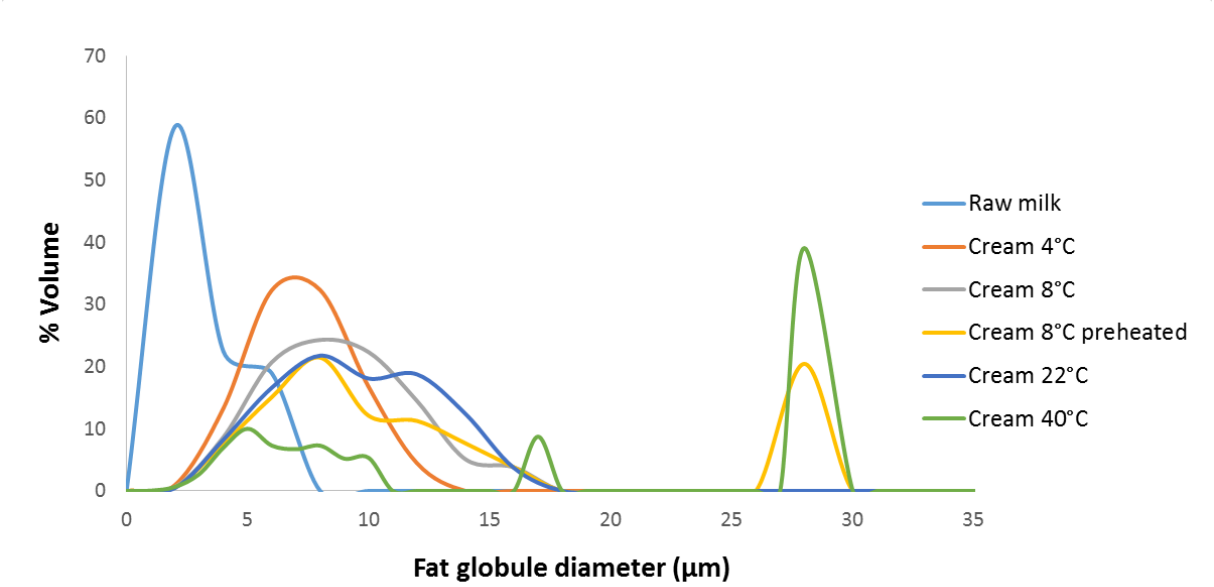

Figure 1.9. Volume distribution of fat obtained from rendering images of cream at different temperatures (Fig. 1.8) by using an image analysis software.

1.3.5 Effect of temperature on behaviour and size of fat globule clusters

Optical microscopy using differential interface contrast (DIC, also called Nomarski) and bright field was used to study the behaviour of fat globule clusters in raw milk when the temperature was risen from 8 °C up to 40 °C (1 °C/5min) and then was lowered down to 8 °C. A series of real-time observations was acquired during the whole thermal cycle and maximum linear diameter and perimeter of three different clusters were considered. Through these observations, clusters proved to disrupt between 36 and 38 °C and the involved fat globules to turn into spherical and smooth free globules (Fig. 1.10). However, when the sample heated up to 40 °C was cooled down to 8 °C for 2 hours, the original cluster of fat globules did not re-establish.

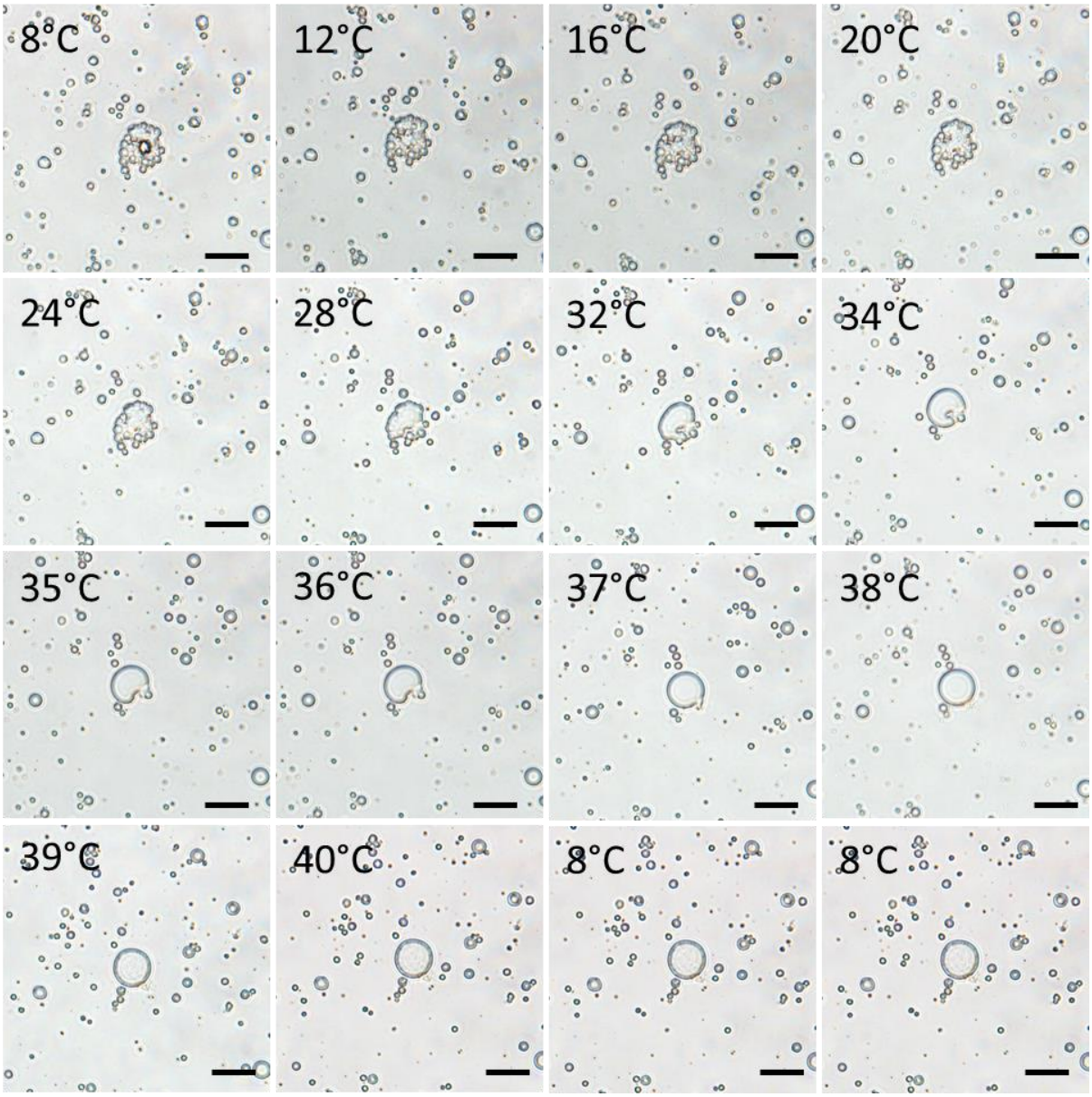

Figure 1.10. Real time images of a fat globules cluster at different temperatures. Sample was heated 1 °C/5 min and images were taken at the end of each heating step. Cooling was performed quickly from 40 to 8 °C and images at 8 °C were taken after 1 and 2 hours. Bars are 10 µm in length.

A further trial was performed to test fat globule ability to re-establish a clusters after heating up to 40 °C and cooling back to 8 °C for 6 hours (Fig. 1.11). Consistently with previous observations (Fig. 1.10), the clusters we considered at 8 °C (Fig. 1.11, arrows) broke around 36-38 °C and no other large clusters formed at 40 °C. A slight increase in clustering activity was observed when the sample was cooled down to 8 °C and kept at this temperature for 3 hours. However, clusters did not increased in size after a further 3-hour step at 8 °C. The

clustering process at low temperature was slower and less intense than the cluster breaking that happens at 36-38°C (Fig. 1.10).

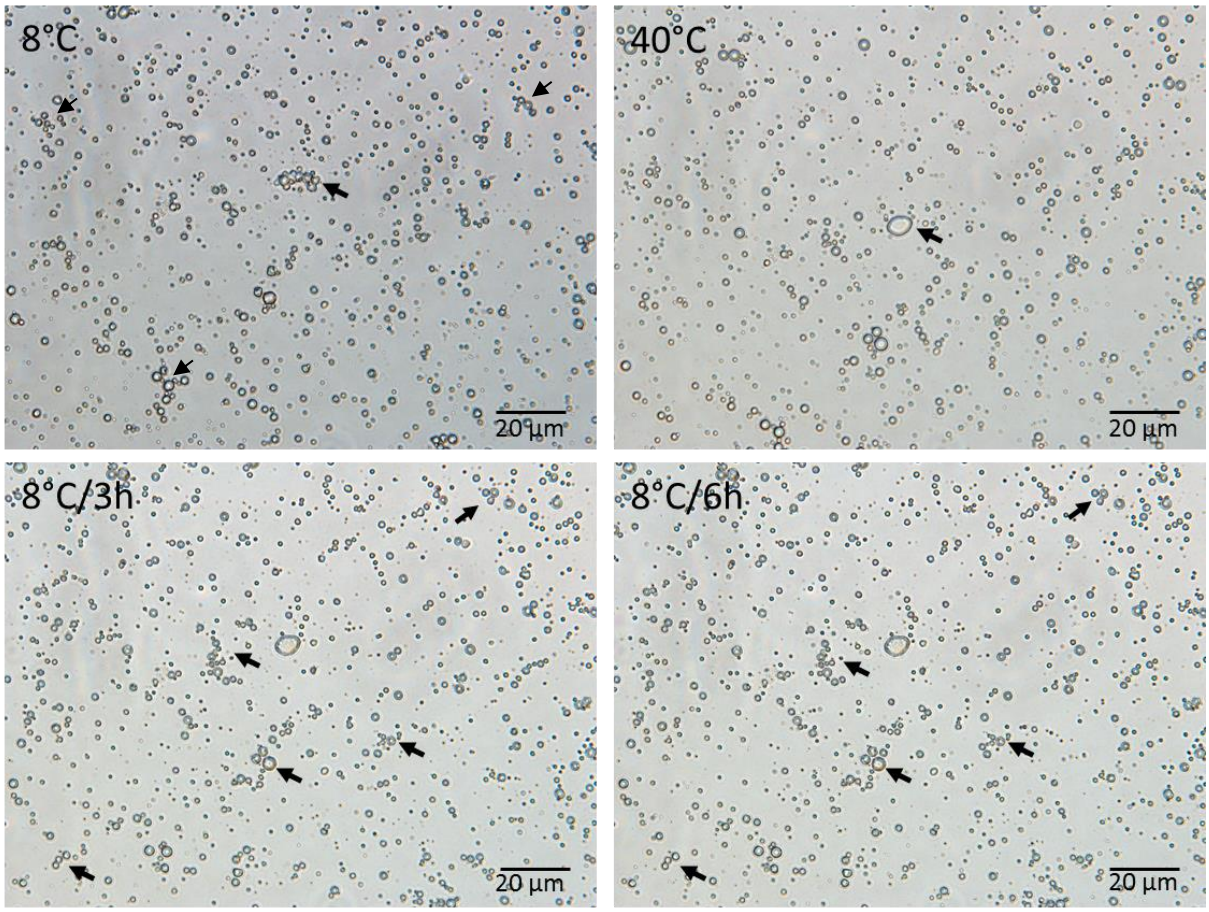

Figure 1.11. Real time images of fat globules behaviour during heating from 8 to 40 °C and subsequent cooling down to 8 °C. A total time lapse of 7 hours was considered.

Maximum linear diameter and perimeter of fat globules clusters were measured in real time during heating from 8 to 40 °C (Fig. 1.12). Consistently with light images, both the measured parameters decreased with increasing temperature. The most important changes were observed in the range 35-38 °C, where disruption of clusters takes place. However, both the parameters trends were no affected by clusters size but instead the maximum linear diameter trend was affected by the size of clustered fat globules. In fact, the diameter trend of "cluster 1" (Fig 1.12 a) was different with respect to the others because it was composed of a large globule and some small globules. Therefore, the diameter slowly decreased when small globules came off the cluster. Differently, when only small fat globules came off a large drop in size was measured, (clusters 2 and 3).

Maximum linear diameter is an important parameter since it affects the creaming rate of fat globules. However, our results showed that no diameter changes were taking place in the temperature range of natural creaming (8-20 °C). Consequently, no variations in creaming rate may depend on changes in clusters diameter in that temperature range.

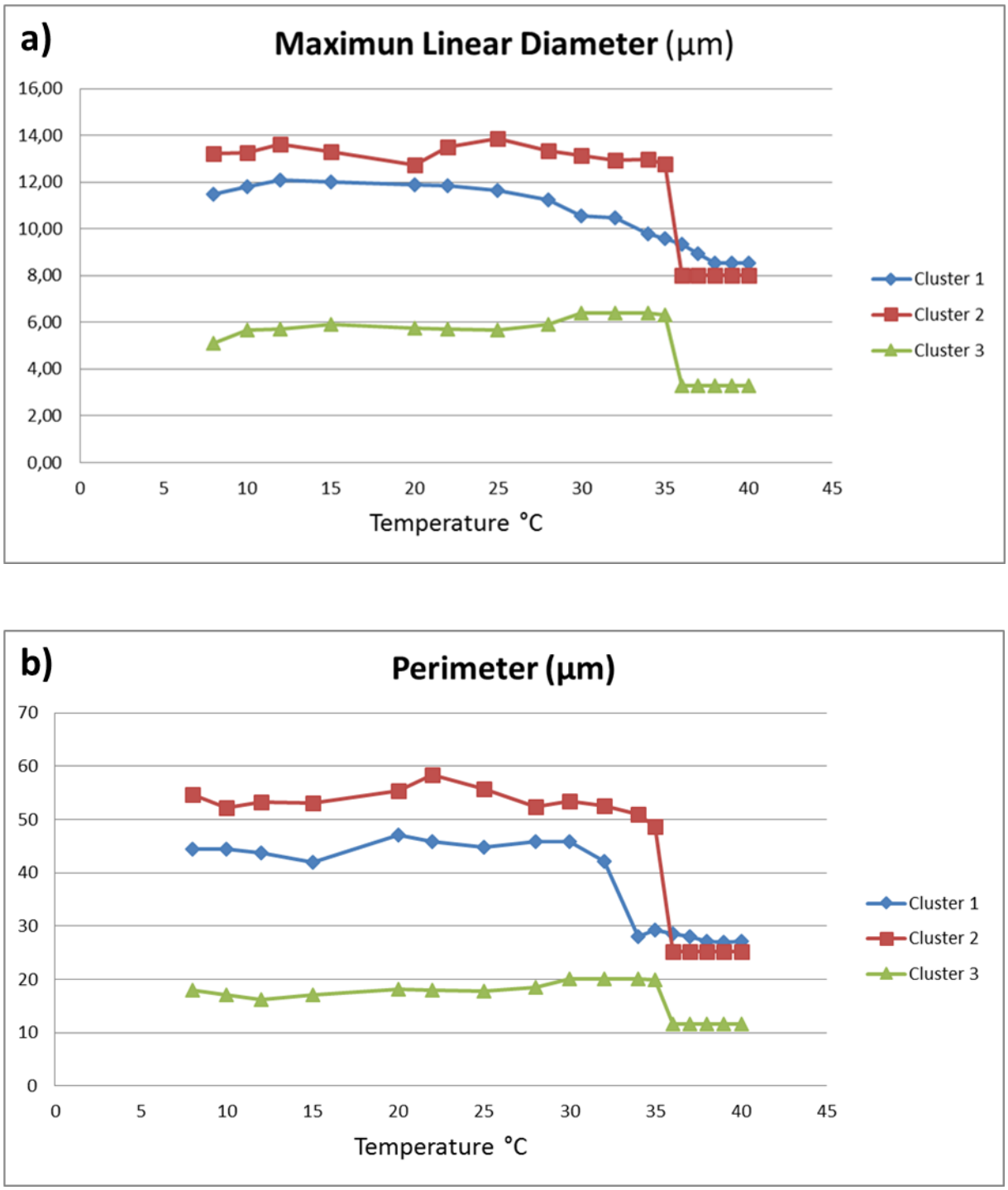

Figure 1.12. Maximum linear diameter (panel a) and perimeter (panel b) of three different fat globules clusters. Measurements were collected in real time by Olympus software associated to the microscope.

1.4 DISCUSSION

The fat content of raw milk destined to manufacturing of Grana Padano and Parmigiano-Reggiano PDO cheeses must be lowered by natural creaming according to the product specification of these cheeses (European Union Regulation, 2011a; European Union Regulation, 2011b). This process, which lasts for 8-12 hours at a temperature between 8 and 20 °C, also allows the removal of the majority of microorganisms, spores and somatic cells with the cream. However, even very few spores of *C. tyrobutyricum* remaining in the cheese curd may cause the late blowing defect (LBD).

The experimental procedure we adopted correctly reproduced the natural creaming phenomenon with high efficiency in spores and bacteria removal (>90%) after an overnight fat separation at 8°C. The accuracy of adopted conditions in keeping the surface of fat globule intact was assessed by DilC_{18}(3)-DS fluorescent staining. MFGMs were brightly, but heterogeneously stained and the absence of fluorescence in some portions could be regarded either as a lack of a lipid bilayer (Evers et al., 2008) or the presence of co-existing fluid and gel phases which impair membrane staining. More recently, Lopez et al., (2011) suggested the local differences in the thickness of the MFGM to be due to the liquid-ordered domains of sphingomyelin with long-chain saturated fatty acids. Such a heterogeneous composition and complex structure of the MFGM are likely to have an impact on both the persistent interactions among fat globules and the coalescence phenomena we have sometimes observed by light fluorescence microscopy (Figures 1.1 c, d).

As regards the supposed stable interaction between bacteria and fat globules in cream, light microscopy clearly showed that this interaction does exist. In fact, most of the time both spores and bacterial cells appeared firmly adherent to fat globules, even in presence of sample streaming on the microscope slide (Figure 1.2 a). However, the staining procedures for both light and fluorescence microscopy did not give any information on the nature of this binding. The close adhesion of either bacteria or spores to fat globules was confirmed by TEM examination of replicas of cryofixed cream. By this technique bacteria seem to stick to MFGM (Fig. 1.3) but, despite the high resolution, no molecules possibly involved in this mechanism could be visualized. Much more details on adhesion mechanism came from the examination of ultrathin sections by TEM. An electron-opaque amorphous material apparently sticking bacteria to MFGM, but not fat globules among themselves, seems to be responsible for adhesion and hence for bacteria rising during creaming (Fig. 1.4). Thus, the rising would not be merely due to physical entrapment of bacteria in the fat clusters, as

suggested by Rossi (1964), but to a more complex mechanism. Indeed, the involvement of milk immunoglobulins in the interactions among fat globules was proposed since a long time, as suggested by the pioneering experiments of Bottazzi et al. (1972). At this regard, Bottazzi and Zacconi (1980) isolated from cream a proteinaceous material that they called "active fraction", able to agglutinate each other either fat globules or bacteria. This fraction proved to contain milk IgM, however the contribution of other molecules was stated (Zacconi and Bottazzi, 1982). Beta-lactoglobulin and proteins from MFGM, like Muc1 and peripheral proteins PAS 6/7, were reported to contribute to this phenomenon (Evers, 2008; Sando, 2009) but their role was only indirectly demonstrated because the fat globule aggregation was not observed in heat-treated milk. Honkanen-Buzalskiand Sandholm (1981) showed that IgA and IgM were present on the surface of the MFGM, while Euber and Brunner (1984) demonstrated that in absence of IgM, removed by a specific antiserum, gravity separation of fat did not occur. More recently, other indirect evidences of the involvement of immunoglobulins in bacteria adhesion to fat globules have come out from the research work of Barbano and collaborators (Ma and Barbano, 2000; Caplan et al., 2013; Geer and Barbano, 2014a; Geer and Barbano, 2014b). They found that different levels of bacteria in milk influence the degree of gravity separation of fat but not of somatic cells (Caplan et al., 2013), suggesting that bacteria may compete for interaction with the immunoglobulins involved in gravity separation of the fat. As a consequence, high bacteria counts in milk may reduce the extent of creaming. However, the story of immunoglobulin involvement in creaming has turned out more complicated than expected. Very recently, Geer and Barbano (2014b) found that the immunoglobulins themselves were not able to cause the rising of fat, bacteria and spores to the top of the milk but the presence of somatic cells was also necessary. However, in our microscopy studies, we have never seen somatic cells in contact with the fat globules, nor with bacteria, thus it is possible that the contribution of these cells to creaming is not necessarily a consequence of direct interactions but other factors could be involved.

Natural creaming temperature affected both fat globules creaming rate and cream microstructure. Natural creaming at 40, 22 and 8 °C with preheating was faster than creaming at 4 and 8 °C. However, higher creaming temperatures affected cream microstructure causing fat globules coalescence. In particular, higher numbers of damaged globules were observed in the creams raised at 40 °C and at 8 °C with preheating at 37 °C than in the cream raised at 22 °C. At higher temperatures, the difference in mass density between fat globules and skimmed milk is higher and the milk viscosity is lower. Consequently, natural creaming is faster at high temperatures. Furthermore, our experiments showed that the size of fat globule clusters

was rather constant in the temperature range 12-20 °C and, consequently, it does not influence the natural creaming rate at the usual conditions. Also, cluster diameter is not a bulk milk property since it is relative to a small number of fat globules in milk, therefore it is not capable to modify the creaming rate of fat globules.

1.5 CONCLUSIONS

Though we cannot exclude that a number of bacterial cells and spores rises to the top of the milk during natural creaming because physically trapped among fat globules, our study shows for the first time that the majority of these bacteria are actually stuck to fat globules by an electron-opaque material whose nature has to be determined. Immunoglobulins are certainly the best candidates responsible for the adhesion but other compounds, i.e. bacterial exopolysaccharides, may be involved. Biochemical and immunolocalization studies are progressively elucidating the composition of the adhesion material, whose knowledge is determinant to set up protocols for maximizing spore removal during milk creaming in both Grana Padano and Parmigiano-Reggiano cheese making.

2. Chapter 2: Role of immunoglobulins in milk desporification

2.1 INTRODUCTION

Immunoglobulins are natural antibodies that are synthesized by mammals in response to antigenic or immunogenic stimuli such as bacteria and viruses, and thus provide protection against microbial infections. Immunoglobulins have various protective bioactivities, most of which involve binding activity as a first step. Bovine colostrum is produced by cows in the immediate post parturition period and represents a naturally enriched source of immunoglobulins. Consumption of bovine colostrum confers passive immunity to neonatal calves (Lilius & Marnila, 2001). Calves are born agammaglobulinemic and immunoglobulin absorption capacity decreases rapidly within 24h after parturition (Weaver et al., 2000; Beam et al., 2009; Nagalakshmi, 2009). Thus a sufficient intake of colostrum with a high immunoglobulin concentration is important. The initial concentration of immunoglobulin in colostrum varies broadly (from 30 to 200 mg/mL) depending on breed, age, and health status of the cow (Butler, 1986: Larson 1992; McFadden et al. 1997) and decreases by a factor five to six in the first three days. Typically, milk and colostrum contain three main types of immunoglobulin, IgG, IgM and Ig. The most abundant immunoglobulin class in bovine colostrum is IgG, with 43.8 g/L on average. In contrast, IgA and IgM are present at much lower concentrations, with 4.05 and 4.8 g/L respectively (Raducan et al., 2013).

Immunoglobulins in colostrum or milk come from blood through passive transfer (Cummins et al., 2016). All immunoglobulins have the same basic monomeric structure. Each monomer is composed of two identical heavy (~50 kDa) and two identical light (~25 kDa) polypeptide chains, linked by disulphide bonds (Hurley and Theil, 2011), resulting in a total MW of approximately 150 kDa.

The aim of this study was to identify the immunoglobulin classes responsible for both the interactions among fat globules and the possible agglutination of *C. tyrobutyricum* to fat globules during the natural creaming of raw milk prior to cheese making.

2.2 MATERIALS AND METHODS

2.2.1 SDS-PAGE

Immunoglobulins were precipitated from bovine colostrum under the conditions pointed out in this work (see 2.3.1.) and summarized in Fig. 2.1. The protein profile of salt precipitate was analysed by SDS-PAGE in both denaturing and not-denaturing conditions. A known amount of sample (containing 0.015 mg protein in buffer) was mixed with an equal volume of SDS–PAGE denaturing buffer (0.125 M Tris-HCl, pH 6.8, 50% Glycerol, 1.7% SDS; 0.01% Bromophenol Blue) containing 1% 2-mercaptoethanol when indicated, and heated at 100 °C for 10 min. As described in previous studies (Barbiroli et al., 2013) SDS–PAGE was carried out on a fixed porosity gel (12% monomer), by using a MiniProtean apparatus (Bio-Rad, Richmond, VA, USA). Gels were stained with Coomassie Blue.

2.2.2 Immunogold labelling (IGL)

A post embedding was performed on samples prepared and fixed as in paragraph 1.2.4 and 1.2.7 respectively. Thin sections of these samples were first incubated for 5 min at room temperature in phosphate saline buffer (PBS) 0,05 M containing 1% bovine serum albumin (BSA) and 0,01 % Tween 20, and then for 12-24 hours at 4 °C in the appropriate anti-serum to IgG, IgM and IgA diluted 1:100 and 1:1000 with the same solution. After an accurate wash with PBS, section were then incubated for 2 hours at room temperature with anti-serum to IgG, IgM, IgA and labelled with 15 nm colloidal gold.

2.3 RESULTS

2.3.1 Immunoglobulin purification by Ammonium Sulfate precipitation

Various types of processing can be used for harvesting immunoglobulins from colostrum or milk. However, in the last 20 years the proposed techniques have been focused only on IgG, especially those based on column chromatography (El-Loly, 2007; Ayyar et al., 2012). Also, some of these methods involve exposing the immunoglobulins to either heat, acid or high pressure - which may negatively affect the conformation and binding activity of the separated protein molecules. Consequently, attention should be paid to select the most suitable method to harvest immunoglobulin keeping the native characteristics required for our purposes.

In this study immunoglobulins were concentrated from bovine colostrum collected on the second day postpartum, i.e. when the colostrum achieve the physical stability to allow manipulation (Tsioulpas et al., 2007). Colostrum was laboratory processed through several steps (Fig. 2.1) to obtain native immunoglobulins. Fat and casein were separated by centrifugation and precipitation at pH 4.6 respectively. Immunoglobulins were purified by salt precipitation with both 45 and 80% $(NH_4)_2SO_4$. Subsequently, the precipitate was analysed by 12% SDS-PAGE to determine the salt concentration most suitable for maximising the precipitation of immunoglobulins while unwrapping the other soluble proteins. The addition of 80% w/w $(NH_4)_2SO_4$ did not result in an increase of immunoglobulin precipitation (fig 2.1a) and, contrarily, increased the precipitated amount of other whey proteins, especially α-lactalbumin and β-lattoglobulin. Consequently, the pellet obtained after the addition of 45% w/w $(NH_4)_2SO_4$ was used. The assessment of the actual presence of immunoglobulins in the precipitate has been achieved by gel-electrophoresis under both reducing and not reducing conditions (Fig 2.1). Heavy and light immunoglobulin chains in the reducing gel gave origin to two different bands. These bands were absent in non-reducing gel, instead a single band appeared having a larger MW (Fig 2.1 c, red arrows). Heavy chain migrated close to the 67 kDa marker, according to the MW from 53 to 65 kDa reported by Sites et al. (1976) for this immunoglobulin component. Light chain was approximately 25 kDa. Based on the electrophoretic patterns, purification steps and precipitation at 45% $(NH_4)_2SO_4$ were optimized to obtain a final product augmented in immunoglobulins and depleted in casein, α-lactalbumin and β-lactoglobulin. This result is clearly visible comparing the lane of native colostrum with that of 45% precipitate colostrum

in reducing gel (Fig. 2.1 b). Concentrated immunoglobulins were dialyzed against PBS and used for natural creaming trials.

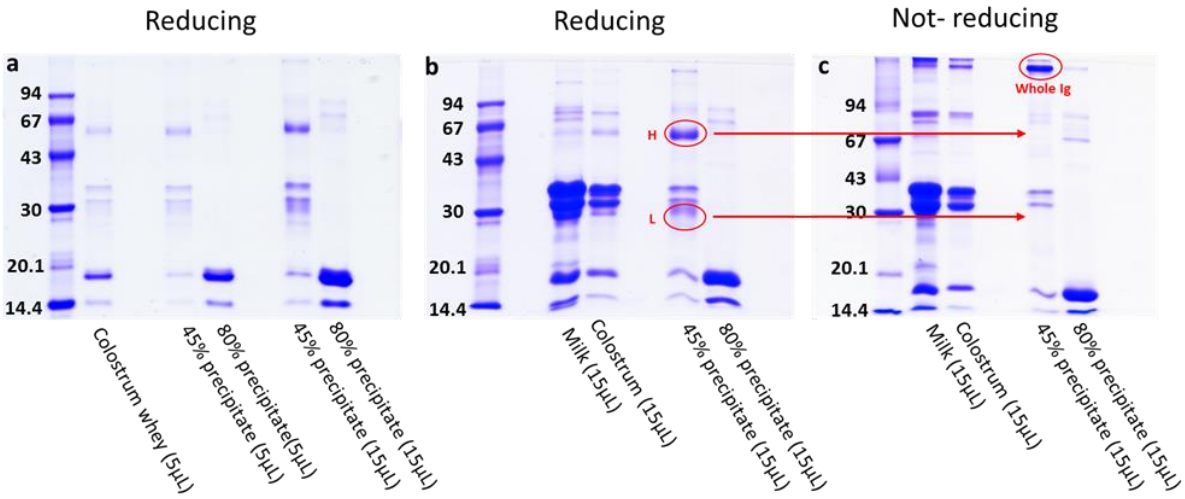

Fig. 2.1. SDS-PAGE separation of proteins precipitated by both 45 and 80% saturated $(NH_4)_2SO_4$ in both reducing and not-reducing conditions.

2.3.2 Role of immunoglobulins in natural creaming of milk

Natural creaming was reproduced at laboratory scale under conditions selected with the aim of causing as little damage as possible to the involved components (Fig. 2.2). Microfiltered skimmed (0.3% fat) milk was used as a medium depleted of fat globules, cells and spores. Washed milk fat globules, washed *Clostridium* spores and immunoglobulins were added at five different levels according the experimental plan. A parallel set of samples was prepared using the same milk heated at 80°C for 10 min to inactivate immunoglobulins present in milk. In this way we could also study the effect of either heated or unheated immunoglobulins on promoting rising of both fat globule and spore. The most probable number (MPN) of spores into the top cream layer was evaluated as well as the amount of raised cream after natural creaming for a fixed time of 8 hours.

Milk added with fat globules showed a thicker cream layer than the corresponding sample made using heated milk (tab. 2.1). It seems that a heat-sensitive factor that affects the fat globules is present in microfiltered skim milk. Spore rising was shown to be strongly dependent on heat treatment, because lower spore numbers were counted in the cream layer of the sample with heated microfiltered milk than in the unheated one. Moreover, the addition of immunoglobulins caused an important increase in spore rising with respect to the sample

where no immunoglobulins were added. Caplan *et al*. (2013) showed that heat treatment at ≥76.9°C for 25 s stopped spores and fat globules from rising, possibly because of denaturation of native immunoglobulins.

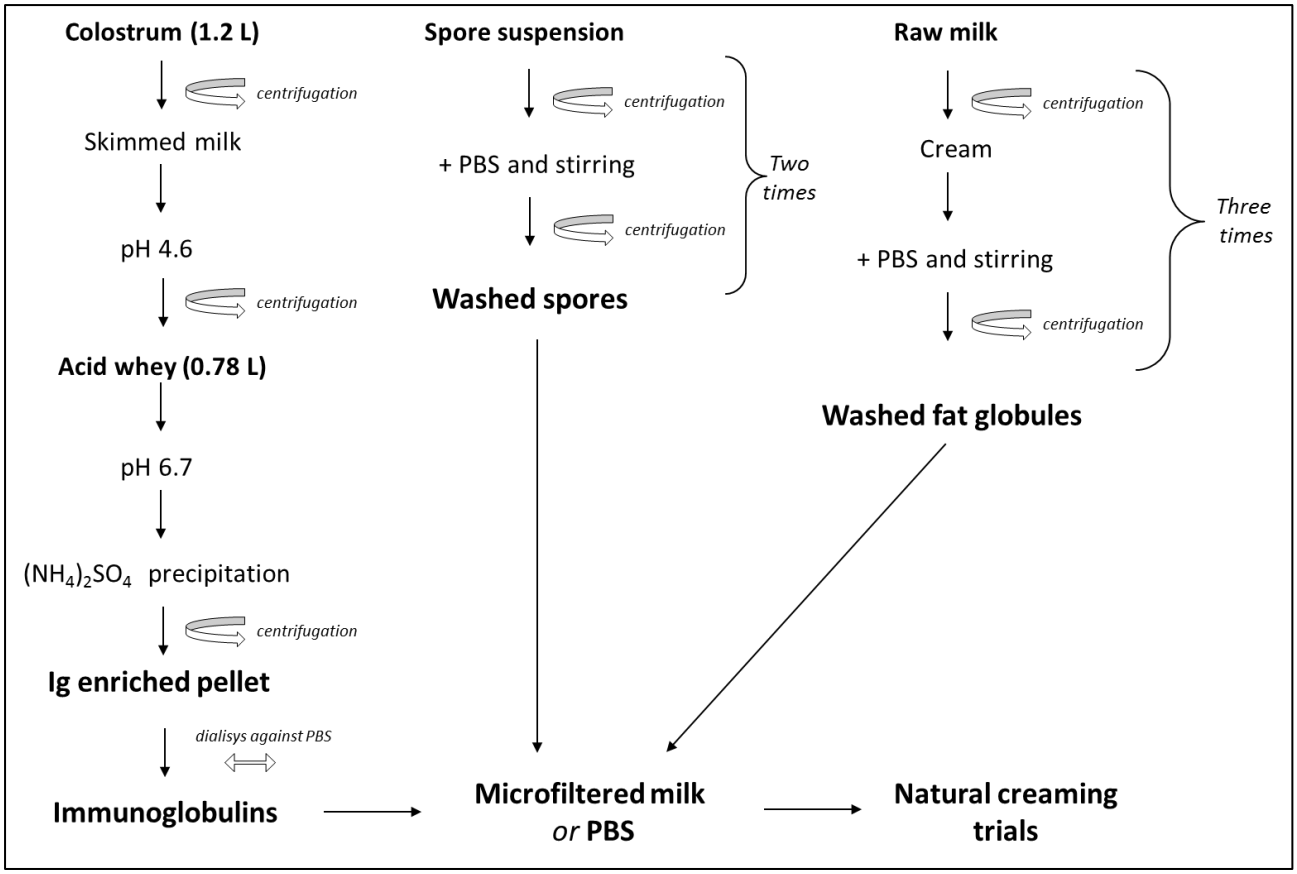

Fig 2.2. Experimental design applied for reproducing natural creaming using immunoglobulins precipitated from colostrum, spores washed out from broth and fat globules washed out from raw milk.

Sample	Cream *(mL)*	Spores *(MPN/mL)*
MMilk + fat globules	1.5	na
Heated MMilk + fat globules	1.2	na
MMilk + fat globules + spores	1.5	330
Heated MMilk + fat globules + spores	1.2	80
MMilk + fat globules + spores + Igs	1.5	490
Heated MMilk + fat globules + spores + heated Igs	na	80

Tab. 2.1. Numbers (MPN) of spores raised in cream during natural creaming of fat globules in microfilterd milk (MMilk) added with spores and immunoglobulins.

A second set of experiments was carried out to evaluate the effect of increased concentration of native immunoglobulins on rising of both spores and fat globules. A simpler model system has been set up using PBS as a medium suitable to observe the effect of added immunoglobulins in the absence of those naturally present in milk. The use of PBS also guaranteed to exclude effects due to other soluble molecules present in milk.

Both the amount of cream and the number of spores in the top cream layer increased after the addition of immunoglobulins when compared to the sample without immunoglobulins (tab. 2.2). Spore rising has shown to be strongly affected by the addition of immunoglobulins. Considering that fat globules rising is able *per se* to concentrate 60-99% of bacteria in the cream layer (Abo-Elnaga et al., 1981; D'Incecco et al., 2015), the spore surge we observed from 220 to 490 MPN/mL should be considered as a relevant improvement. This could also explain why we did not observe a further increase in raised spores when the amount of added immunoglobulins was increased three times. Another reason could be the absence of free antigen sites available for additional immunoglobulins binding. It is worth noting that 220 spores MPN/mL were found in the cream sample where immunoglobulins were not added. This data could be explained by the physical entrapment of spores within clusters of rising fat globules. Instead, a smaller spore number, 80 MPN/mL, was detected on top of the samples where no fat globules were added.

Sample	Sampling	Cream *(mL)*	Spores *(MPN/mL)*
PBS + fat globules	*top*	0.4	na
PBS + fat globules + spores	"	0.4	220
PBS + fat globules + spores + Igs	"	0.5	490
PBS + fat globules + spores + 3Igs	"	0.5	490
PBS + spores	"	na	80
PBS + spores + Igs	"	na	80
PBS + spores + Igs	*bottom*	na	330

Tab. 2.2. Spores counted at the top and the bottom of a model system where fat globules, spores and immunoglobulins were added in different combinations to PBS.

The results obtained from natural creaming trials involved three phenomena: (i) the fat globules clustering, (ii) the agglutination of bacteria to fat globules and (iii) the rising of fat globules. Moreover, fat globules are essential for spores to reach the top of the milk because spores deposited at the bottom of the milk when no fat globules were present into the system. When added, immunoglobulins seemed to be able to attach bacteria to fat globules, as higher numbers of spores were detected in the top cream layer of the sample. Fat globule rising *per se* is not an immunoglobulin-dependent phenomenon. Nevertheless, creaming can be fastened through the addition of immunoglobulins that increase the size of fat clusters. The faster rising can be explained by the Stokes' Law. However, evidence that clustering of fat globules was promoted by heat-activated components, such as immunoglobulins, came from the real time observation of raw milk by optical microscopy while the temperature was risen (Fig. 2.3). In fact, clusters appeared to be persistent at low temperature (8 °C) but progressively broke up during heating. Clusters completely dissolved into single fat globules around 36-37 °C (Fig. 2.4) and this status was observed up to 70 °C (Fig. 2.4). Because of their ability in trapping bacteria, clusters of fat globules have an important role in natural creaming of milk (D'Incecco *et al*. 2015). Previous studies indirectly showed that immunoglobulins are responsible for cross linking fat globules together and, because of their propensity to undergo cold-induced aggregation, some immunoglobulins are considered cryoglobulin. This is in agreement with our observation of clustered fat globules only at low temperature. The ability of fat globules to stick together after the addition of a serum component has been previously observed (Babcock 1889).

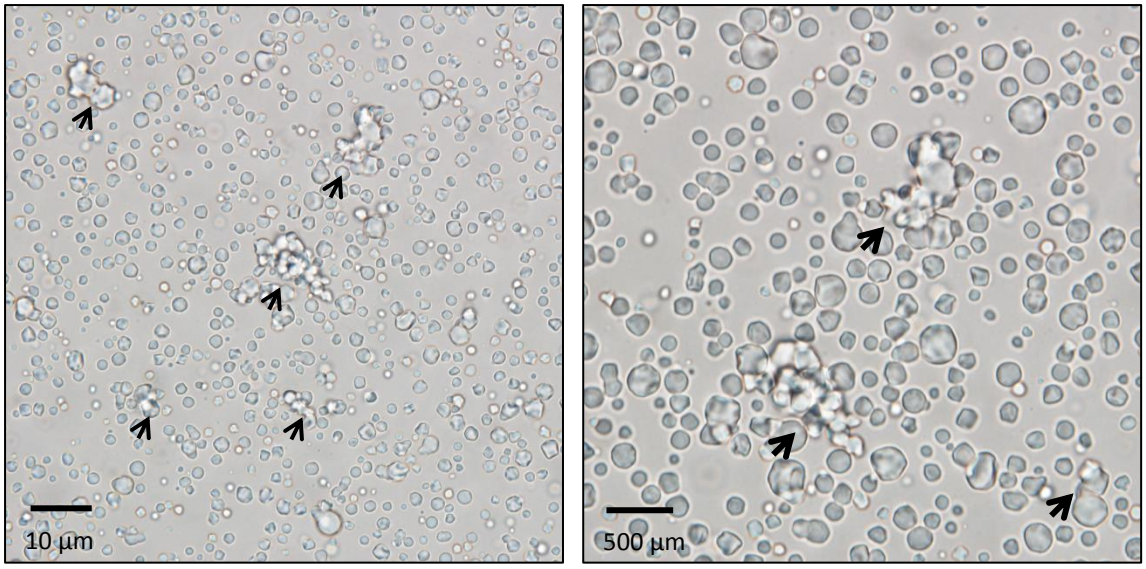

Fig. 2.3 Light microscopy images of fat globule clusters (arrows) in raw milk kept at 8 °C.

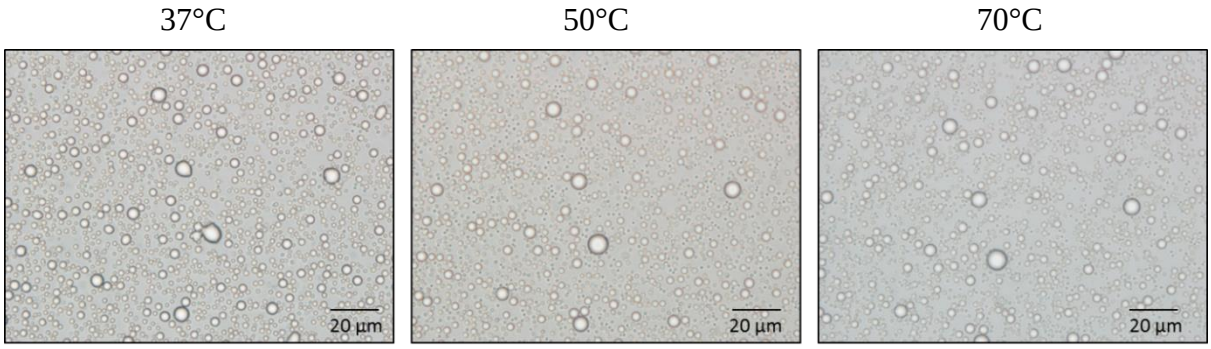

Fig 2.4 Real time-light microscopy images of raw milk heated up to 70 °C. Clusters split up at 36-37 °C and single fat globules only were observed until the end of the heating step.

Previous research has shown that immunoglobulins are a necessary component for the gravity separation of fat globules (Euber and Bunner, 1984). That said, no literature has been found studying the effect of adding immunoglobulins on improving spore rising during natural creaming of milk. Our experimental design was planned not only to test the immunoglobulins role but also to evaluate the improvement of cheese milk healing by the addition of increasing amounts of native immunoglobulins separated from colostrum whey. More details about the role of immunoglobulins in either cross-linking fat globules or agglutination of bacteria were obtained by performing immunogold labelling.

2.3.3 Immunogold labelling

Further research work was undertaken to identify the type of immunoglobulins involved in increasing rising fat globules or interaction of these latter with *C. tyrobutyricum* spores in milk upon natural creaming. An experiment was aimed to determine whether all the immunoglobulin types, i.e. IgG, IgM and IgA, were equally involved in promoting either fat globule clustering or the bacteria agglutination to fat globules. For this purpose, creaming trials were conducted in triplicate for each immunoglobulin type. Immunogold labelling was performed on sections of resin embedded samples, i.e. cream, cream previously added of *C. tyrobutyricum*, and pure culture of *C. tyrobutyricum*. From TEM observation, IgM was rarely observed to be involved in the interactions among fat globules and between globules and bacteria while no contribution could be evidenced for IgG.

In contrast, the gold-labelling showed IgA to be always present in the material linking together either fat globules (Fig. 2.5) or a bacterium to a fat globule (Fig. 2.6).

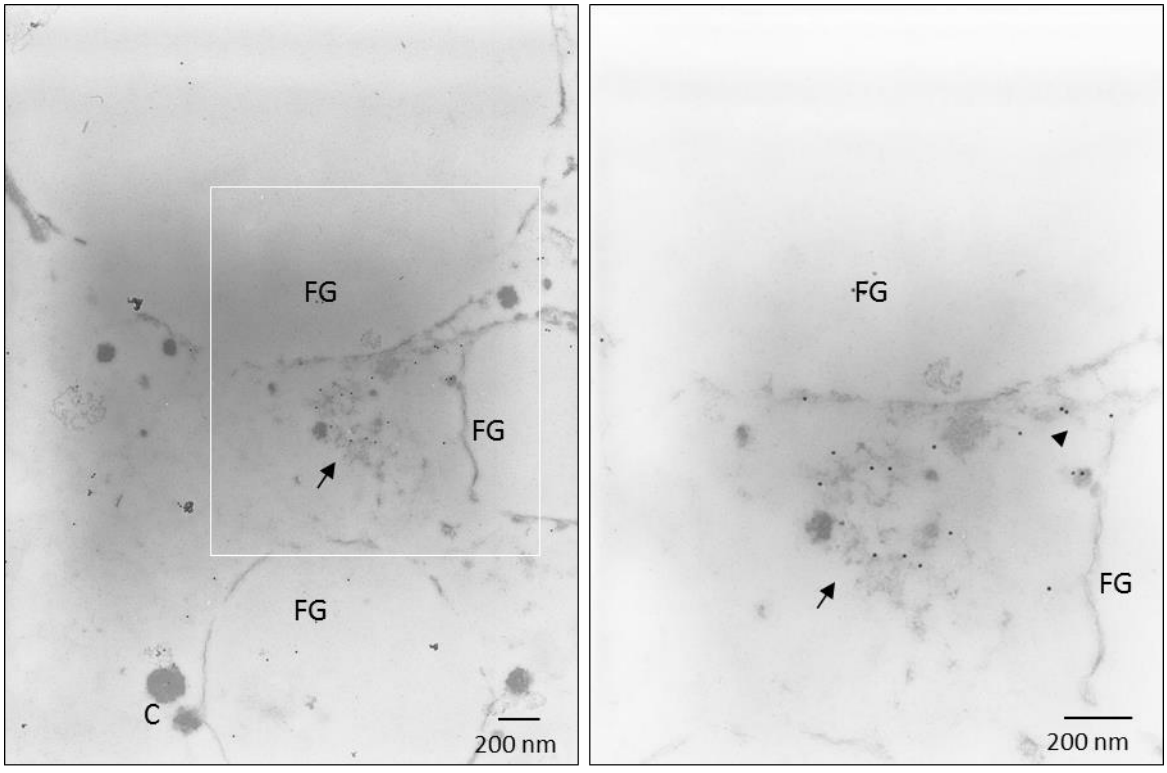

Figure 2.5. TEM micrographs of double immunogold labelling on fat globule cluster. IgA is labelled with gold-labelled secondary antibody 15 nm in length. Higher magnification of the white frame is on the right side.

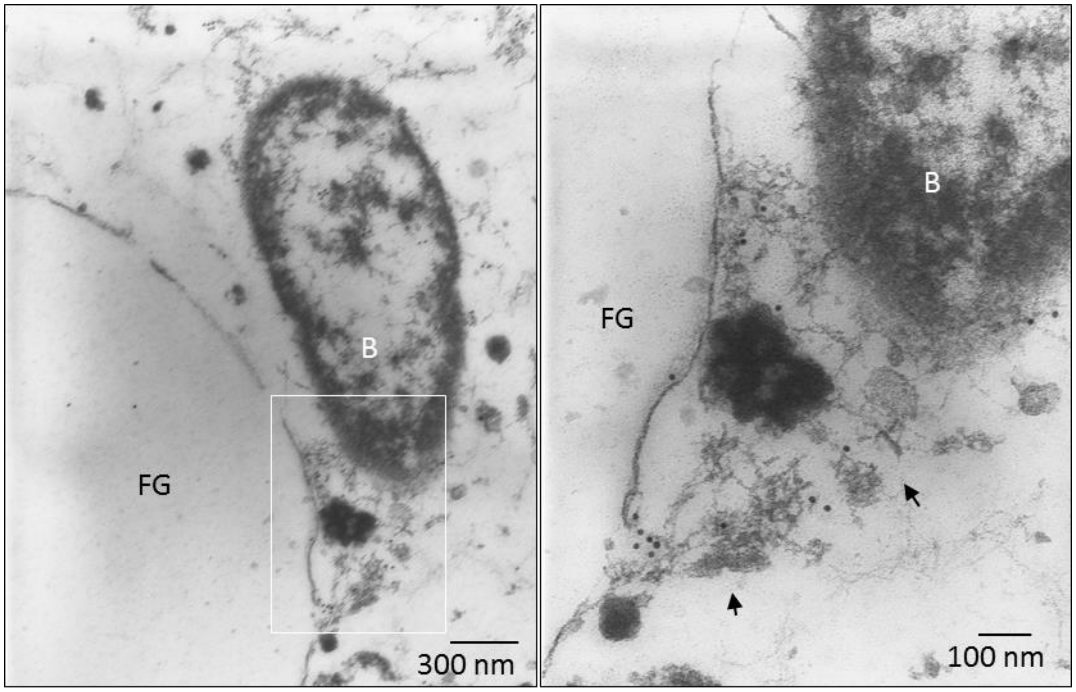

Figure 2.6. TEM micrographs of double immunogold labelling on bacterium (B) attached to fat globule (FG) via electron-opaque material. IgA is labelled with gold-labelled secondary antibody 15 nm in length. Higher magnification of the white frame is on the right side.

This was an amorphous material, formless and apparently having low density. Due to the number of gold spots labelled on it (Fig 2.7), this material looked like a complex of IgA molecules, although we cannot exclude that other molecules take part to it.

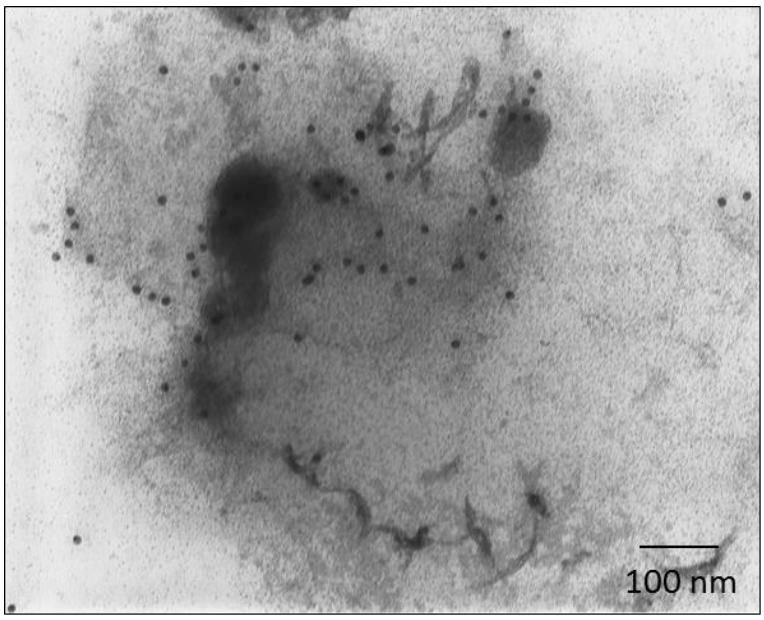

Figure 2.7. Electron-opaque material labelled with IgA. Gold particles are 15 nm in length.

Surely, IgA was at least one molecule responsible in cross-linking fat globules and agglutinating bacteria to fat globules. These results are consistent with those of Caplan et al. (2013). They hypothesized that a competition may take place between bacteria and fat during natural creaming because milk with a high bacteria count gave a cream having a higher percentage of total bacteria but a lower percentage of fat compared with a milk initially having a lower bacteria count.

IgA was labelled on two different zones with respect to fat globules: on the electron-opaque material among clustered fat globules and on the MFGM (Fig. 2.8). In this last case, IgA looked to be a constituent of the MFGM itself, especially when the labelling was exactly on the MFGM (Fig. 2.8b, arrow), or to be strongly associated to it.

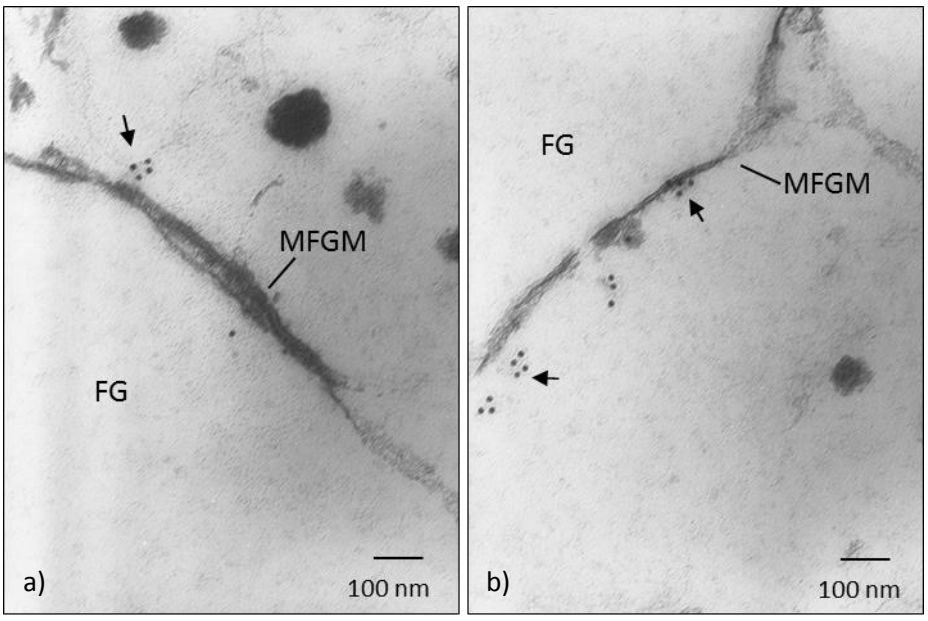

Figure 2.8. TEM micrographs of gold-labelled IgA associated to MFGM. Gold particles are 15 nm in length.

Our consideration is consistent with the findings of Honkanene-Buzalski and Sandholm (1981). These authors showed that the major part of IgA should be regarded as extrinsic membrane protein because it was released from the MFGM when solubilised with Triton X 100, and or treated with guanidine HCl. A theory (Larson, 1979) explaining why bovine IgA remains largely absorbed to the MFGM is that dimeric IgA binds to secretory compounds in the membranes of epithelial cells and this complex of sIgA is then transported across the epithelial cell to be released at the apical surface. Consequently, sIgA is bound to the MFGM

when a lipid droplet, composed of triglycerides, buds off the apical plasma membrane being enveloped by it (Fig. 2.9) The reason why IgA remains largely associated to the MFGM instead of being released into the lumen could have to do with the higher hydrophobicity of sIgA when compared to that of other animal species (Goudswaard et al., 1979).

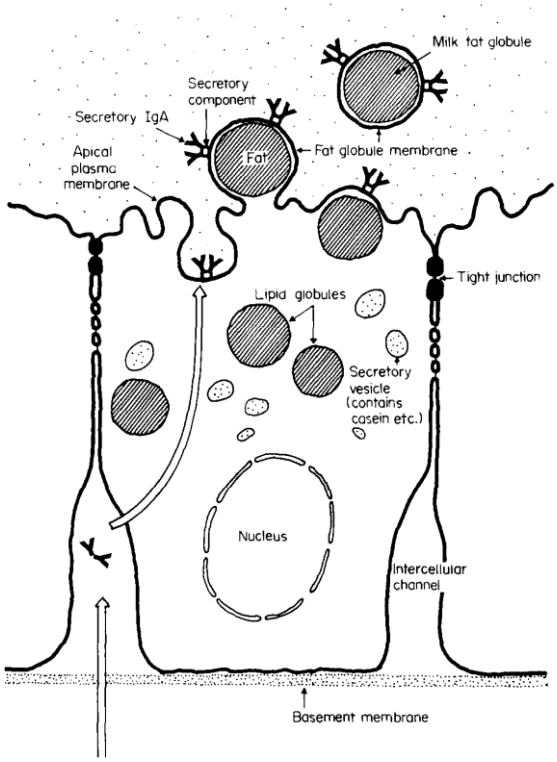

Figure 2.9. A schematic representation of the possible mechanism of MFGM-associated immunity in bovine milk proposed by Larson (1979).

Many IgA molecules were labelled on the cell wall of *C. tyrobutyricum.* Differently, no IgM and IgG were observed. *C. tyrobutyricum* was shown to possess anti-IgA receptors on its cell wall (Fig. 2.10). IgA was also observed on cell wall fragments far from the cell (Fig. 2.10 b,c).

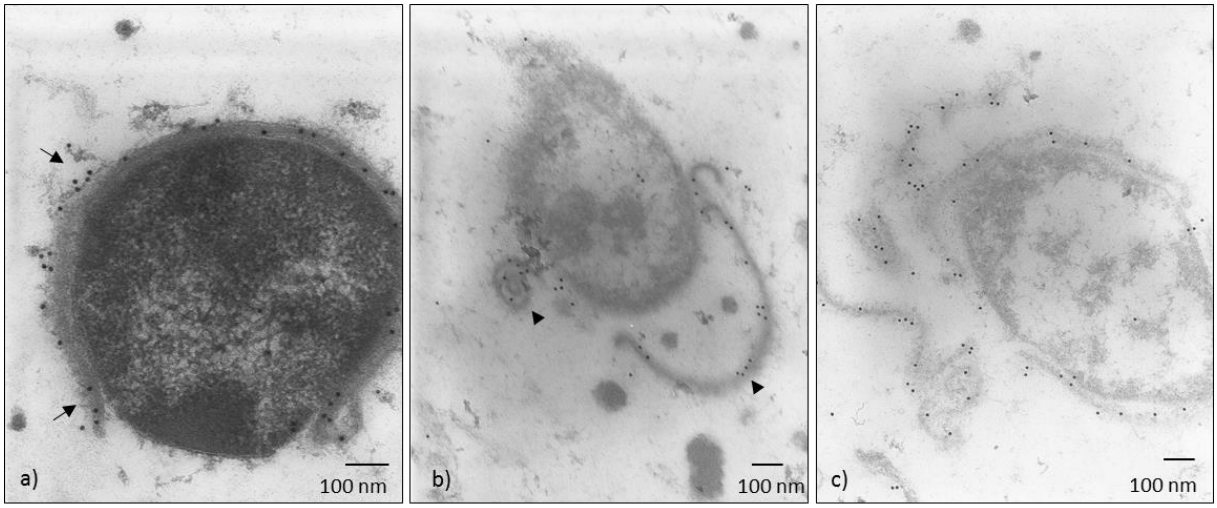

Fig. 2.10. TEM micrographs of double immunogold labelling on *C. tyrobutyricum* cells. Fifteen nm in length gold particles are associated to IgA on *C. tyrobutyricum* cell wall.

2.4 DISCUSSION

In the opinion of this author, it is important to distinguish between the agglutination of bacteria to each other, and the agglutination of bacteria to fat globules taking place during cream rising. The former is a biological event that should not be unexpected because it is part of the natural response of immune system against an antigen and doesn't require any fat globule role. In fact, Hurley and Theil, (2011) reported IgA as the major immunoglobulin class found in mucosal secretions that prevents infection by agglutinating microbes. Antimicrobial properties such as agglutination of microbes were also reported for sIgM (Brandtzaeg and Johansen, 2007). This natural agglutinating activity was demonstrated either in bovine colostrum preparations against a variety of pathogenic bacteria (Stephan *et al*., 1990; Loimaranta *et al*., 1998) or in normal milk (Choemon *et al*., 1976) and colostrum (Todd *et al*., 1989) against *Lactic streptococci*. Moreover, the agglutination of bacteria (in starter cultures in particular) is considered an unfavourable event in cheese making because it reduces cheese quality and yield (Todd et al 1989). In fact, agglutinated starter cells sediment to the bottom of the vat, causing uneven acid production within the coagulating milk.

The rising of bacteria, markedly of spore-forming species, during natural creaming of milk before vat processing, should be regarded as a positive event. In fact, it determines a spontaneous healing of the milk and consequently decreases the occurrence of late blowing defect in the cheese. The rising of bacteria is a not deeply studied phenomenon that provides for two steps: the agglutination of bacteria to fat globules and the subsequent co-rising of the two particles. According to our results, the capability of *C. tyrobutyricum* to be agglutinated to fat globules is subject to the presence of anti-IgA and anti-IgM proteins on the bacterial wall. The entity of the agglutination depends on two factors: the frequency a specific antigen is expressed on *C. tyrobutyricum* wall surface and the IgA and IgM content in the milk, which may indicate an antibody's specificity for *C. tyrobutyricum* surface antigens.

Very few studies focused, directly or indirectly, on the agglutination of bacteria to fat globules during natural creaming of milk. Franciosi *et al*., (2011) showed that psychotropic bacteria in milk intended for Trentingrana cheese making were mainly concentrated in the cream layer. Geer and Barbano (2014) showed that the addition of colostrum to skim milk was able to partially restore the natural rising of *Clostridium's* spores. However, to the author best knowledge, only Honkanen-Bulzaski and Sandholm (1981) differentiated among immunoglobulin classes working against milk bacteria and, consistently with our results, showed that *Staphylococcus aureus* appears associated to fat globules raised in presence of

IgA and IgM. No clustering and no bacteria agglutination were observed in presence of IgG. On the contrary, Stadhouders and Hup (1970) showed that the addition of what they called "whey euglobulin" to a suspension of fat globules clearly increased the binding of *S. cremoris*, but no creaming step was performed in that study.

Our findings indicated that milk immunoglobulin classes are not involved in the same way in cross-linking fat globules and agglutinating bacteria to fat globules, with IgG resulting to play no role. In depth examination of immunoglobulins characteristics reported in the literature identified some possible explanations. IgA and IgM differ from IgG for both physiological and structural reasons. IgA and IgM are found in milk and colostrum in the form of secretory IgA and IgM, namely sIgA and sIgM (Hurley and Theil, 2011) and much of these are produced by plasma cells in the mammary tissue. During the trans-epithelial transport to the apical end of the mammary cell, IgA and IgM are bound to a secretory component (Mostov and Kaetzel, 1999; Hunziker and Kraehenbuhl, 1998) that remains attached to these immunoglobulins after their secretion into milk. The secretory component is a highly glycosylated polypeptide that is known to have itself a protective role (Phalipon *et al*., 2002). Also, IgA and IgM are the only polymeric immunoglobulins (dimeric and pentameric, respectively) in milk and colostrum. In the polymeric structures, monomers are covalently bound through a joining (J) chain (Mix *et al.,* 2006 and Woof 2007). The J chain also results in additional features, such as high valency of antigen-binding sites, allowing them to agglutinate bacteria and creating a high affinity for the polymeric immunoglobulin receptor (pIgR) that is responsible for the trans-epithelial transport of IgA and IgM into mucosal secretions.

2.5 CONCLUSIONS

This study demonstrated that IgA and, to a lesser extent, IgM were among the components responsible in either clustering fat globules or agglutinating *C. tyrobutyricum* to fat globules during the natural creaming of milk. IgG was shown to have any implication in these interactions. *C. tyrobutyricum* showed to have anti-bovine IgA wall proteins.

Immunoglobulins can be concentrated from colostrum or milk prior to their addition to GP cheese milk with the aim of improving the desporification of milk by natural creaming.

3. Chapter 3: Behaviour of *Clostridium tyrobutyricum* during Grana Padano cheese making

3.1 INTRODUCTION

Hard cheeses are susceptible to defects that may develop during the prolonged ripening, as a consequence of the growth of gas-producing Clostridia, gram-positive, endospore-forming, anaerobic bacteria, which are responsible for the late blowing defect (LBD) in a variety of hard and extra-hard cheeses (Le Bourhis et al., 2007; Garde et al, 2015; Bermudez et al., 2016). When favourable environmental conditions occur in cheese, *Clostridium spp*. spores can germinate into vegetative cells that in turn produce acetic acid, butyric acid, carbon dioxide, and hydrogen by the fermentation of lactate, residual sugars and citric acid (Garde et al., 2012). The abundant gas causes splits and holes to form within the cheese body, generally in combination with an unpleasant flavour and consequent loss of product. Among clostridia, *C. tyrobutyricum* is considered the principal responsible for LBD in Grana Padano (GP) cheese (Coccolin et al, 2004; Bassi et al., 2015; Morandi et al., 2015, Cosentino et al., 2015). Many approaches were proposed to prevent LBD in cheese: bactofugation or microfiltration of milk (Elwell & Barbano, 2006), addition of nitrate or lysozyme (Brasca et al., 2013), addition of lactic acid bacteria (LAB) strains biologically active against gram-positive bacteria (Martinez-Cuesta et al., 2010; Gomez-Torres et al., 2014) or addition of jenny milk considering its high content of lysozyme (Cosentino et al., 2013; Galassi et al., 2012). However, all these methods have technical or legal limitations (Avila et al. 2015). Currently, addition of lysozyme from hen's egg white (E1105) is the only tool authorized to prevent LBD in GP, since this cheese is registered as a Protected Designation of Origin (PDO) cheese. The consolidated GP cheesemaking is described in the product specification (http://www.granapadano.it/) and consists of five main steps: natural creaming of raw milk, in-vat cheesemaking, in-mould acidification, brine salting and ripening. The natural creaming of raw milk is carried out to lower the fat content to 2.1-2.2% and thus to standardize the fat-to-casein ratio, which is important for the unique grainy cheese texture. In addition, during the 8-10 h of natural creaming at 8-20°C, most of the bacteria, somatic cells, and spores rise together with the fat globules, and thus are removed with the cream (Bottazzi, 1971; Abo-Elnaga et al., 1981). This cleaning effect is partly achieved thanks to stable interactions occurring between fat globules and spores or vegetative cells (D'Incecco et al., 2015). During vat cheese making, milk is coagulated at 33-35°C and the curd is gradually heated up to 53-

54°C while it is cut into small granules under gentle stirring. Then stirring is stopped and the curd granules deposit at the bottom of the vat to compact under the hot whey for about 1 h. The curd is then removed from the vat and cut into two portions that are kept in molds for about 48 h. During this period, the temperature remains high for several hours in the cheese core, thus promoting the fast growth of the most thermophilic LAB species at the expenses of lactose and the consequent drop of pH to 5.2-5.3. Subsequent steps are the brine salting at 22-24 °C for 20 to 30 days and the ripening at 16-18°C and 85% relative humidity for a minimum of 9 months. During the ripening period, the cheese pH value slowly increases up to 6 and the following phenomena take place: (i) loss of moisture, (ii) breakdown of casein and consequent accumulation of peptides and free amino acids, (iii) lipolysis and (iv) depletion of glucidic sources available for microbial growth (Pellegrino et al., 2015).

Although it was demonstrated that the spores of *C. tyrobutyricum* remaining in cheese milk after creaming are able to survive the cheese making process, nowadays no information is available on the behaviour of vegetative cells. Also, the official method for enumerating *Clostridium* spp. endospores by the most probable number (MPN) involves a preliminary heat treatment of the sample to destroy vegetative cells. The aim of this research work was to investigate the morphological, physiological and metabolic changes induced to *C. tyrobutyricum* by the cheese making conditions of GP. Using a new experimental approach, both vegetative cells and spores of *C. tyrobutyricum* were separately submitted to the whole cheese making and sampled at the most crucial steps including the cheese ripening. Their behaviour was thus investigated and tentatively interpreted by combining the information obtained using microscopy techniques (SEM and TEM) with microbiological and chemical data.

3.2. MATERIAL AND METHODS

3.2.1 Production of bacterial cell and spore suspension

C. tyrobutyricum strain UC7086, previously isolated from a cheese with LDB and part of the Università Cattolica del Sacro Cuore culture collection, was used for the experimental cheese manufacture. The strain was cultured in Reinforced Clostridial Medium (RCM) (Oxoid, UK) with 50% (w/w) sodium lactate syrup (Merck, Germany) added to reach a final concentration of 2.8% (w/v) and incubated at 37°C in anaerobic chamber (Don Whitley Scientific, Shipley, UK). Spore suspensions of C. tyrobutyricum UC7086 were prepared modifying the biphasic method of Cerf et al. (1967) and according to Bassi et al. (2009). Purified spore crops were then plate counted and finally stored at 4°C until use.

3.2.2 Experimental cheese manufacturing and sampling steps

A dedicated cheese manufacture was carried out at a GP dairy using the usual process conditions described in a previous paper (D'Incecco et al., 2016) and without addition of lysozyme. Two vats (1000 L milk each) were worked in parallel to obtain a total of four cheeses. Aliquots (10 mL) of pure cell culture of *C. tyrobutyricum* UC7086 in whey and of spore suspension in water, both at the final concentration of 10^8 CFU/mL, were separately put into dialysis tubes (100,000 Da) that were carefully sealed and differently labelled by colour bands to allow further identification. Eight cell-containing tubes (C-tubes) and eight spore-containing tubes (S-tubes) were kept suspended into each vat during the whole cheese making. After curd cutting and cooking, the stirring was interrupted and the tubes were pushed at the bottom of the vat where the curd grains were compacting. Overall, one C-tube and one S-tube were taken at different steps of the cheese manufacturing process (Fig. 3.1): rennet addition (RE), end of curd cooking (54°C) (EC), curd extraction from the vat (CX), end of curd acidification in mold (24 h after extraction) (EA), end of brine salting (ES), after 3-month (3C) and 6-month (6C) ripening. All tubes, including the control (untreated), were processed in the same way after their sampling from either milk or cheese. Briefly, the tube content was carefully recovered and divided into four portions. One portion was subjected to plate counts for *C. tyrobutyricum* enumeration, one was used for scanning electron microscopy (SEM), one was included in resin for transmission electron microscopy (TEM), and one was analysed by ion exchange chromatography to evaluate the free amino acid pattern (FAA).

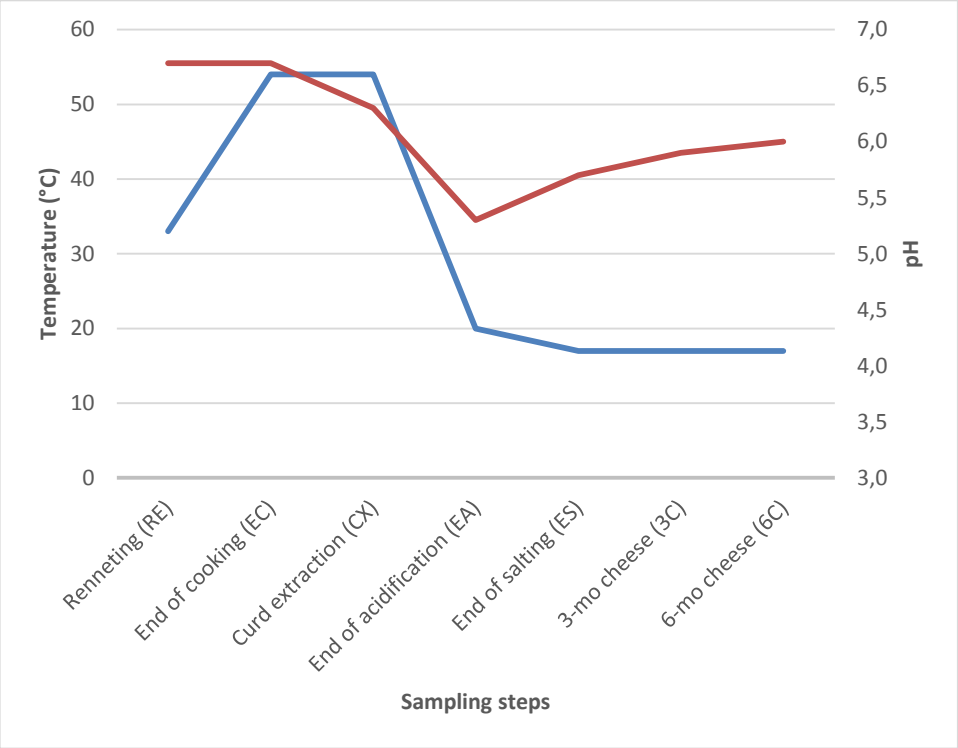

Figure 3.1. Trends of temperature and pH value during Grana Padano cheese making and subsequent ripening.

3.2.3 Plate counts

Each sampling of dialysis tubes content during the cheese making process was processed for *C. tyrobutyricum* cells and spores quantification by plate count analysis. RCM agar medium (Oxoid Ltd., Wade Road, Basingstake, Harnpshire, Engl.) with the addition of 0.005% of neutral red solution and 200 ppm of D-cycloserine (Jonsson et al., 1989) was used for selectively enumerating yellow (UV-light fluorescent) colonies of *C. tyrobutyricum* vegetative cells. *C. tyrobutyricum* spores were estimated either on plates of RCM with neutral red and D-cycloserine after a pasteurization treatment of 10 minutes at 80°C. All plates were prepared and incubated at 37 °C in anaerobic conditions.

3.2.4 Scanning electron microscopy

Samples for SEM were prepared as follows: 1 ml of each tube cellular pellet was centrifuged, concentrated in a smaller volume of physiological solution and 5 µl fixed on a positively charged nylon membrane (Roche Diagnostics GmbH Germany). These membranes were then

dehydrated stepwise in ethanol 75%, 85%, 95% and 100% for 1 h each at room temperature. Critical point drying was performed in a Baltec CPD030 dryer. Specimens were coated with gold for electrical conductivity by sputtering (Balzer Union Med 010) and analysed with a Quanta SEM microscope ESEMTM technology (FEI, Oregon, USA) under both low and high vacuum SEM conditions: high vacuum 7x10-5 Pa, and low vacuum 130 Pa.

3.2.5 Transmission Electron Microscopy

The portion of tube pellet was immediately fixed with 1 mL of fixative solution (glutaraldehyde 1%, paraformaldehyde 3% in cacodylate buffer, w/v). The mixture was kept for 2 h at 8°C and then mixed with 1 mL of melted (35–40°C) low-temperature gelling agarose (2% in water). The suspension was layered onto a microscope slide before it gelled, allowed to set, and then cut into 1-mm3 cubes. Cubes were further fixed in the same fixative solution as above for 30 min at 4°C, and then washed with cacodylate buffer for 1 h and post-fixed in osmium tetroxide (1% in cacodylate buffer) for 2 h. Dehydration was carried out in an ethanol series, and then samples were embedded in Spurr resin and cured at 60 °C for 24 h. Ultrathin sections, 50 to 60 nm thick, were stained with uranyl acetate and lead citrate and examined with a Philips E208 transmission electron microscope (Aachen, Germany).

3.2.6 Free Amino Acid analysis by ion exchange chromatography

The pattern of free amino acids (FAA) was determined using the method described by Masotti et al. (2010). Briefly, the solid samples (curd, cheese) were grinded, solubilized with sodium citrate, homogenized and deproteinized with sulphosalicilic acid. The obtained extracts as well as the liquid samples (milk, supernatant of tube material, culture media) were diluted (1:1) with lithium citrate buffer at pH 2.2, filtered and analysed by ion exchange chromatography. A Biochrom 30plus (Biochrom Ltd, Cambridge, UK) amino acid analyser was used and operated under the conditions provided by the manufacturer for the chromatographic separation. These imply an eight-step elution program with lithium citrate buffers of increasing pH and ionic strength, post-column derivatisation with ninhydrin, and detection at 440 and 570 nm. The quantification was carried out using four-level calibration lines of the 21 amino acids (all from Sigma Aldrich) solutions in the range 0.75-22.5 mg/L and using norleucine (Sigma Aldrich) as an internal standard. Repeatability values of ISO Standard 13903:2005 were fulfilled.

3.2.7 *C. tyrobutyricum* cell growth in model cheese and milk

A cell culture of *C. tyrobutyricum* UC7086 at logarithmic phase and with a concentration of 1.2 x 102 CFU/mL was anaerobically inoculated (10%) in two tubes containing 20 mL of (a) sterilized milk, and (b) sterilized milk added with both arginine and lactate at the final concentrations of 0.5 g/L and 28 g/L, respectively. After 10 days of incubation at 37 °C in anaerobic chamber, samples were processed for both the total bacterial count and FAA analysis as above described. Similarly, cheese environment was modelled using a 3-month ripened cheese not containing lysozyme. A set of six 25-ml tubes, each containing 5 g of grated cheese, were kept for 24h at 4°C in anaerobic bags equipped with Anaerocult A packs (Merck, Germany) to remove oxygen. Three of the tubes were anaerobically inoculated with 0.2 mL of a cell culture of C. tyrobutyricum UC7086 at logarithmic phase and with a concentration of 3.8 x 106 CFU/mL, while the other three tubes were used as negative control samples. All tubes were incubated at 37 °C in anaerobic chamber and a test and a control tube were taken at 0, 2, 7 and 14 days. Cheese samples from the tubes were processed for plate counts of clostridia cells and spores and for FAA analysis as above described.

3.3 RESULTS AND DISCUSSION

With the aim of studying *C. tyrobutyricum* behaviour during the whole cheese manufacturing process, we have set up an innovative experimental approach. Vegetative cells and spores of *C. tyrobutyricum* were separately confined into dialysis tubes that were kept immersed into the milk during the whole vat processing and then included into the cheese curd to undergo the subsequent steps of acidification, brining and ripening. By this way, at each of the selected sampling steps, it was possible to take both cells and spores having been continuously and directly in contact with the changing environment (milk, curd, cheese) outside the tubes and having undergone the whole sequence of the technological conditions in a real cheese making. The selected sampling steps were: renneting (RE), end of cooking (EC), curd extraction (CX), end of acidification (EA), end of brining (ES), 3-month aged cheese (3C) and 6-month aged cheese (6C).

3.3.1 *C. tyrobutyricum* counts in tubes sampled during cheese manufacture

To distinguish between cell and spore amounts, pellets were preliminarily pasteurized. The initial concentration of *C. tyrobutyricum* vegetative cell (C-tubes) and spore (S-tubes) solutions in the tubes were 10^8 cfu/mL. At milk renneting, vegetative cells within the C-tube showed a -log decimal decrease (from 10^8 to 10^7 cfu/mL) that can be associated to a physiological drop-off of cell vitality in the passage from laboratory to plant-scale. During curd cooking (EC), when the process reaches the highest temperature of 54°C, vegetative cells further decreased to 8 x 10^5 cfu/mL and disappeared in the curd at the extraction, i.e. after 40 min of compacting in the hot whey. No cultivable cells were found in C-tubes at the next sampling steps, suggesting the high temperature attained during vat processing to be lethal for *C. tyrobutyricum* vegetative cells. Nevertheless, some vegetative cells seemed to sporulate since few spores (around 200 cfu/mL) were detectable starting from the end of that step (Fig. 3.2). The activation of sporulation might be mediated by the lack of specific nutrients or by oxygen intake during the cutting of the curd under continuous stirring. A one-log increase in spore numbers was then observed in the 3-month old cheese; due to the lack of sampling in the time interval between the end of brining and the 3rd month of ripening, we supposed that, during this period, *C. tyrobutyricum* spores could germinate, reproduce and sporulate in a new cell-cycle. Anyway, these processes are very difficult to separate from each other with lab-techniques, since they are part of the asynchronous life cycle of

sporulating bacteria. The same spore number was found in the C-tube taken from the 6-month old cheese.

Spore numbers in the S-tubes remained almost unchanged until end of salting. At the end of curd cooking (EC) and at the end of curd acidification (EA), however, spore numbers were slightly lower due to possible germination onset, likely stimulated by heating, in the first case, and by the drop of pH value (5.3) in the second one (Fig. 3.3). Low pH represents a favourable condition for spores. A two-log decrease in spore counts was observed in S-tubes taken from cheese at 3 months of ripening, when values reached 10^6 UFC/ml, suggesting a deeper germination rate in this phase. Despite these changes, very few vegetative cells (90-95 CFU/ml) were cultivable in the S-tube, with a slight increase observed in the curd at the extraction (CX) and a small decrease at the end of brining (Fig. 3.3). We supposed that only a small portion of vegetative cells was able to outgrow during the curd cooling from 54 °C (curd extraction) to 20 °C (end of acidification) even if growth temperature has been demonstrated to be strain-dependent for *C. tyrobutyricum* (Ruusunen et al., 2012). In this step the cheese also undergoes acidification (pH drops from 6.3 to 5.2) which is faster in the core with respect to the outer zones (Pellegrino et al., 1997); cell growth could be influenced by this aspect depending on the tube location within the cheese.

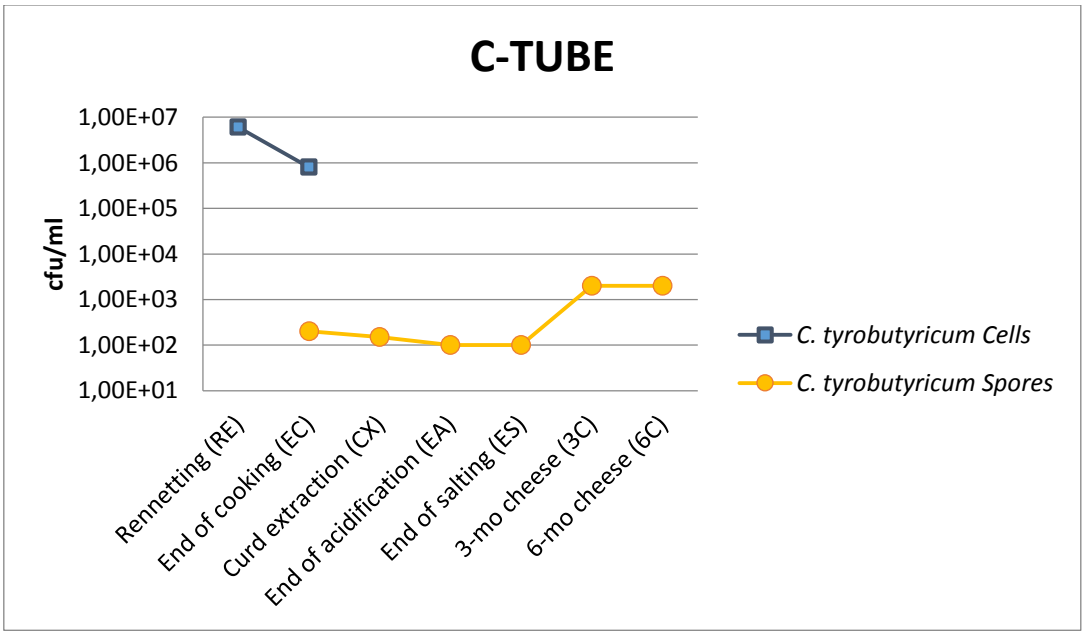

Figure 3.2. Evolution of cell and spore concentrations within the C-tube throughout the cheese manufacturing and ripening process.

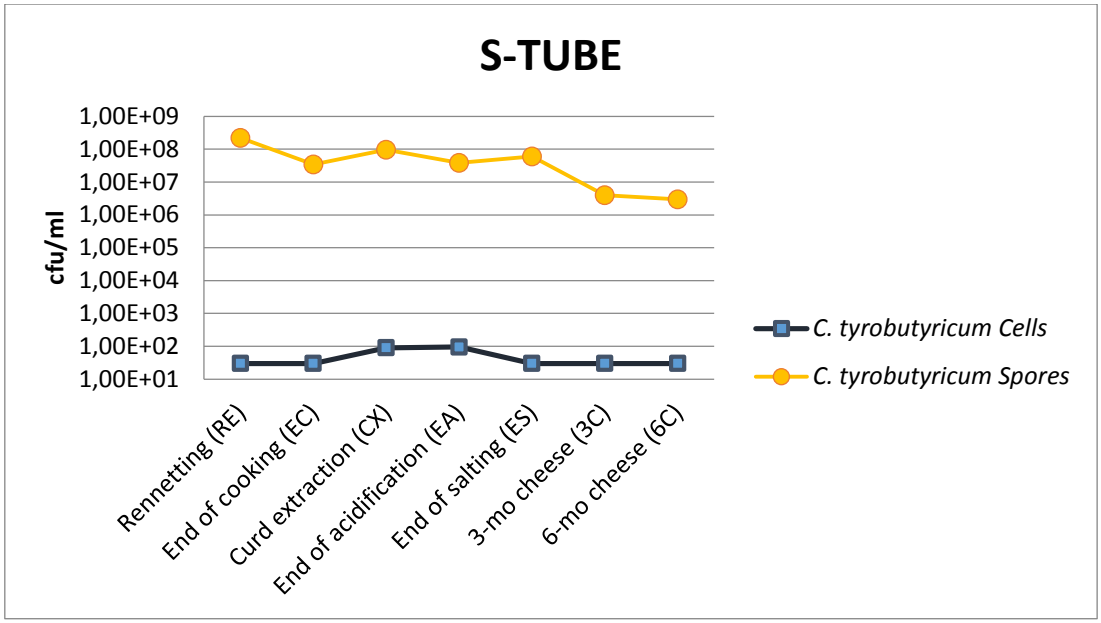

Figure 3.3. Evolution of cell and spore concentrations within the S-tube throughout the cheese manufacturing and ripening process.

3.3.2 Scanning and Transmission Electron Microscopy of tubes sampled during cheese manufacture

Both SEM and TEM were used to monitor morphological changes of *C. tyrobutyricum* cells and spores throughout the whole cheese making process.

SEM analysis of the C-tube pellet gave overlapping results with data obtained with microbiological methods. At renneting (RE), only *Clostridium* vegetative cells were detected (Fig. 3.4 a) whereas some spores began to be visible at the end of cooking (Fig. 3.4 b) reflecting the 2-log spore counts found at this step. At the curd extraction step, cells were almost lysed and few spores were visible and detectable (Fig. 3.4 c). The sample preparation for microscopy analysis was more difficult for the tubes taken from the cheese since these were completely dry and the collected pellets had to be hydrated before observation. At the end of acidification and after brining, we supposed to observe only dead cells and some dormant spores (not shown).

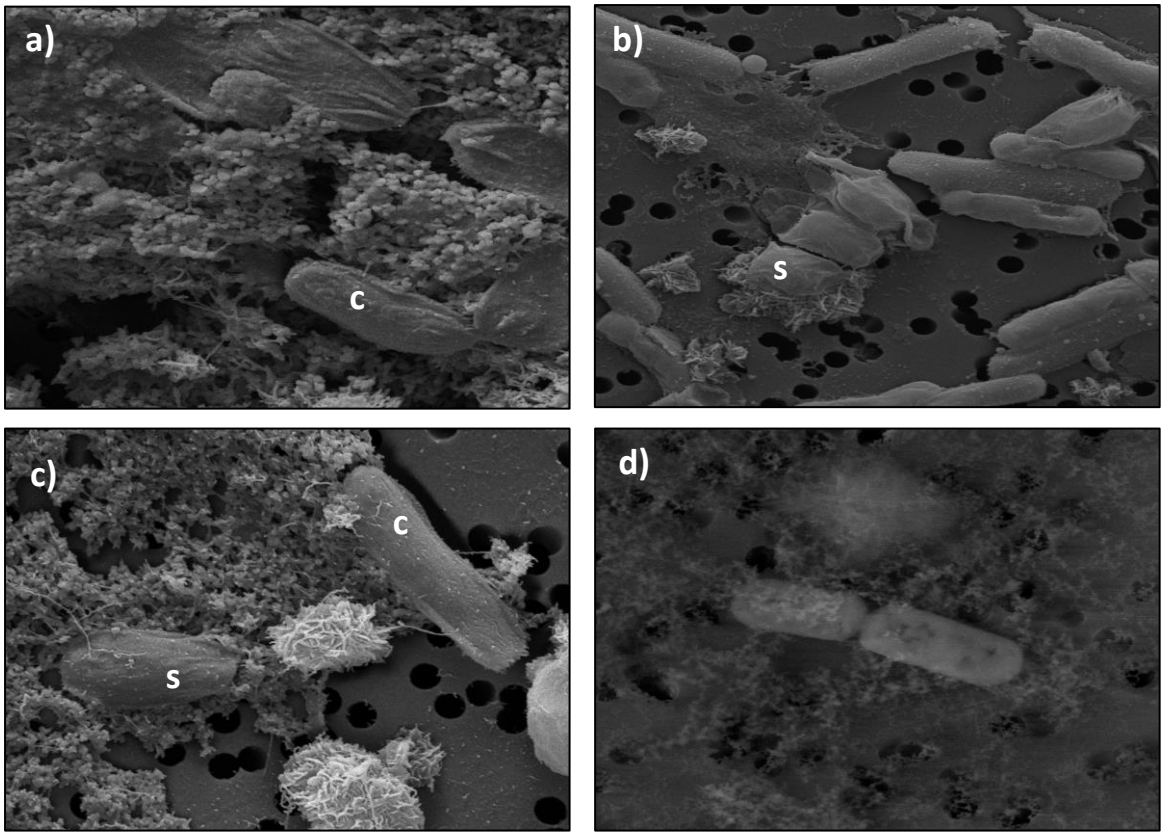

Figure. 3.4. SEM analysis of C-tube content at the different steps of GP cheese making: a) renneting; b) end of curd cooking (54°C); c) curd extraction; d) end of curd acidification.

The S-tube taken at RE contained only spores (Fig. 3.5 a); these spores appeared to change their basal morphology slightly and this behaviour is similarly observed also at the end of cooking (Fig. 3.5 b). It's only at the curd extraction and at the end of acidification that some vegetative cells appear (Fig. 3.5 c, d). The brining phase showed no evident modification with a mixed situation that showed faint cells in autolysis together with spores.

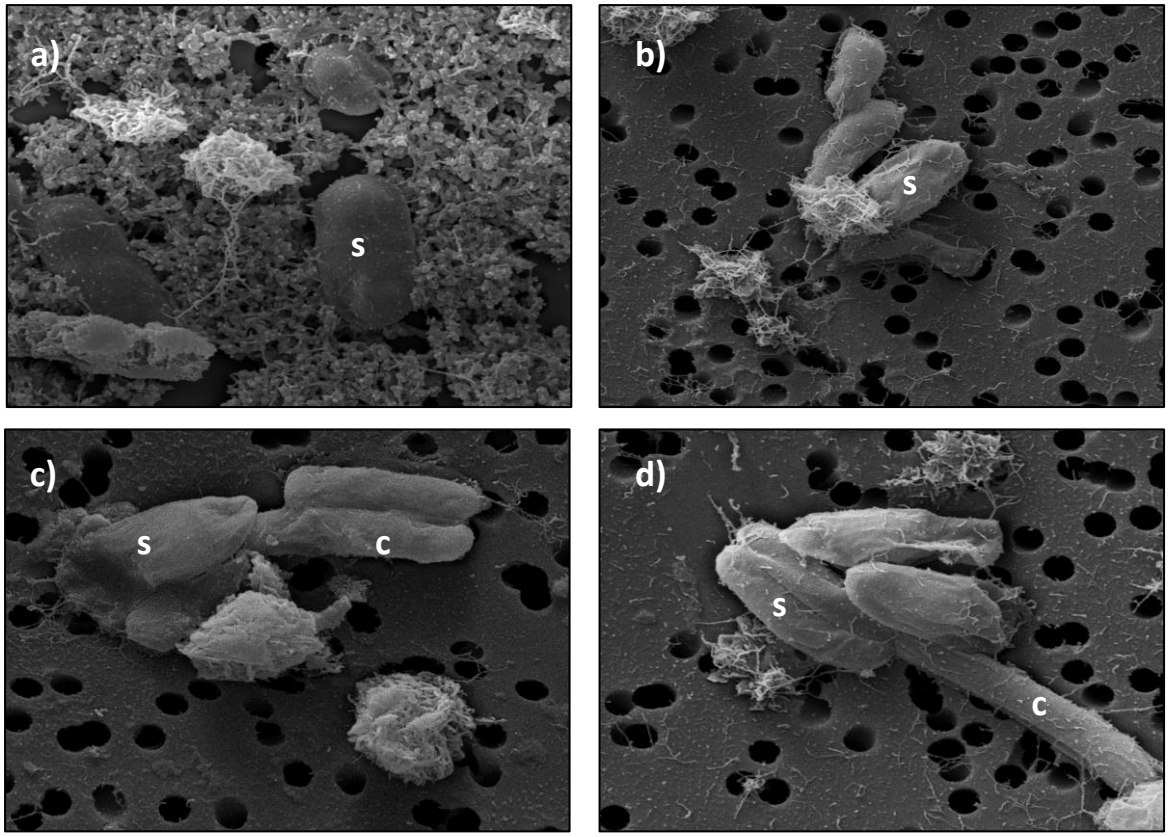

Fig. 3.5 SEM analysis S-tube content at the different steps of GP cheese making: a) renneting; b) end of curd cooking (54°C); c) curd extraction; d) end of curd acidification.

TEM analysis of tube pellets was performed in parallel with SEM. C-tube images showed the presence of intact vegetative cells until renneting, whereas some damaged vegetative cells were observed at the end of curd cooking, consistently with SEM and plate count evidences (not shown). Interesting morphological changes of the cells appeared at the curd extraction, that is after 2 hours at 54-55°C from the previous sampling and when the pH has dropped down to 5.6. In particular, a black spot (Fig. 3.6 a-c, arrows) was observed inside most of the cells and some spores were also detected. In the curd that had slowly cooled down and acidified (pH 5.3), cells showed to be further changed since the black spot was often surrounded by an organized oval structure (Fig. 3.6 d-f). Starting from the outside inwards, the structure consists of a 10 nm thick wall that encloses around a hundred of circular organelles, a thin wall and the black spot in the middle (Fig. 3.6 f). The black spot looks denser with respect to the surrounding organelle matrix, probably due to a lower water content. At the end of salting, that is 18 days later, cells appeared evidently damaged and spores were still present. Even after 6 months of ripening, when the sampling was rather tricky, spores were observed in cheese together with damaged vegetative cells (not shown).

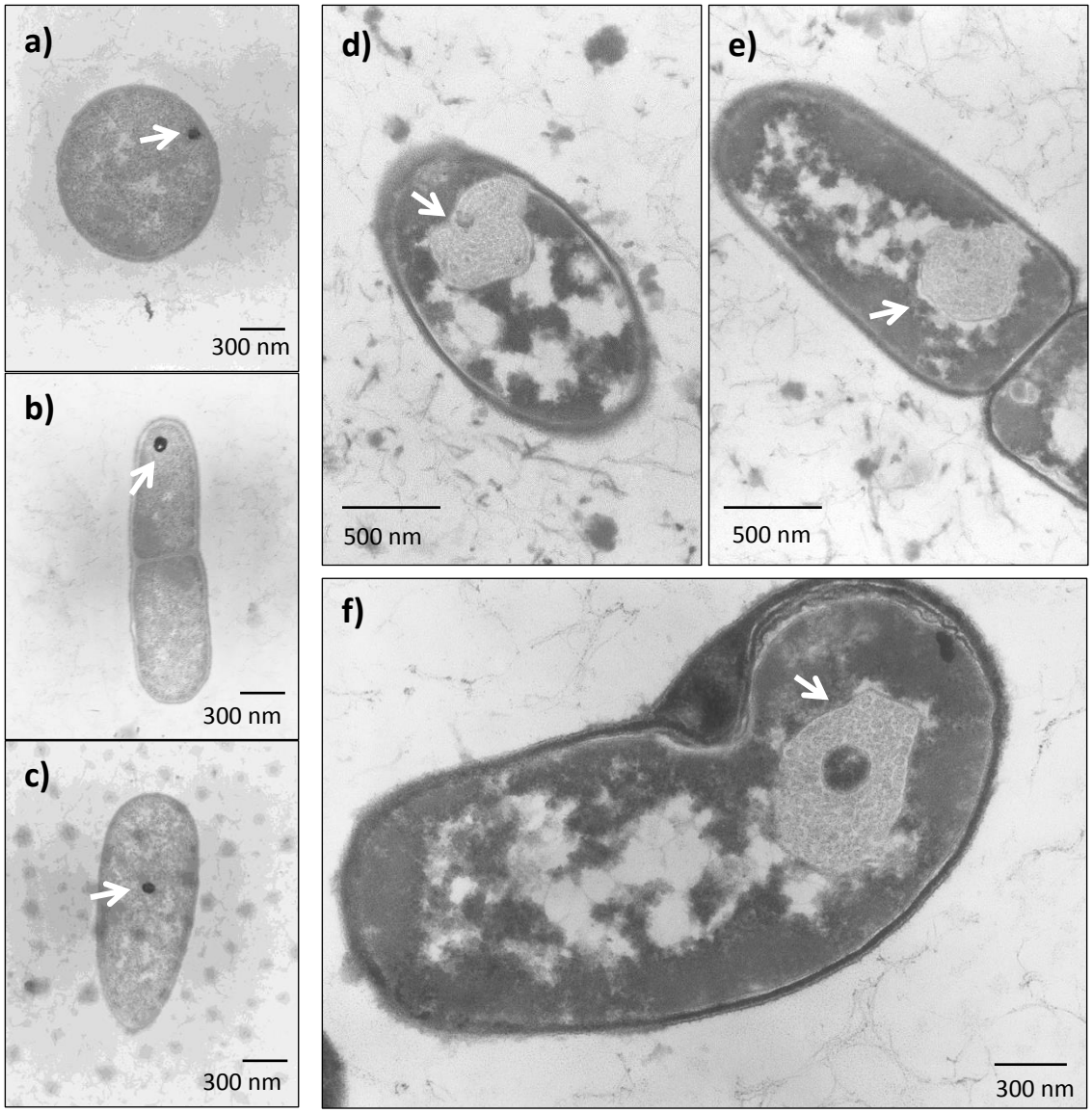

Fig. 3.6 TEM micrographs of C-tube content at the different steps of GP cheese making process; a-c) curd extraction; d-f) acidified curd.

Spores within S-tubes looked the same until curd extraction. The typical dormant spore structure was observed, well organized in exosporium, coat, cortex, inner membrane and core, as reported by others studies (Bassi et al., 2009; Brunt et al., 2015). Some spores changed their internal structure in the acidified curd (Fig. 3.7 c), probably due to the germination phase, as confirmed by the plate count and SEM analysis. These spores appeared to have a core increased in size and a smaller exosporium with respect to the dormant spores that however were still present (Fig. 3.7 a-c).

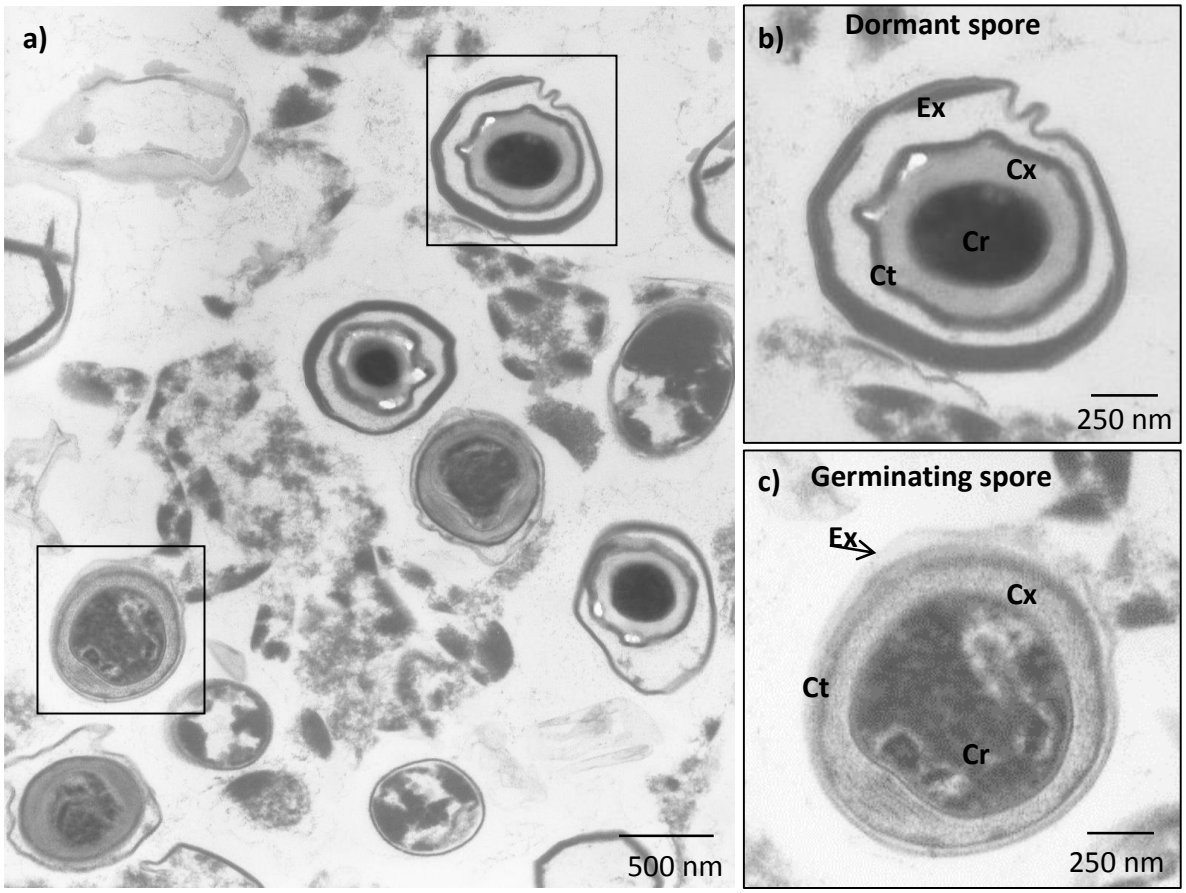

Fig. 3.7 TEM micrographs of S-tube content at acidified curd step of GP cheese making. Black frames in panel "a)" are shown with higher magnification in panels "b" and "c", where ultra-structural details are tagged: (Ex) exosporium; (Ct) coat; (Cx) cortex and (Cr) core.

After core hydration, the stage II of the spore germination was reported to involve the core expansion (Setlow, 2003; Brunt et al., 2015). At the end of brine salting, cells appeared to be deeply damaged (not shown), like those observed in the cheese after 6 months of ripening (Fig. 3.8), when spores always lacked of exosporium and the dense core was easily observed.

Fig. 3.8. TEM micrograph of S-tube content at six months of ripening when both (C) cells and (S) spores were observed.

Two main events were observed through our samplings: (i) the vegetative cells sporulation during the vat processing and (ii) the spore germination at the end of curd acidification. The vegetative cell sporulation was likely trigged by the absence of nutrients and the presence of oxygen. Instead, beside of requiring favourable environmental conditions, the germination process is known to be trigged by numerous molecules, the so-called germinants (Moir et al 2002; Setlow, 2003). In our case, lactic acid could be among the germinants responsible for the spore activation, since it is available after the curd extraction (Pellegrino and Resmini, 2001). Bassi et al. (2009) and Brunt et al., (2015) reported that a solution of lactate/alanine had a germinant effect toward spores of both *C. tyrobutyricum* and *C. sporogenes*. As reported by Pellegrino et al. (2007), within the moulded GP cheese, there is a combined presence of high temperature (52-56°C for 10 h at least) and low pH (5.0-5.3) which is able to inactivate several enzymes. This combination could be recognized by the spores as a suitable condition for growth. Heath treatments are known to enhance the spore germination (Keynan and Evenchick, 1969; Brunt et al., 2015) and activation is the term used to indicate germination enhancement (Foster and Johnstone, 1990). However, the biochemical mechanisms behind these phenomena have not been clarified yet.

3.3.3 Free amino acid patterns

The pattern of the FAA was determined within the C- and S-tubes as well as in the matrices (milk, whey, cheese) outside them to have information on FAA utilization by *C. tyrobutyricum* in the selected steps of cheese making. In a preliminary test, we assessed that the FAA could move freely through the dialysis membrane both directions (not shown), confirming that the chosen membrane represented a suitable tool to keep the bacterium confined without affecting exchange of solutes, namely FAA. Nevertheless, in view of comparing the FAA levels detected within the tubes with those in the different matrices outside them, the relative values were necessarily considered.

In a recent study, Pellegrino *et al*. (2015) showed that the initial FAA content of the milk, i.e. 80-100 mg/L, increased by 5-10% throughout the vat processing of GP cheese. In agreement with this observation, no changes occurred until milk renneting and coagulation (not shown). At the curd extraction from the vat, the contents of individual FAA within C- and S-tubes were not significantly different from each other and from that of the whey just drained off (Table 3.1). It is worth noting, however, the higher content of γ-amino butyric acid (GABA) we found within both C- and S-tubes with respect to the whey. Formation of this non-protein amino acid was undoubtedly due to vegetative cells of *C. tyrobutyricum* and was so fast at the sampling moment that the equilibrium with the outside environment (whey) was not reached.

It is known that production of GABA, catalysed by the glutamate decarboxylase, represents a common way to contrast acidic conditions for several bacterial species (Ueno, 2000; Brasca et al., 2016). Therefore, we can argue its production to be related to the stressing conditions, including initial acidification (Fig. 3.1), that have also brought to *Cl. tyrobutyricum* sporulation observed at the end of curd cooking (Fig. 3.2). The amount of GABA was significantly lower in the subsequent steps in spite of the large availability of glutamate. For other few FAA (Val, Leu, Tyr, Arg) the content was slightly lower within the tubes, as it will be further discussed.

The four subsequent sampling steps implied the removal of tubes from the cheese. Therefore, one out the four produced cheeses was cut at a time and, besides the tubes, two cheese portions (1-cm thick) were also taken around them: z1, in contact with the tube, and z2, surrounding z1. The FAA level in these two portions allowed us to highlight the possible presence of a concentration gradient indicating a movement of the individual FAA either inwards or outwards the tube. The whole cheese was sampled as well and considered as a reference. Data were not different between the cheese portions z1 and z2 taken around either

C- or S-tubes respectively, therefore mean values of the two are presented (Tab. 3.1). No relevant differences were observed in the FAA levels between C- and S-tubes at any sampling step, in accordance with the lack of an extensive cell growth. Furthermore, none of the FAA was depleted, indicating that availability of FAA was not a limiting factor for cell growth itself. This observation is supported by findings of Storari et al., (2016), who have recently reconstructed the presence of genes putatively involved in the biosynthesis of 19 amino acids in the genomes of four *C. tyrobutyricum* strains isolated from hard and semi-hard cheeses, including UC7086 used in this study. For a few FAA however, a systematic difference was observed between the content in the C- and S-tubes. Among these, alanine had an interesting behaviour because its content was always lower in the S-tubes. As already mentioned, this amino acid in combination with lactate has been reported to be a germinant of *C. tyrobutyricum* spores (Bassi et al., 2009). However, probably more FAA can have this role depending on strain and environmental conditions (Storari et al., 2016), supporting the need of further investigation.

The most relevant impact of the presence of *C. tyrobutyricum* in cheese involved arginine (Table 3.1). Arginine content progressively decreased within the both the tubes during cheese ripening and was depleted in 6-month ripened cheese. The utilization of arginine within the tubes was confirmed by the decreasing concentration observed from z2 to z1 cheese portions indicating the slow permeation of the amino acid into the tube itself to re-establish the equilibrium. The opposite behaviour was observed for citrulline and ornithine (Table 3.1). In fact, these two non-protein amino acids form by the degradation of arginine through the arginine deimidase (ADI) pathway (Zúñiga et al., 2002). Partial deamidation of arginine to citrulline and, to a lower extent, to ornithine also occurred in the samples representing the whole cheese at the various sampling steps (Table 3.1). This is in fact the usual pattern we observed in GP cheese as a result of the metabolism of selected non starter LAB (D'Incecco et al., 2016). The ADI pathway is adopted by a variety of microorganisms to contrast acid stress and, in the step leading to ornithine, also to produce ATP (Zúñiga et al., 2002).

Cheeses contaminated with *C. tyrobutyricum* and developing the late blowing defect were reported to have higher pH than the control cheeses as a consequence of lactate consumption (Le Bourhis et al. 2007). However, to our knowledge no literature data concerning the adoption of direct mechanisms to obtain the deacidification of the environment is available for *C. tyrobutyricum*.

Sampling	Sample name	Asp	Thr	Ser	Asn	Glu	Gln	Gly	Ala	Cit	Val	Met	Ile	Leu	Tyr	Phe	Gaba	Orn	Lys	His	Arg	Pro
Curd at the	Cell tube	3,01	3,48	2,53	0,78	43,30	2,67	8,07	6,04	0,42	1,43	0,30	1,51	1,90	1,12	0,84	6,78	0,51	5,30	0,84	3,46	5,74
extraction	Spore tube	3,00	3,38	2,53	0,63	42,75	3,20	8,28	5,70	0,48	1,41	0,15	1,68	1,74	1,03	0,53	7,25	0,41	5,15	0,98	3,23	6,03
	Whey	3,22	3,30	2,38	0,55	40,16	3,18	7,57	5,91	0,93	4,28	0,25	1,74	2,43	1,67	0,80	2,21	0,59	5,65	0,65	4,48	6,64
Cheese after	Cell tube	2,15	1,83	4,32	1,47	9,96	7,77	3,43	11,10	0,00	2,03	1,11	3,37	7,20	2,28	2,04	2,28	0,05	13,71	4,14	7,39	11,90
24 h moulding	Spore tube	2,19	1,84	4,04	1,54	10,33	7,95	3,45	10,64	0,00	2,06	1,10	3,48	7,52	2,41	2,19	2,02	0,03	13,18	4,34	7,76	11,50
	z1	2,26	2,70	3,73	2,99	10,00	6,55	1,83	10,77	0,00	5,03	1,65	3,51	8,30	3,96	3,23	0,58	0,00	13,06	3,41	7,70	8,76
	z2	2,22	2,69	3,33	2,82	9,87	6,91	2,24	10,89	0,00	5,53	2,03	3,05	8,23	3,46	3,12	0,00	0,00	14,34	3,41	7,17	8,98
	Whole cheese	2,62	2,58	3,50	2,30	10,83	6,38	2,28	9,73	0,00	5,74	1,98	3,12	7,86	3,21	3,23	0,00	0,00	13,90	3,04	7,22	8,47
Cheese	Cell tube	2,80	2,54	4,34	3,55	13,03	11,16	2,36	5,89	0,05	6,61	2,21	4,14	8,43	2,38	2,57	0,62	0,22	9,88	2,76	4,58	10,41
after brining	Spore tube	2,43	2,36	4,73	3,53	13,78	11,39	2,13	4,30	0,07	6,78	1,87	3,73	9,64	2,06	2,56	0,82	0,29	10,28	2,08	4,27	10,39
	z1	2,18	3,32	3,48	4,10	13,55	7,94	1,86	4,75	0,00	6,20	2,03	4,16	9,16	2,59	3,00	0,00	0,36	12,54	3,64	5,41	8,72
	z2	2,25	3,39	3,37	3,92	13,42	7,24	1,85	4,86	0,00	6,03	2,28	4,27	9,35	2,90	3,46	0,00	0,20	12,76	3,53	5,68	8,70
	Whole cheese	2,35	2,88	3,29	4,31	12,44	5,78	2,44	4,43	0,00	6,32	1,90	4,45	9,92	3,10	4,02	0,00	0,00	11,78	3,25	7,75	7,50
Cheese	Cell tube	3,67	2,22	1,12	4,01	17,56	7,08	2,38	5,33	1,06	5,13	2,08	5,24	8,94	1,08	4,58	0,44	1,56	11,67	2,13	1,23	10,37
after 3 months	Spore tube	3,54	2,18	1,56	4,27	18,51	6,57	2,63	4,06	1,02	4,92	1,99	5,17	9,05	0,99	4,36	0,68	1,53	11,62	2,24	1,28	10,63
ripening	z1	2,09	2,13	1,84	4,72	16,88	5,00	2,65	3,94	0,96	7,54	2,35	4,58	10,28	1,30	4,95	0,00	2,47	12,25	4,20	1,74	9,73
	z2	1,60	2,20	2,42	4,95	15,60	5,78	2,32	3,24	0,00	7,05	2,16	4,08	10,88	2,60	4,76	0,00	0,22	11,45	3,98	6,32	8,64
	Whole cheese	1,88	3,07	3,09	4,40	15,94	5,80	2,21	2,92	0,00	7,08	2,22	4,85	9,20	2,71	4,67	0,00	0,14	11,63	3,81	5,45	8,95
Cheese	Cell tube	5,88	1,91	1,78	2,87	22,59	2,79	3,08	4,48	2,25	2,99	1,89	6,77	9,80	0,40	4,28	0,29	1,60	12,61	1,38	0,00	10,56
after 6 months	Spore tube	5,08	2,14	2,00	3,16	22,82	2,84	2,82	3,60	2,36	2,88	1,91	6,67	9,30	0,68	4,41	0,58	1,61	12,36	1,25	0,00	10,87
ripening	z1	2,83	2,18	1,27	3,11	19,79	3,26	2,41	3,55	1,28	8,73	2,15	5,20	10,53	2,61	5,89	0,06	2,23	13,00	2,14	0,27	8,21
	z2	2,39	2,05	1,42	4,13	18,29	2,06	2,60	3,22	0,59	8,13	2,24	4,69	10,83	2,78	5,59	0,00	0,50	11,43	3,54	4,14	9,37
	Whole cheese	2,45	3,06	3,81	4,21	17,87	2,48	2,24	2,61	1,27	7,62	2,25	5,12	9,34	2,96	4,76	0,00	0,19	11,42	3,10	3,41	9,72

Table 3.1. Concentration of FAAs (g/100 g FAA) throughout GP cheese making and ripening. Depending on the sampling step, analysed samples are: cell and spore tube contents; the whey taken at curd extraction; the cheese portion (z1) in contact with the tube; the cheese portion (z2) surrounding z1; a portion representing the whole cheese.

3.3.4 Model milk and cheese trials

In order to shed more light on the adoption of the deacidification mechanisms by vegetative cells of *C. tyrobutyricum*, two simple model systems were set up reproducing milk and cheese environment respectively and vegetative cells of UC7086 were inoculated at the exponential growth phase. In the inoculated sterilized milk (control), where no acidification took place and counts only increased by one log after 10 h of incubation, the arginine content and trace levels of citrulline and ornithine remained unchanged (Fig. 3.9). When lactate was added and the content of arginine was 10 fold increased, counts reached 6.5 log and approximately 30% of arginine was deaminated to citrulline and ornithine (Fig 3.9).

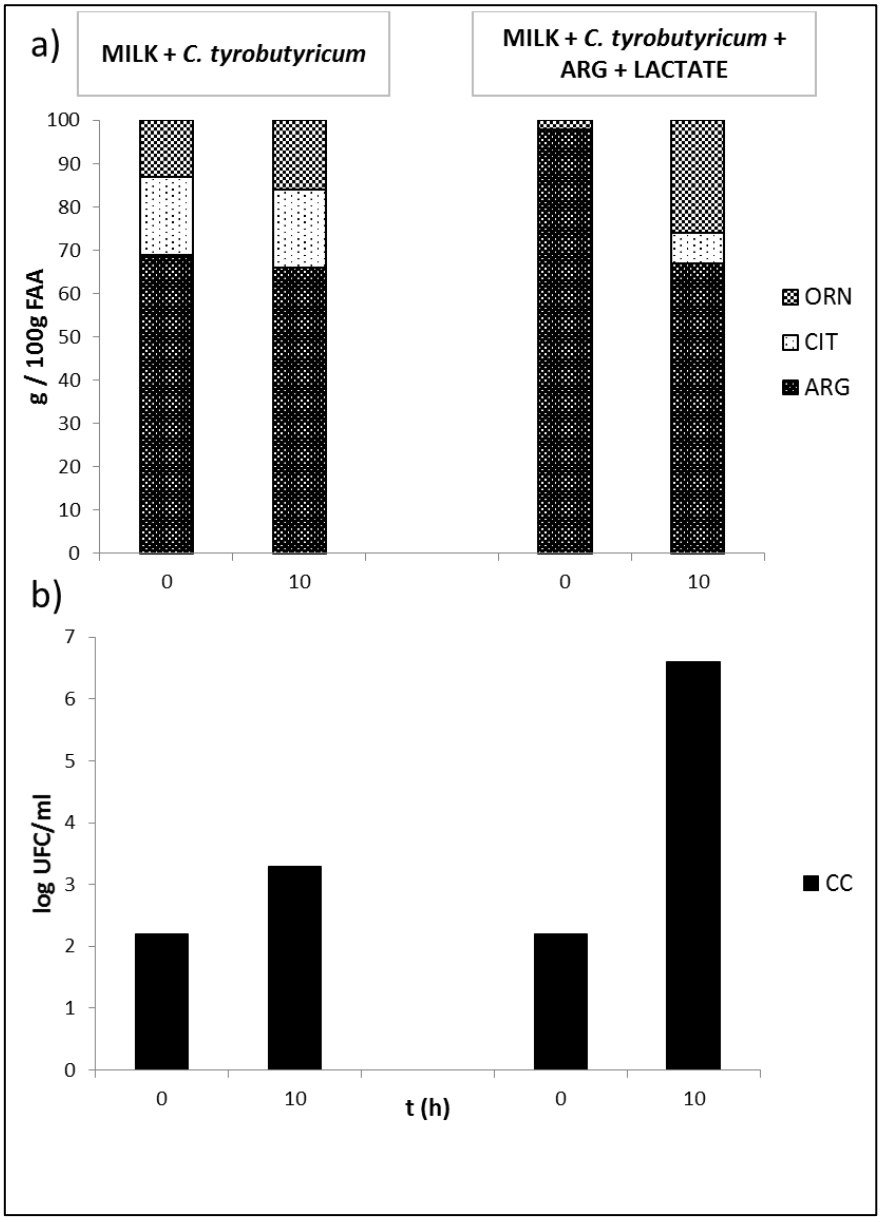

Fig 3.9. Degradation of free arginine (a) by *C. tyrobutyricum* inoculated in sterilized milk and counted (b) at different incubation times.

In the model cheese, a slow degradation of arginine took place in the control sample as an expected result of activity of minor LAB species (Fig. 3.10 a). However, when *C. tyrobutyricum* was inoculated, arginine degradation was much faster and after 14 days only citrulline and ornithine were detected. Cells dead in cheese after 14 days but 4 log UFC/mL spore were counted (Fig. 3.10 b). Interestingly, in both milk and cheese model systems inoculated with *C. tyrobutyricum* no production of GABA was observed throughout the incubation periods, although glutamate was largely available (not shown). Taken together, these observations confirmed that *C. tyrobutyricum* is able to deaminate free arginine in cheese through the ADI pathway. In contrast, the ability to decarboxylate glutamate to GABA was observed only at the highly stressing temperature attained during vat processing and sporulation was observed in parallel. To our knowledge, no literature data concerning the presence of glutamate decarboxylase genes in *C. tyrobutyricum* are available and therefore this aspect needs to be further investigated.

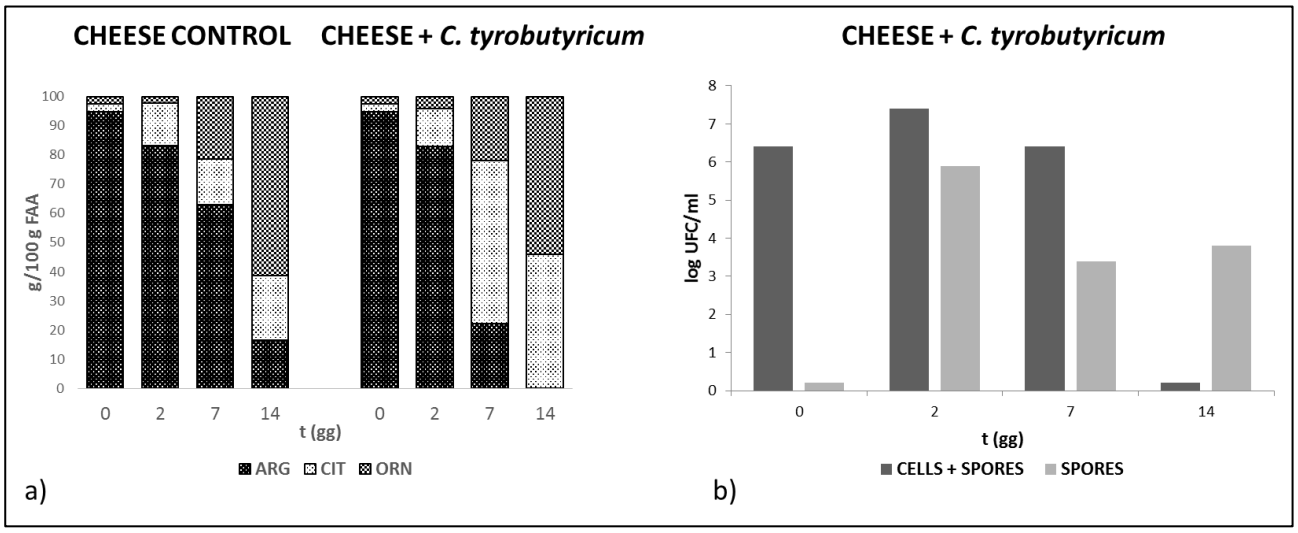

Fig. 3.10. Degradation of free arginine (a) by *C. tyrobutyricum* inoculated in model cheese and counted (b) at different incubation times.

3.5 CONCLUSIONS

In conclusion, our data showed that vegetative cells of *C. tyrobutyricum* sporulated during the vat processing, probably due to the presence of oxygen and rise of temperature. Spores germinated after the curd extraction, when the lactic acid fermentation makes lactate available. From this step on, vegetative cells were no longer cultivable, possibly because damaged during the subsequent salting. The capability of the vegetative cells to sporulate during the vat processing focusses the importance of their preventive removal by natural creaming, avoiding a potential risk of LBD. Specific metabolic pathways involving free amino acids of *C. tyrobutyricum* have been pointed out for the first time.

4. Chapter 4: Side effects of Lysozyme in Grana Padano cheese

4.1 INTRODUCTION

Nowadays hen's egg white lysozyme (EC 3.2.1.17) (LZ) is used in Grana Padano as well as in other hard cheeses to prevent the "late blowing" defect (Brasca et al, 2013; Jiménez-Saiz et al., 2013). In fact, LZ is efficient in lysing the vegetative cells of Clostridia, specifically of *Clostridium tyrobutyricum*, by splitting β (1–4) linkages between N-acetylmuramic acid and N-acetylglucosamine of the peptidoglycan of the bacterial cell wall (Hughey and Johnson, 1987). These bacteria are capable of producing spores that survive the thermal treatment applied in making hard cheeses and can later germinate and produce gas causing the defect. The origin of the contamination by this bacterium has been identified in the wide use of silage in livestock feeding (Jonsson, 1991; Vissers et al., 2006).

The different sensitivity to LZ of various bacteria, both Gram positive and negative, is due to the different cell wall composition and structure and, thus, to the binding of the enzyme to its specific substrate (Bester and Lombard, 1990; Carini et al., 1985; Hughey and Johnson, 1987). Due to its wide spectrum, LZ activity can also occur against lactic acid bacteria (LAB) involved in curd acidification and cheese ripening. The interference of the enzyme with the acidification process occurring during hard cheese production has been indirectly studied by considering the sensitivity of LAB responsible of curd acidification. For example, LZ inhibitory activity has been extensively evaluated for the main species present in the natural whey starter used to produce Grana Padano, i.e. *Lactobacillus helveticus*. It was found that sensitivity of *L. helveticus* was strain-dependent, and acquisition of resistance can be due to strain adaptation rather than selection of spontaneous mutants (Fortina et al., 1998; Neviani et al., 1991). Resistance to LZ was also reported for *Lactobacillus delbrueckii* (Vinderola et al., 2007). Moreover, a correlation was observed between LZ resistance and bacteriophage sensitivity in *L. helveticus* (Neviani et al., 1992) and the authors suggested the possibility of using LZ as a selective agent to isolate phage-resistant starter strains.

To author's knowledge, few literature data are available on LZ resistance of non-starter LAB (NSLAB). These are part of the raw milk cheese microbiota and are not involved in curd acidification but play a relevant role in cheese ripening (Gatti et al 2014). Carini et al. (1985) reported LZ resistance of *L. casei* species. Ugarte et al. (2006) studied NSLAB isolated from soft and semi hard Argentinean cheeses and found most of the species to tolerate 2.5 mg $100g^{-1}$ of LZ. More recently, LZ sensitivity of NSLAB was studied as one of the criteria suitable to evaluate their probiotic aptitude (Solieri et al., 2014). A strain-dependent resistance to LZ at the concentration of

10 mg 100g-1, close to that adopted in Grana Padano, was found for *L. rhamnosus*, *L. paracasei*, *L. casei*, *L. harbinensis*, and *L. fermentum*.

The aim of this work was to investigate the effects of LZ in cheese with respect to both the microbial populations and proteolysis pathways responsible of cheese ripening. In particular, the focus was on Grana Padano PDO cheese, usually made with LZ and extensively studied for its microbial and chemical features (Pellegrino et al., 1997; Masotti et al., 2010; Santarelli et al., 2013; Pogacic et al., 2013). Eight cheese makings were therefore conducted at four different dairies, using in parallel, the same milk either added or not with LZ. The 16 derived cheeses were analysed after 9 months of ripening, i.e. the minimum ripening period for Grana Padano PDO cheese, and after 16 months. The microbial populations were characterized by Length Heterogeneity-PCR (LH-PCR) considering both the intact and lysed cells. Furthermore, the free amino acids (FAA) patterns of the cheeses were evaluated. Since FAA mostly result from the action of intracellular proteinases and peptidases released after the bacterial cell lysis, different patterns could be expected between cheeses produced with and without addition of LZ.

The work described in this chapter is already published as a research article (D'Incecco et al., 2016).

4.2 MATERIAL AND METHODS

4.2.1 Cheese manufacture

Grana Padano cheeses were manufactured at four dairies belonging to the Consorzio Tutela Grana Padano, following the traditional manufacturing process (European Parliament and Council, 2012). At each dairy, the cheese makings were carried out on two different days for a total of eight trials. For each cheese making trial, raw bulk milk was partially skimmed (fat content: 2.2-2.3%) by natural creaming, divided into two vats (1000 L each), one of which was added with 20 g LZ (Sacco, Cadorago, Italy) carefully dispersed in 200 mL water, and the two vats were worked in parallel. The natural whey starter (titratable acidity: 30-32°SH/50 mL), obtained from the residual whey of the previous days' cheese-making, and the calf rennet were added to coagulate the vat milk at 32°C in 8-10 min. The curd was gently cut into small granules while progressively heated up to 52-54°C, then it was allowed to compact at the bottom of the vat for 60 min before extraction. The cheeses (two wheels per vat) were molded for 48 h to allow lactic acid fermentation (pH was measured in the core of the wheels) and then salted in brine for 18-20 days. During ripening, all the cheeses were regularly inspected by X-ray tomography (Philips CT Brilliance 16P, Zürich, Switzerland) to evidence possible development of defects. The twin cheeses obtained from each vat were cut after 9 and 16 months of ripening respectively. A portion representative of the whole wheel was taken from each, grated and deep-frozen until analysis. Samples for microbiological analyses were kept at 4°C until arrival at the laboratory and immediately analyzed. Cheese samples either containing or not LZ were coded as LZ+ and LZ- respectively, whereas numbering from 1 to 8 identifies the cheese making trial they come from.

4.2.2 Bacterial counts

Bacterial counts were determined on de Man, Rogosa and Sharpe (MRS) agar (Oxoid, Basingstoke, United Kingdom). Representative samples (10 g) of the grated cheese were suspended in 90 mL of 20 g L^{-1} tri-sodium citrate (pH 7.5) (Sigma–Aldrich, St. Louis, USA) and homogenised for 2 min in a blender (Seward, London, United Kingdom). For enumerating mesophilic lactobacilli, as main microbiota of cheese during ripening, decimal dilutions of cheese homogenates were made in quarter-strength Ringer solution (Oxoid, Basingstoke, United Kingdom) and spread plated in triplicate on MRS. The plates were incubated at 30 °C for 72 h under anaerobic conditions.

4.2.3 DNA extraction

Bacterial genomic DNA was extracted directly from samples by using a General Rapid Easy Extraction System (GREES) DNA kit (InCura S.r.l., Cremona, Italy) according to the manufacturer's instructions. Cheese samples were pre-treated in order to discriminate the DNA from whole and lysed cells as described by Gatti et al. (2008). Briefly, cheese samples resulted in two fractions, the free-cell fraction was obtained by filtration and the whole-cell fraction was obtained by treating samples with DNase to digest free DNA arising from lysed cells. DNA was extracted from 1 mL of the filtered untreated fraction (lysed cells) and from 1 mL of the treated fraction (whole cells).

4.2.4 Length heterogeneity (LH)-PCR

LH-PCR was used in order to determine the microbial community composition. V1 and V2 16S rDNA gene regions were amplified with primers 63F and 355R (Lazzi et al., 2004). The forward primer was 5′-end labelled with a 6-carboxyfluorescein (6-FAM) dye. Amplicons were then separated by capillary electrophoresis in an automated sequencer (Applied Biosystems, Foster City, USA). PCR and capillary electrophoresis conditions were as described by Bottari et al. (2010). The fragment sizes (base pairs) were determined with GeneMapper software version 4.0 (Applied Biosystems), local Southern method to generate a sizing curve from the fragment migration of the internal size standard (GS500 LIZ®; Applied Biosystems) and a threshold of 150 fluorescence units. The fragment analysis software converted fluorescence data into electropherograms. The peaks represent fragments of different sizes and the areas under the peaks are the amount of the fragments. Total area were considered to directly correlate to the total amount of the DNA arising from whole or lysed cells depending on the two fractions previously described. Each peak, corresponding to amplicon of specific length on the electropherogram profile, was attributed to bacterial species according to published databases (Lazzi et al., 2004; Gatti et al., 2008) and the areas under the recognized peaks were used to estimate the amount of the assigned species in the samples. Total area under all the peaks (sum of attributed and unattributed peaks) of the LH-PCR electropherograms was used for measuring total amount of DNA arising from both intact and lysed cells.

4.2.5 Determination of free amino acids by ion-exchange chromatography

4.2.5.1 Free amino acid extraction

The grated cheese was weighted (1.5 g) in a 100 mL beaker, added with 40 mL 0.2 N tri-sodium citrate buffer at pH 2.2 (SCB), kept under magnetic stirring for 15 min then carefully homogenized

with Ultra-Turrax (5 min at low speed). The extract was filtered (Whatman 42 paper filter, GE Healthcare, Milan, Italy) and 10 mL of the filtrate were transferred into a 25 mL volumetric flask, dropwise added with 10 mL 7.5% (w/v) 5-sulphosalicylic acid (pH 1.7-1.8) under stirring, diluted to the mark with SCB and filtered. Finally, 10 mL of this filtrate were transferred into a 100 mL volumetric flask, added with 2 mL norleucine solution (60 mg norleucine in 100 mL SCB) as an internal standard, made up to the mark with 0.2N Lithium citrate pH 2.2 (dilution buffer), and filtered on 0.2 µm disposable filter (Minisart® RC 25, Sartorius, Goettingen, Germany) prior to injection. All cheese samples were analysed in duplicate.

4.2.5.2 Amino acid standard solutions

A stock solution was prepared containing: 15 mg of arginine, asparagine, citrulline, glycine, glutamine, γ-aminobutyric acid, methionine, ornithine, threonine, tyrosine; 30 mg of alanine, aspartic acid, phenylalanine, isoleucine, histidine, serine; 40 mg of leucine, proline, valine, glutamic acid and lysine (Sigma-Aldrich) per 100 mL of SCB. Aliquots of 0.5, 1.0, 2.0 and 5.0 mL of this solution were transferred into 100 mL volumetric flasks, added with 2 mL of the norleucine solution, and made up to the mark with dilution buffer to prepare working solutions with four different concentrations.

4.2.5.3 Chromatographic conditions

A Biochrom 30+ chromatograph (Biochrom Ltd., Cambridge, UK) equipped with an Accelerated Lithium Column (Biochrom Ltd.) was used and the elution conditions recommended by the manufacturer were followed. Reagents of analytical grade and MilliQ water (Millipore, Vimodrone, Italy) were used. Ready-to-use Ninhydrin reagent was purchased from Erreci s.r.l. (Pieve Emanuele, Italy).

4.2.6 Statistical analysis

Statistical treatment of data was performed by means of SPSS Win 12.0 program (SPSS Inc., Chicago, IL, USA). Data were analysed by Principal Component Analysis (PCA) by means of Statistica (StatSoft Inc., Tulsa, OK, USA) and comparison of means was carried out by Student's t-test. A $P<0.05$ was assumed as significance limit.

4.3 RESULTS AND DISCUSSION

4.3.1 Microbial characterization of 9-month ripened cheeses

Microbial counts in MRS at 30°C (i.e. mesophilic lactobacilli) and community composition were different in all couples of samples and not clearly correlated with presence or absence of LZ. However, some peculiarity emerged. Overall, cultivable bacterial population varied of almost two log units among samples (Table 4.1). The plate count in LZ+ cheeses showed a great variability (ranging from 4.44 log cfu/g in sample 6 to 6.64 log in sample 7). Differently, the counts in LZ- cheeses were higher and less variable. In particular, the cultivable population in LZ- cheeses were higher than in the corresponding LZ+ for 6 out of the 8 couples (Table 4.1).

The LH-PCR was performed with DNA extracted from intact cells to estimate which bacterial species were still present in the cheeses after 9 months of ripening. Only peaks attributed to the database set (Lazzi et al., 2004; Gatti et al., 2008) were considered. The same species evidenced in Grana Padano by Santarelli et al. (2013) and by Pogacic et al. (2013), i.e. Lactobacillus delbrueckii, L. helveticus, L. rhamnosus, L. fermentum and Pediococcus acidilactici, were found in cheeses but never simultaneously in the same sample. L. helveticus, L. delbruecki and L. rhamnosus were the most frequently detected species in LZ+ cheeses, while in LZ- cheeses L. helveticus, L. rhamnosus and L. fermentum prevailed, with L. delbruecki only found in two LZ- cheeses (Table 4.1). Pediococcus acidilactici was seldom found, preferentially in LZ- cheeses.

The evaluation of the free DNA fraction allowed estimating which LAB underwent lysis during 9 months of ripening leaving their DNA still amplifiable. This method, developed by Gatti et al. (2008) to highlight LAB lysis in Parmigiano-Reggiano, was also adopted by Santarelli et al. (2013) for Grana Padano. Lysed species found in the presently studied cheeses were L. delbrueckii, L. helveticus, L. rhamnosus and, in one sample, L. fermentum. Interestingly, lysed L. delbrueckii was detected in the same samples where the intact cells were still present, seven out of eight of these samples being LZ+ (Table 4.1). Differently, lysed L. helveticus in LZ+ cheeses was always below the detection limit. Recently, Sgarbi and colleagues demonstrated the ability of NSLAB to grow using cell lysates of SLAB as the exclusive source of nutrients (Sgarbi et al., 2014). Total area under all of the peaks (attributed and unattributed) in the LH-PCR electropherograms either from intact or lysed cells was used for measuring the respective total amounts of DNA (Table 4.1). The amount of DNA of intact cells was higher than the amount of DNA of lysed cells for 14 out of 16 samples, irrespective of LZ presence. Importantly, higher amount of DNA arising from lysed cells was observed in 6 out of 8 LZ+ cheeses (Table 4.1).

Considering individual species, in the LZ- cheeses L. delbrueckii was below the detection limit in six out of eight samples, whereas presence of L. fermentum was often higher than in the corresponding LZ+ cheese. Taking together microbial counts and LH-PCR results, lower numbers of cultivable population and higher amount of DNA arising from lysed cells found in LZ+ cheeses are reasonably due to the hydrolytic activity of the additive (Hughey et al., 1987). On the other hand, its efficacy on different LAB species depends on their different sensitivity which was found to be strain specific in L. helveticus (Neviani et al., 1991; Fortina et al., 1998), L. casei group (Solieri et al., 2014), and potentially variable in L. delbrueckii (Vinderola et al., 2007).

Despite this variability, PCA showed that LZ+ samples spread along the first component, mostly due to the high amounts of L. delbrueckii (both intact and lysed), intact L. helveticus, DNA from lysed cells on one side, and to high MRS plate counts and high amount of L. rhamnosus on the other side (Figure 1a and 1b). Moreover, LZ- cheeses appeared to distribute along the second component, where the amount of L. fermentum and P. acidilactici showed greater weight. The positioning of the samples (cheeses) was likely determined by LZ, whose presence affected both SLAB (L. helveticus and L. delbrueckii) and NSLAB (L. rhamnosus, L. fermentum and P. acidilactici) species with a direct effect on LZ-sensitive species and a consequent effect of selection on the others.

Sample	Log cfu/g	peaks area of recognized species (whole cells DNA)					peaks area of recognized species (lysed cells DNA)				Total DNA area	
	MRS plate count	*Lactobacillus delbrueckii*	*Lactobacillus helveticus*	*Lactobacillus rhamnosus*	*Lactobacillus fermentum*	*Pediococcus acidilactici*	*Lactobacillus delbrueckii*	*Lactobacillus helveticus*	*Lactobacillus rhamnosus*	*Lactobacillus fermentum*	Whole cells	Lysed cells
	MRS*	Ldw*	Lhw*	Lrw*	Lfw*	Paw*	Ldl*	Lhl*	Lrl*	Lfl*	DNAw*	DNAl*
1LZ+	6,07	840	16156	11394	1928	<LOD	2587	<LOD	<LOD	<LOD	31153	2587
1LZ-	6,26	<LOD**	3910	1260	15929	<LOD	<LOD	<LOD	<LOD	<LOD	21099	576
2LZ+	6,28	1365	215	13141	<LOD	<LOD	995	<LOD	784	<LOD	15223	1779
2LZ-	6,25	<LOD	8992	<LOD	37974	<LOD	<LOD	<LOD	<LOD	1443	48232	3739
3LZ+	6,12	<LOD	3434	64202	7011	<LOD	<LOD	<LOD	2402	<LOD	79422	3339
3LZ-	6,25	<LOD	223	12306	4896	<LOD	<LOD	<LOD	1374	<LOD	18224	1374
4LZ+	4,58	4188	1586	<LOD	14287	<LOD	1465	<LOD	<LOD	<LOD	20061	24360
4LZ-	5,99	<LOD	8799	2360	<LOD	6162	<LOD	1024	518	<LOD	17321	16294
5LZ+	5,74	3282	6928	5422	<LOD	3446	1747	<LOD	<LOD	<LOD	19078	30697
5LZ-	5,83	<LOD	5853	16483	56959	<LOD	<LOD	778	<LOD	<LOD	80651	7632
6LZ+	4,44	10652	28041	<LOD	2393	<LOD	2089	<LOD	<LOD	<LOD	41086	6834

6LZ-	5,50	<LOD	6658	5082	16437	1916	<LOD	<LOD	<LOD	<LOD	30093	815
7LZ+	6,64	4464	5578	7826	<LOD	4403	1295	<LOD	877	<LOD	22271	16750
7LZ-	6,64	1957	13958	23302	<LOD	8643	482	1948	1094	<LOD	47860	8432
8LZ+	5,87	2535	2669	4717	<LOD	<LOD	610	<LOD	<LOD	<LOD	10538	1988
8LZ-	6,23	503	1507	20791	<LOD	4738	<LOD	1519	<LOD	<LOD	27539	5133

Table 4.1 Microbial characterization of 9-month ripened cheeses produced with (LZ+) or without (LZ-) lysozyme.

* code used in PCA analysis

**below limit of detection

4.3.2 Free amino acid pattern in 9-month ripened cheeses

During cheese ripening, casein is progressively degraded into peptides and free amino acids (FAA) by a pool of proteolytic enzymes coming from both starter and non-starter microflora and acting in combination. Since the pattern of peptides is changing over time (Ferranti et al., 1997), we have disregarded this intermediate fraction and focused the attention on the pattern of free amino acids (FAA) that proved to represent an accurate descriptor of proteolysis behaviour in Grana Padano cheese (Cattaneo et al., 2008).

The total content of FAA on cheese protein basis was in the range 17-22% (data not shown), in agreement with previously published data for Grana Padano cheese of the same age (Masotti et al., 2010). The values were not significantly different (P=0.48) between cheeses produced with and without LZ, indicating that proteolysis has proceeded at the same rate. The whole data set was thus analyzed by PCA to highlight possible differences among cheese samples. The plot showed a significant dispersion of the observations, and the cheese samples did not cluster together depending on the presence or absence of LZ (Fig. 4.1 a). Nevertheless, within each couple of twin cheeses, the LZ+ cheeses always fell on the upper side with respect to the corresponding LZ- cheese. Interestingly, this positioning appeared to be due to four FAA, namely arginine, citrulline, ornithine and ϒ-aminobutyric acid (g-ABA) (Figure 4.1 b), although their content only accounts for 5-6% of the total FAA. In particular, g-ABA is a non-protein amino acid generated through decarboxylation of glutamic acid as a defence mechanism for resistance to an acidic environment (van de Gukte et al., 2002). The ability to produce g-ABA was reported for several SLAB species typically present in Grana Padano natural whey starter, including L. helveticus, L. delbruecki, as well as for L. plantarum, L. brevis, all producing a glutamate decarboxylase (Li and Cao, 2010). Although the values were very low, the average content of g-ABA was approximately double in LZ+ cheeses (Table 4.2) and confirmed the presence of g-ABA-producing strains. The other three FAA are all involved in a common metabolic pathway, being citrulline and ornithine non-protein amino acids deriving from arginine catabolism. Thus we have focused our attention on this pathway.

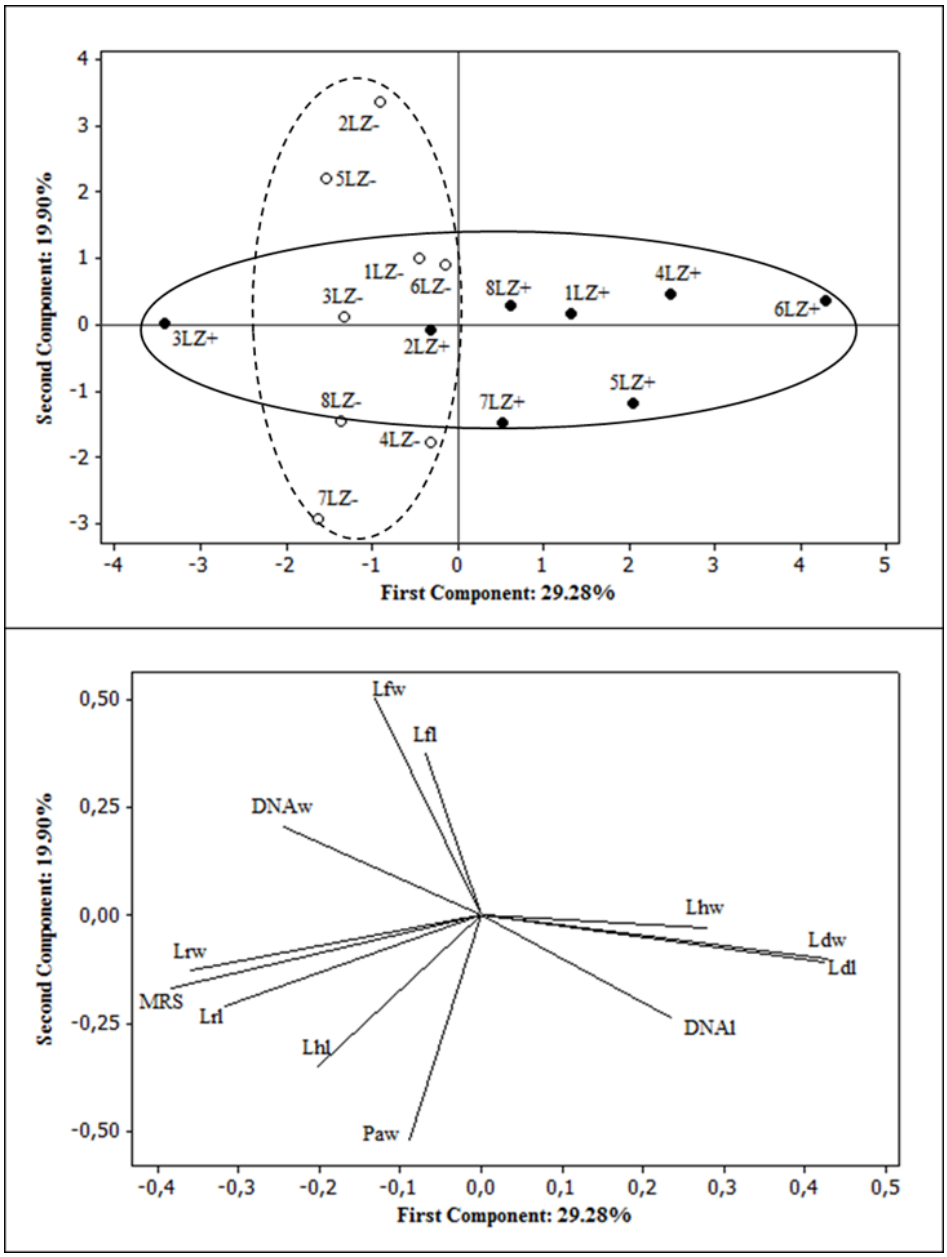

Fig. 4.1. PCA of different LAB species in cheeses produced with (LZ+) or without (LZ-) addition of lysozyme. Component plot (Panel a), and loadings of individual species (Panel b). Abbreviations are as in Table 4.1.

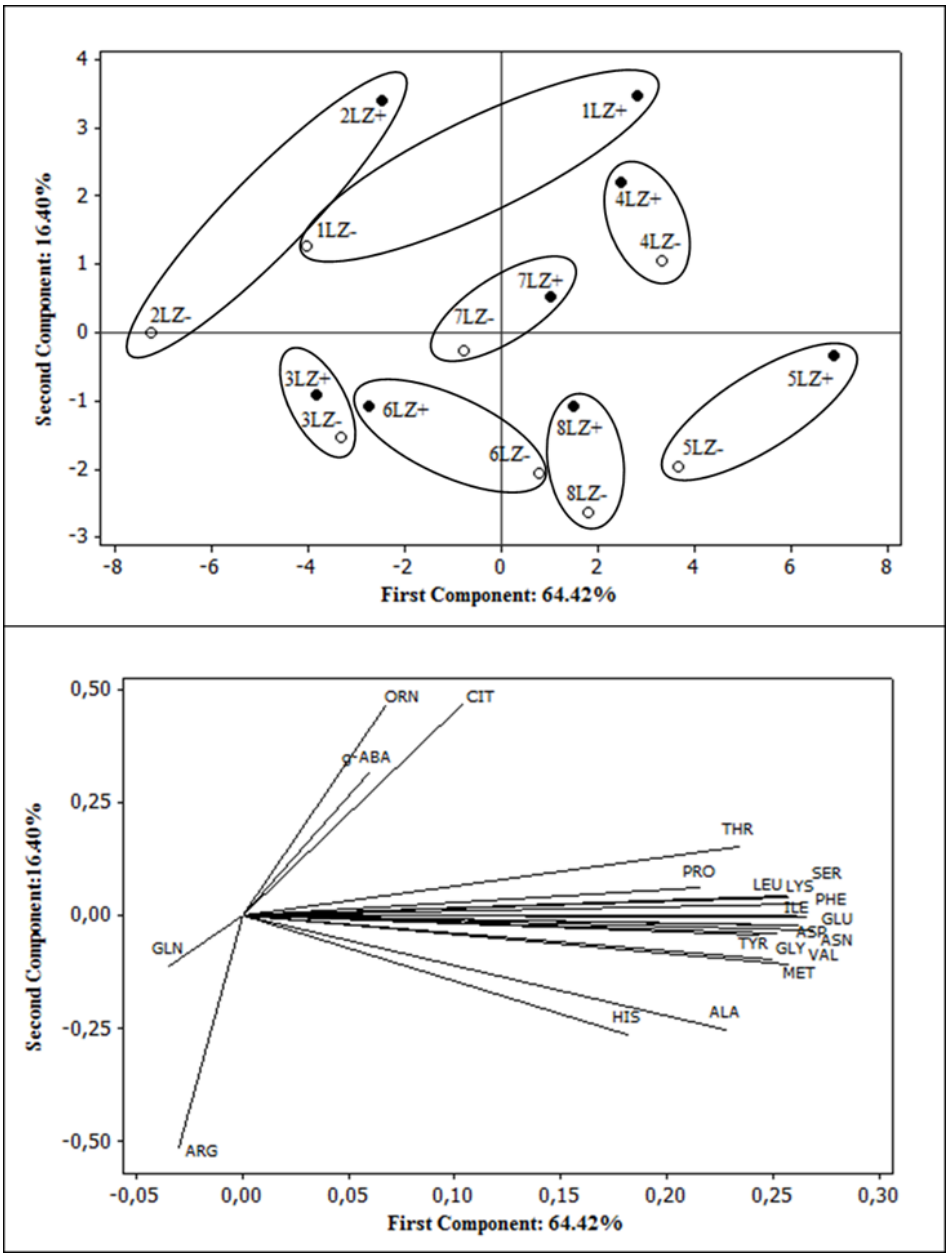

Fig. 4.2. PCA of free amino acids composition of cheeses produced with (LZ+) or without (LZ-) addition of lysozyme. Component plot (Panel a), and loadings of individual FAA (Panel b).

4.3.3 Arginine metabolism

The total amount of arginine liberated from casein in cheese was calculated as the sum of free arginine plus citrulline plus ornithine as molar concentration. Values were in the range from 48 to 63 mmoles/kg (Figure 4.3a), roughly corresponding to 22-28% of the arginine in casein (Farrel et al., 2004). By comparing the twin cheeses obtained from different cheese makings (Figure 4.3a), the total amount of arginine liberated from casein was found to be characteristic of the dairy. In contrast, the amount of arginine converted into both citrulline and ornithine was always lower in the

LZ- cheeses, regardless of the dairy of origin, being the amount of ornithine marginal. Not much literature is available to clarify the progress of microbial degradation of arginine in real cheeses (Brandsma et al., 2012; Diana et al., 2014; Laht et al., 2002), since studies are mostly based on single-strain fermentation trials. Our data show that in cheeses it is significantly affected by the presence of LZ, as it is further discussed.

The ability to catabolize arginine through the arginine deiminase (ADI) pathway is rather common in LAB species, typically in heterofermentative LAB (Fröhlich-Wyder et al., 2015; Nicoloff et al., 2001; Price et al., 2012). The accepted model for this pathway (Figure 4.3 b) implies the uptake of free arginine into the bacterial cell by an antiporter system and its degradation into citrulline by ADI. Intracellular citrulline can either be excreted or converted into ornithine by the cytoplasmic enzymes ornithine transcarbamoylase and carbamate kinase. Ornithine is then excreted in the medium. Overall, the ADI pathway brings to the production of one mol of ATP and two mol of ammonia per mol of degraded arginine. Therefore, arginine catabolism is considered to represent both a way to counteract the acid stress and an alternative source of energy.

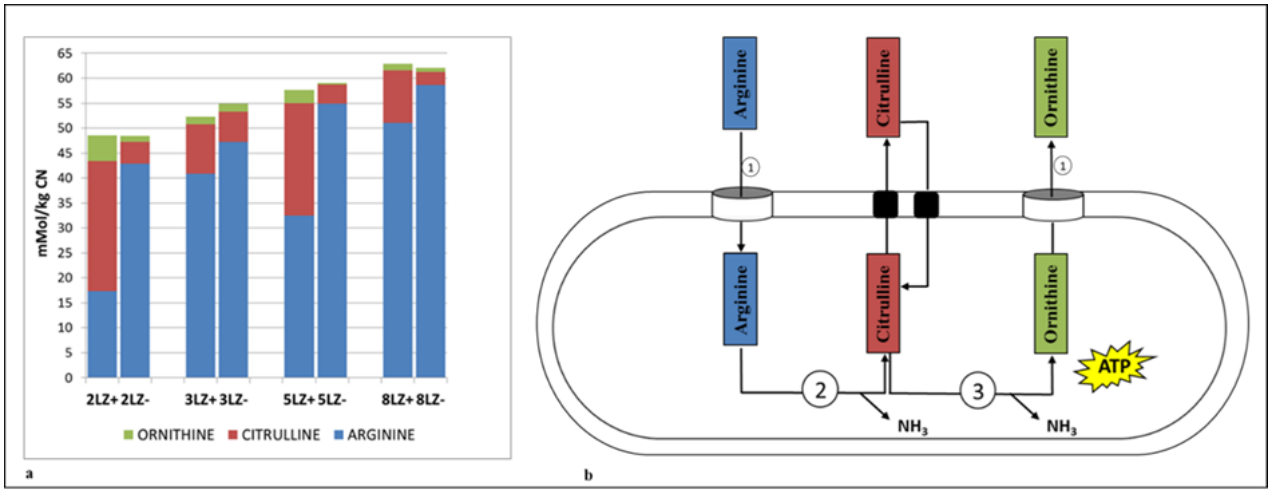

Fig. 4.3. Content of free arginine, citrulline and ornithine in four couples of 9-month ripened cheeses produced with (LZ+) or without (LZ-) lysozyme (Panel a), and scheme of the arginine deiminase pathway (Panel b).

Our data indicated that availability of free arginine did not represent a limiting factor in Grana Padano cheese since it was continuously liberated from peptides. This fact, along with the low levels of citrulline released and extremely low levels of citrulline converted into ornithine, suggested a limited adoption of the ADI pathway during cheese ripening, possibly because of environmental conditions only slightly stressing LAB. Actually, in hard cheeses like Grana Padano, cell stressing conditions, such as high temperature or highly acidic pH, principally occur during the

cheese molding, when growth of SLAB largely prevails (Gatti et al., 2014). As already mentioned, SLAB species typical to Grana Padano are mostly represented by homofermentative species, i.e. L. helveticus and L. delbrueckii subsp. lactis (Gatti et al., 2014). L. helveticus has been reported to harbor an incomplete ADI operon (Christiansen et al., 2008), whereas the complete pathway has been observed in strains of L. delbrueckii subsp lactis (El Kafsi et al., 2014; Nicoloff et al., 2001). The limited adoption of the ADI pathway by SLAB of Grana Padano is supported by our recent data (Pellegrino et al., 2015) showing that, during lactic acid fermentation occurring in the natural whey starter, SLAB mostly coped the strong acidic conditions by converting glutamic acid into g-ABA. Indeed, free arginine was used during cell growth, since most of SLAB species are auxotrophic for this amino acid (Christiansen et al., 2008), but only trace levels of both citrulline and ornithine were detected in whey starter. Considering this, metabolites deriving from ADI pathway could be produced by NSLAB throughout the ripening period more actively in LZ+ than in LZ- cheeses.

To better clarify these aspects, we have analyzed the remaining cheeses after a total ripening period of 16 months. To compare cheeses at different ages, the average relative contents of arginine, citrulline and ornithine in LZ+ and LZ- cheeses were considered (Figure 4.4).

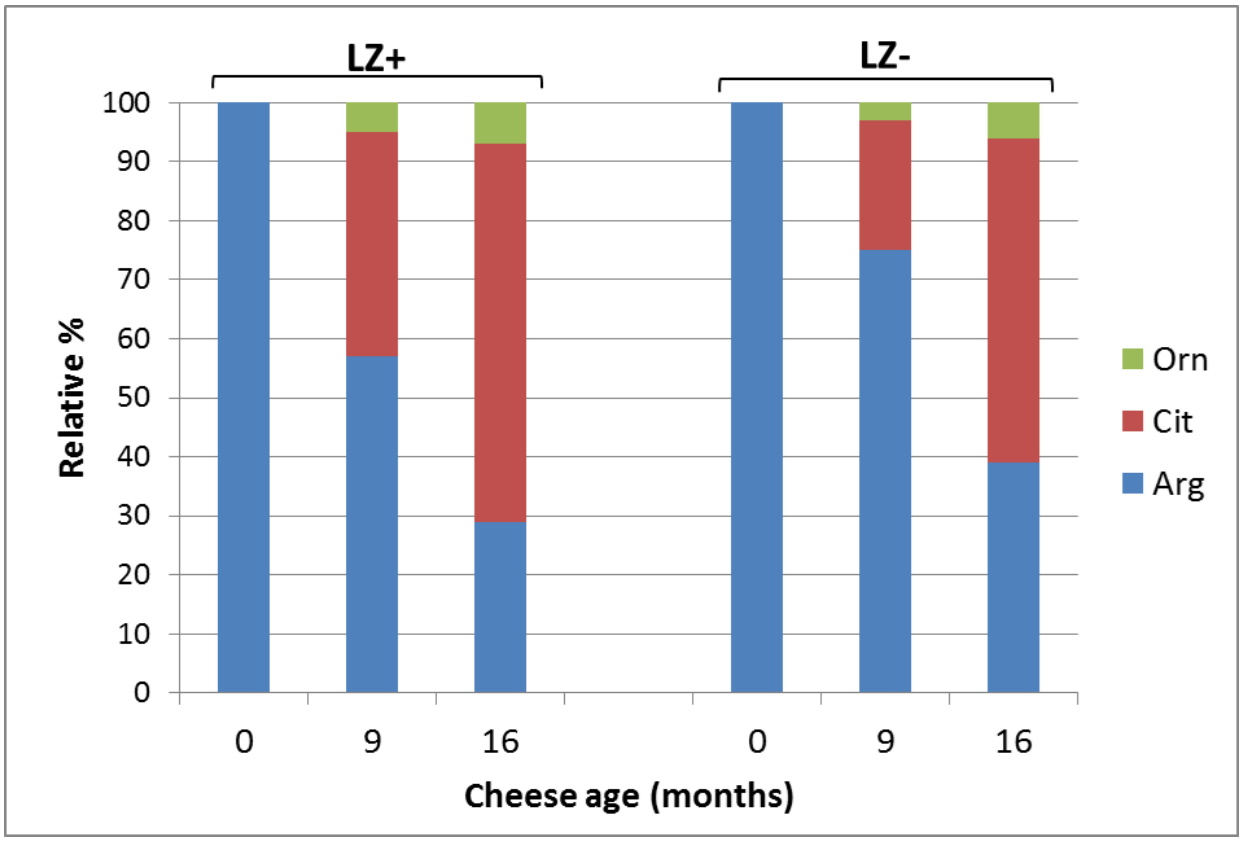

Fig. 4.4. Relative content of arginine (Arg), citrulline (Cit) and ornithine (Orn) in Grana Padano cheeses produced with (LZ+) and without (LZ-) lysozyme and ripened for different periods.

Remarkably, the ADI pathway was in use even in late ripening, being the contents of both arginine and citrulline significantly different between 9- and 16-month ripened cheeses (P= 0.001 and P= 0.000, respectively). Moreover, the presence of LZ still showed a promoting effect on this mechanism, as the residual content of arginine was different (P= 0.000) between LZ+ and LZ- cheeses at 16 months of ripening. Overall, arginine proved to be freely available throughout the whole ripening period and to be progressively converted into citrulline with a minimum further degradation into ornithine. Thus our data indicated that only the first step of the ADI pathway is commonly adopted in Grana Padano and, according to the accepted scheme (Figure 4.3), this step would be likely adopted by living cells in response to acid stress, since it only brings to production of ammonia. This fact is difficult to explain because the pH values in the ripened cheeses were all in the range 5.68-5.84, thus far from being stressing to LAB cells, and no systematic differences were found between LZ+ and LZ- cheeses.

Interestingly, also the microbial profile of the 16-month ripened cheeses confirmed the main features observed in cheeses after 9 months of ripening: the most relevant differences between LZ+ and LZ- cheeses regarded L. delbrueckii, largely dominating in LZ+ cheeses, and L. fermentum dominating in LZ- cheeses (data not shown). To author's knowledge, the only subspecies, belonging to Lactobacillus genus and delbrueckii species, isolated from whey starter and unripened Grana Padano, is lactis, whereas this species was never isolated from ripened Grana Padano cheese, even if presence of intact cells have been revealed by culture independent methods (Pogacic et al., 2013). Recently, the evolutionary adaptation of L. delbrueckii subsp. lactis to the milk environment through the acquisition of functions, including genes encoding for ADI pathway, that allow an optimized utilization of milk resources, has been demonstrated (El Kafsi et al., 2014). Accordingly, ADI pathway could be used as stress response for L. delbrueckii subsp. lactis to stay viable, although not cultivable, and thus isolable, in the ripened cheese.

With respect to L. fermentum, its presence was smaller in LZ+ cheeses at both the ripening stages, in spite of the claimed LZ-resistance (Solieri et al., 2014). Since in these cheeses the degradation of arginine was more intense, this species was unlikely involved in it, although some strains were reported to harbor the genes for ADI pathway (Vrancken et al., 2009a). Through accurate kinetic studies in controlled-condition batch fermentations, Vrancken et al. (2009a, 2009b) evaluated the response of the ADI pathway to different stress conditions in L. fermentum IMDO 130101. These authors demonstrated that both the arginine conversion rate and final citrulline-to-ornithine ratio

were strongly pH- and salt-dependent, whereas the temperature was not influent in the range 20-45 °C. In particular, when pH was set either below 4.0 or above 7.0, arginine was completely converted into ornithine. Differently, at pH in the range 5-6, such as in Grana Padano, citrulline was the main end-product. This strong dependence of the ADI pathway on the environmental pH might explain the prevalence of arginine conversion into citrulline in the studied cheeses regardless of the responsible species.

The different amounts of arginine metabolites in LZ+ and LZ- cheeses may be related also to the known biodiversity of L. rhamnosus (Bove et al., 2011). This species was present in both types of cheese and thus was not discriminant in our study. However, regarding to LZ resistance, Solieri et al. (2014) found a great variability among strains of L. rhamnosus, isolated from Parmigiano-Reggiano cheese, which turned out also to be the most LZ-resistant NSLAB (Solieri et al., 2014). It has been demonstrated that the genetic polymorphisms of L. rhamnosus is a response to cheese environmental adaptation also for arginine repressor (ArgR1) (Bove et al., 2012) and for formation of ammonia trough the ADI pathway (Liu et al., 2003). Thus, we can hypothesize that different strains of L. rhamnosus, having different ability to adopt the ADI pathway, were able to develop in the two types of cheese. This hypothesis needs to be confirmed by further characterization of L. rhamnosus strains that have been isolated from the two types of cheese.

4.4 CONCLUSIONS

The presented results indicate that the functionality of the most relevant LAB species in GP production is not hindered by LZ, but a significant effect on a specific metabolic process, i.e. the degradation of arginine, has been evidenced for the first time. Although it was not possible to identify the LAB species and strains actually responsible for the arginine degradation, a role of the dominant L. helveticus species could be largely excluded. L. delbrueckii subsp. lactis could be one of the responsible species. However, NSLAB species, such as L. fermentum and L. rhamnosus, may also contribute depending on strain ability to degrade arginine.

5. Chapter 5: New insights on fluorescence staining techniques for the detection of *C. tyrobutyricum*

5.1 INTRODUCTION

Clostridium spores spoiling food products may constitute an issue due to their strong resistance to both chemical agents and physical treatments (Sale et al., 1970, Setlow, 2006). Consequently, studies have been mostly focused on spore structure and conditions triggering spore germination. The best candidate tools for these studies are definitely microscopy techniques. Due to the small size, *Clostridium* spores are often observed by electron microscopy that has a high resolution, although the sample preparation is laborious and requires specific skills. An indirect reason for choosing this technique, rather than an optical microscopy approach, is probably the lack of suitable and friendly staining protocols for *Clostridium spp* spores. This is in turn due to the lower interest for Clostridia in comparison with other spore-formers, such as various *Bacillus* species, that are more widely studied (Setlow, 2003).

Schaffer and Fulton (1933) proposed a staining protocol for detecting spores by light microscopy and, despite its limits, it still represents the reference staining protocol for bacterial spores. According to this protocol, spores must be stained on the microscope slide where a heating step is required. This step however causes sample modifications with respect to the native status. An additional drawback of this protocol is that no staining by specific probes is provided allowing the observation of fine details of the structures.

Today's fluorescence microscopy together with confocal laser scanning microscopy (CLSM) are the most rapidly expanding microscopy techniques in biological sciences. Different methods can be applied based on fluorescence but CLSM can take very sharp x,y or 3D images with the advantage that it can be applied on fixed or live cells. High-speed deconvolution can be used for taking live-cell 3D images excluding out focus light by "Super Resolution Microscope".

The goal of this study was to develop a robust and easy-to-apply fluorescence staining technique suitable for a highly sensitive observation of Clostridia spores through Confocal Laser Scanning and Super Resolution Microscopy. *Clostridium spp.* most relevant for the "late blowing defect" in cheese were stained with fluorescence probes with the aim of getting information on both structural details and physiological properties.

5.2 MATERIAL AND METHODS

5.2.1 Double staining protocol for Confocal Laser Scanning Microscopy and Super Resolution Fluorescence Microscopy of *Clostridium spp*

C. tyrobutyricum, *C. butyricum*, *C. sporogenes* and *C. beijerinckii* were submitted to the live/dead cell staining Hoechst 34580 (HO)/Propidium iodide (PI). Five hundred µL of culture broth were centrifuged (5 min at 10,000 *g*) and the pellet was washed once with sterile PBS. Then 50 µL of Propidium Iodide (50 µg /mL water) and 50 µL of Hoechst (25 µg /mL water) were added to the pellet and mixed. The suspension was incubated at 37 °C for 30 min in the dark, then was centrifuged (10,000 *g*, 5 min) and, after removing the supernatant, 200 µL of agar solution (0,25 g/ 50 mL) at ~45°C was added to the pellet. The mixture in the tube was quickly vortexed and then observed using an inverted confocal laser scanning microscope from Leica Microsystem (Heidelberg, Germany). The same sample staining technique was used for the Super Resolution Fluorescence Microscopy on a DeltaVision OMX, 3D-Structured Illumination Microscopy (3D-SIM). Hoechst 34580 was excited at a wavelength of 405 nm and Propidium iodide at 488 nm. The emission filters were set at 392 - 440 nm for the former stain and 535 - 617 nm for the latter.
In another set of experiments, lectin wheat germ agglutinin Alexa Fluor conjugate (WGA 488; Invitrogen, Mulgrave, Victoria, Australia) was used at the final concentration of 10 µg/mL to label glycosylated molecules of bacteria.

5.2.2 Preparation of an intentionally contaminated cheese for Confocal Laser Scanning Microscopy

An experimental cheese with the addition of *C. tyrobutyricum* spores was made at laboratory scale for testing the efficacy of a fluorescence staining protocol for detecting spores in the cheese matrix by CLSM.
Full-fat pasteurised milk (four litres) from a local shop was heated to 32 °C in a thermostatic bath and inoculated with 1% (vol/vol) of *C. tyrobutyricum* spore suspension. Glucone-delta-lactone (1 g/L) as acidifying agent and rennet (0.06 mL/L) (Hannilase L, 690 IMCU/mL, Chr. Hansen, Bayswater, Australia) were added to milk under gentle stirring. Once coagulation was achieved, the curd was cut into small pieces with a knife and gradually heated by increasing the temperature up to 38 °C in a total of 60 min. The curd was kept at that temperature until the pH dropped to 6.1-6.2, then whey was drained off. When the pH reached approximately 5.4, the curd was milled before being pressed overnight. Cheese was stored at 15 °C for 1 month.

5.2.3 Triple staining protocol for Confocal Laser Scanning Microscopy of *Clostridium* spores in cheese

The lipid-specific stain Nile red was prepared from a stock solution of Nile red (1 mg/mL, containing 0.5 mL/L dimethylsulfoxide (DMSO, Sigma Aldrich) and diluted in MilliQ water to a final concentration of 0.1 mg/mL just prior to staining. The protein-specific stain Fast green FCF (Sigma-Aldrich) was prepared from a stock solution (1 mg/mL water) and diluted to a final concentration of 0.1 mg/mL. Samples for CLSM observation were prepared from the intentionally contaminated cheese. Thin slices (2 x 2 x 1 mm) were taken from the cheese interior and soaked for 10 min by adding in sequence Nile red, Hoechst 34580, and Fast green working solutions before washing with MilliQ water. The stained cheese slices were placed on a microscope slide (ProSciTech, Thuringowa, Queensland, Australia), mounted with glycerol-based anti-fading agent (AF2, Citifluor Ltd., Leicester, London, U.K.) and secured with a glass coverslip (0.17 mm thick) (ProSciTech). The CLSM equipment was an inverted confocal laser scanning microscope from Leica Microsystem (Heidelberg, Germany).

5.3 RESULTS AND DISCUSSION

5.3.1 CLSM of *C. tyrobutyricum*, *C. butyricum*, *C. sporogenes* and *C. beijerinkii*

CLSM was successfully used for developing a fast and robust protocol for fluorescent staining of spores and vegetative cells of *C. tyrobutyricum*. With this purpose, Hoechst 34580 / Propidium Iodide (HO/PI) staining was used, for the first time, to distinguish viable, dead and sporulated cells of *C. tyrobutyricum*. The blue fluorescent Hoechst 34580 dye crosses the cell membrane and binds to all nucleic acids. In contrast, Propidium iodide, as a membrane integrity probe, stains nucleic acids in cells with permeabilized membranes. When stained with both HO and PI, vegetative cells of *C. tyrobutyricum* displayed either blue or red fluorescence when alive or dead, respectively. This double staining also allowed to distinguish the spore within the sporulated mother cell when both the fluorescent emissions were observed simultaneously (Fig. 5.1).

The proposed protocol for HO/PI staining was also tested on other three Clostridia that can cause the late blowing defect: *C. butyricum*, *C. sporogenes* and *C. beijerinkii* (Fig. 5.2, 5.3, 5.4). The staining proved to be suitable for all the tested strains and allowed to observe interesting morphologic features not previously reported for these species. In all of the strains, spores were oval and surrounded by dead structures. However, *C. tyrobutyricum* and *C. butyricum* spores were in sub-terminal position within dead cells still keeping the rod shape. Differently, spores of both *C. sporogenes* and *C. beijerinckii* were surrounded by thin dead structures that in the latter species showed a characteristic long tail.

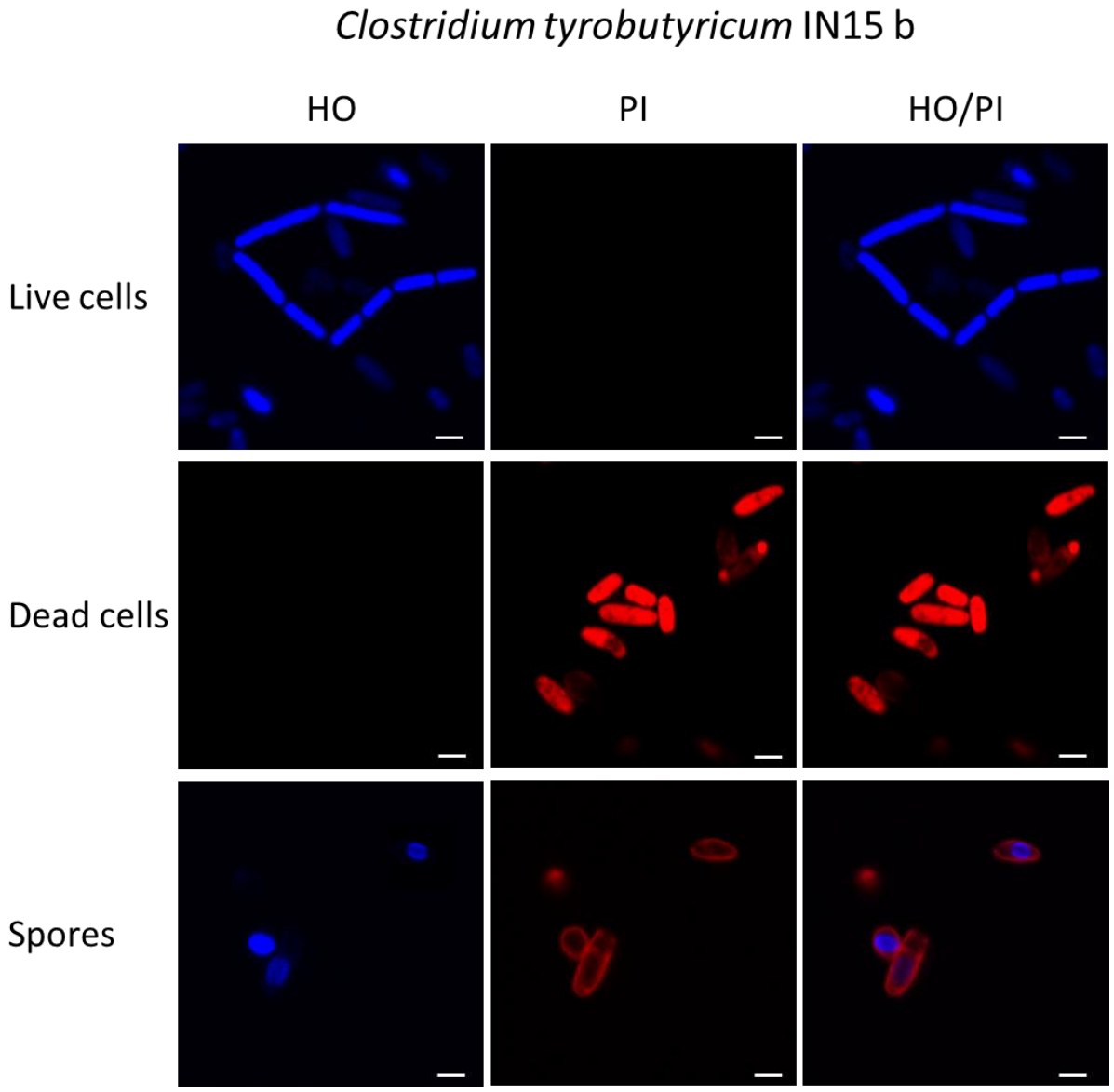

Figure 5.1. CLSM images of *C. tyrobutyricum* IN15b double stained with Hoechst 34580 and PI. Bars are 3 µm in length.

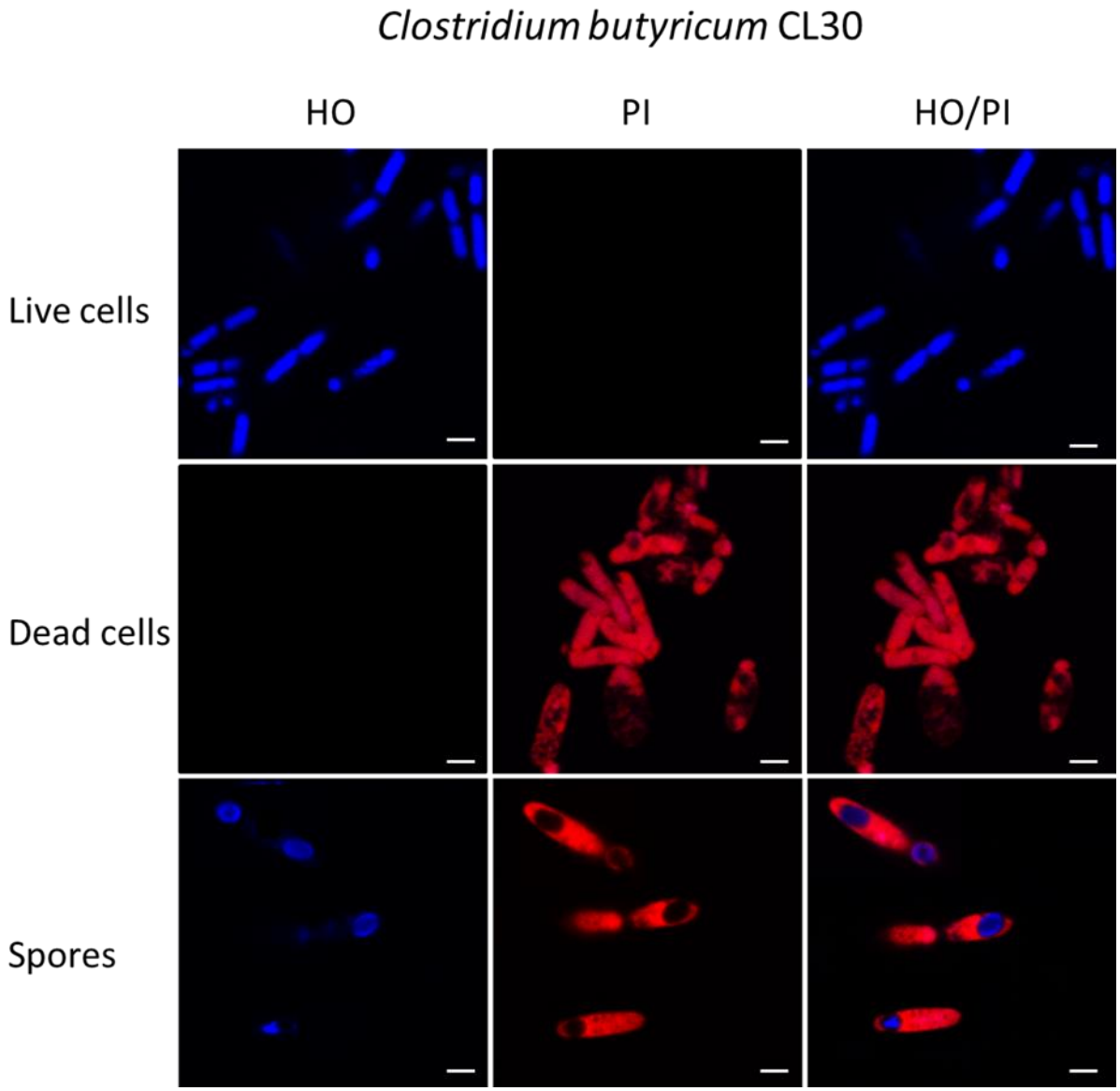

Figure 5.2. CLSM images of *C. butyricum* CL30 double stained with Hoechst 34580 and PI. Bars are 3 µm in length.

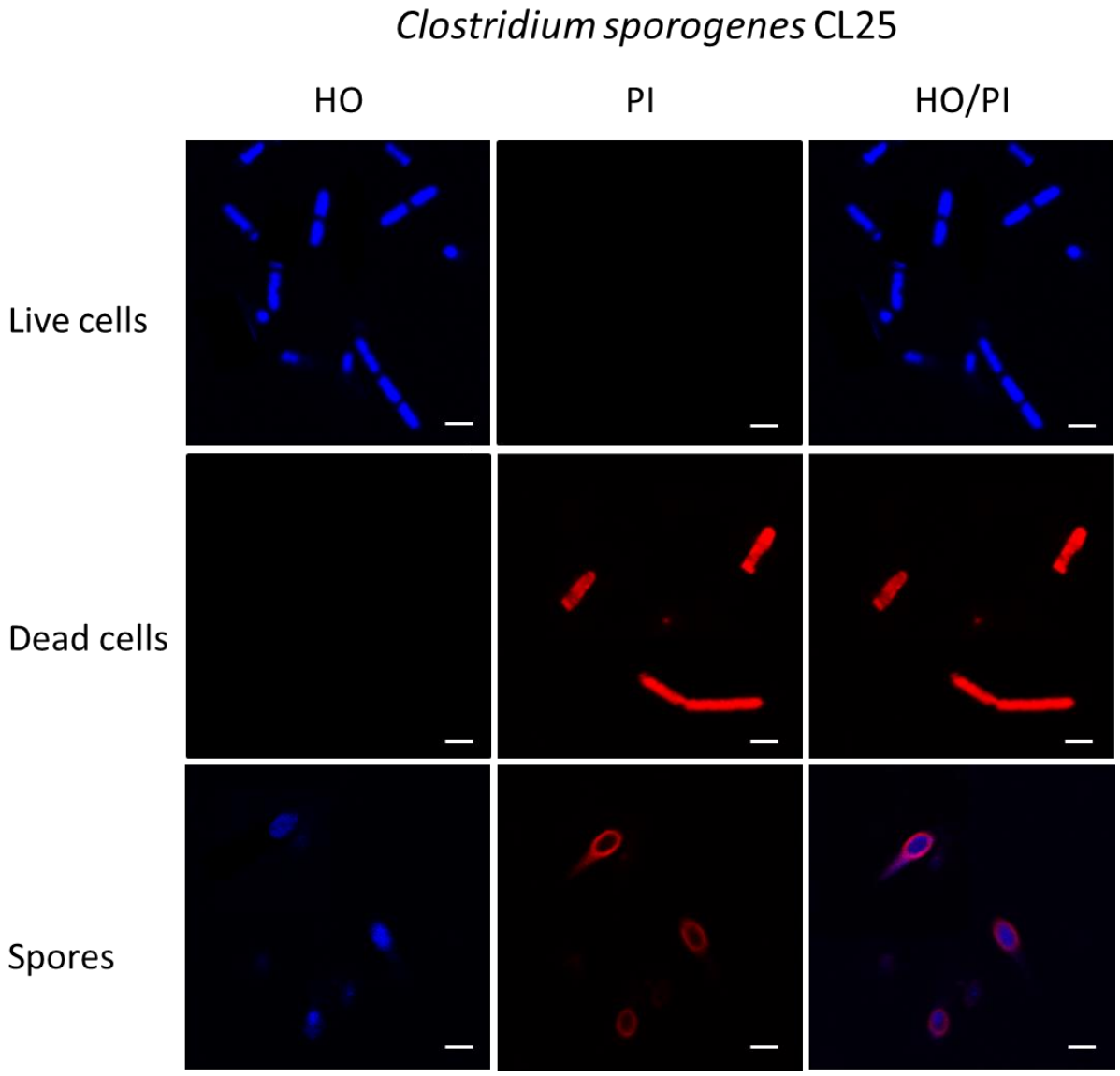

Figure 5.3. CLSM images of *C. sporogenes* CL25 double stained with Hoechst 34580 and PI. Bars are 3 µm in length.

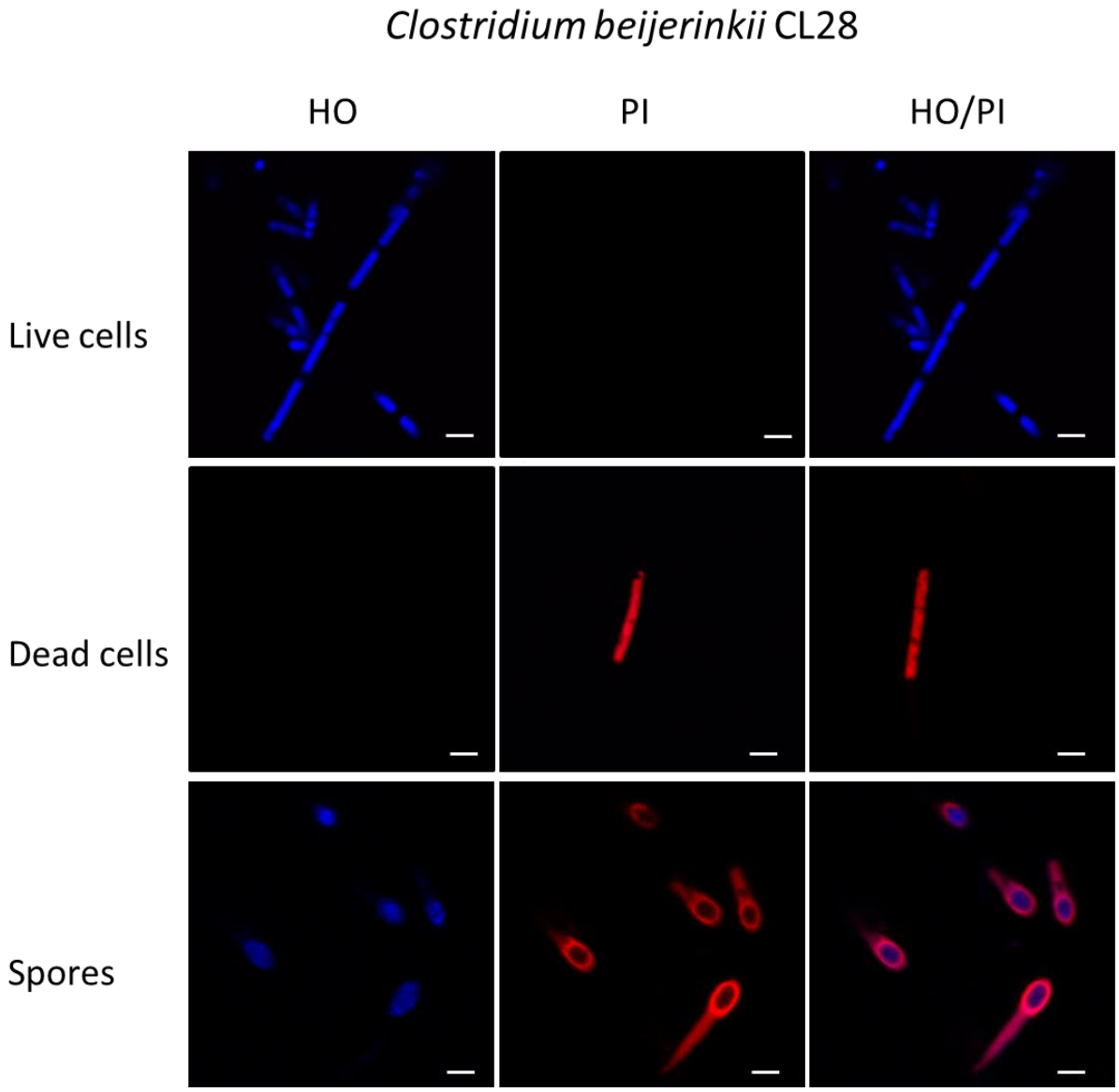

Figure 5.4. CLSM images of *C. beijerinckii* CL28 double stained with Hoechst 34580 and PI. Bars are 3 µm in length.

The double staining was used to follow the behaviour and morphologic changes of vegetative cells of *C. tyrobutyricum* when heated at 55°C for 2 h. Vegetative cells at the exponential growth phase mostly died after the heat treatment (Fig. 5.5 b, d). However, some cells survived forming the endospore (Fig. 5.5 b). Differently, vegetative cells were still alive in the control sample that was kept for 2 h at the optimum growth conditions at 37°C (Fig. 5.5 f). These results confirmed the behaviour of *C. tyrobutyricum* we observed during vat milk processing (paragraph 3.3.1).

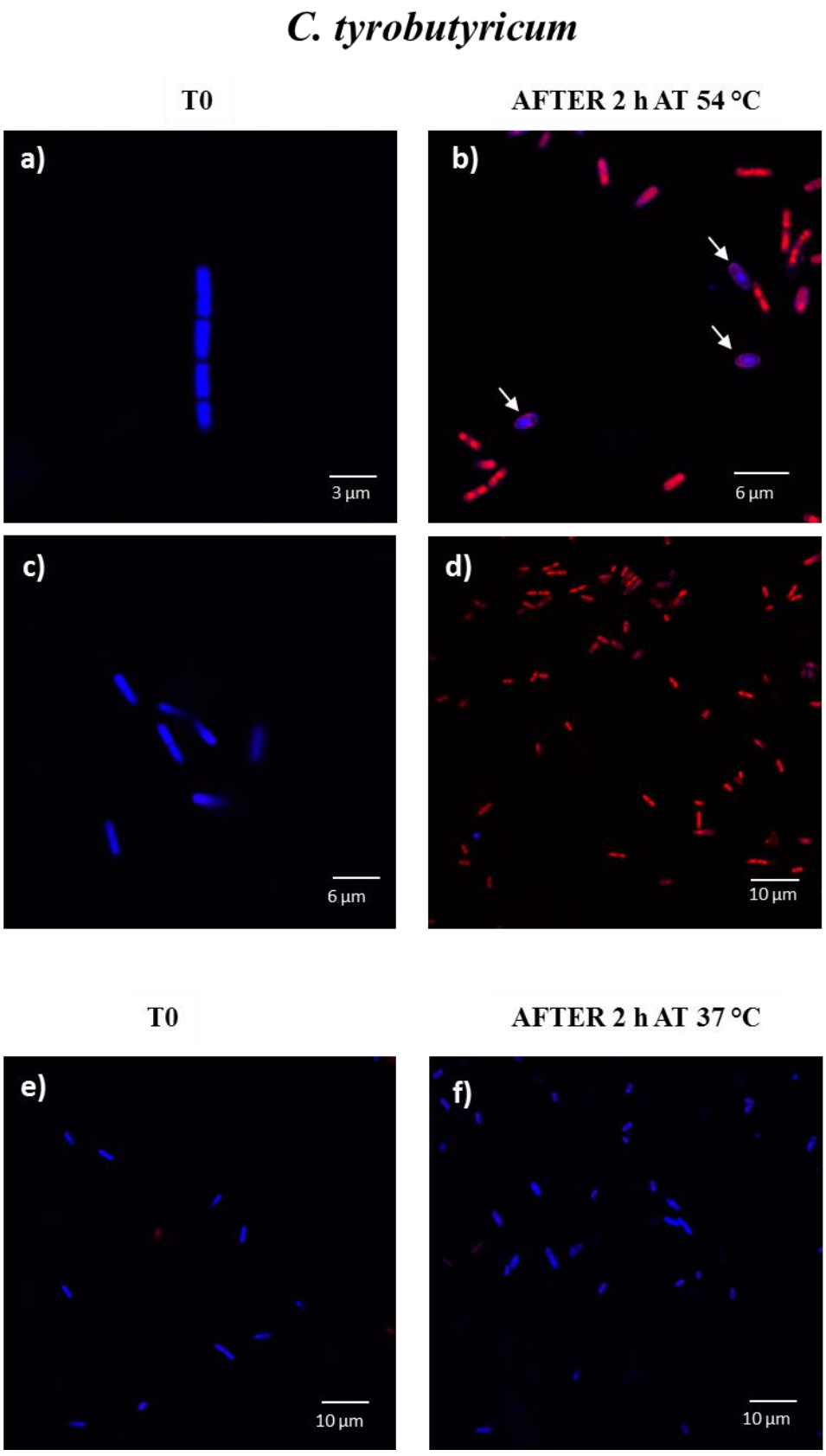

Figure 5.5. CLSM images of double stained *C. tyrobutyricum* under heat treatment. Spores formed after heat treatment (arrows, panel b).

The HO/PI staining protocol here proposed for endospore staining represents a large improvement with respect to the most known and commonly used protocol of Schaeffer and Fulton (1930). Our staining can be performed directly on the microscopic slide but also in the culture tube. The latter condition makes it possible the recovery of pre-stained bacteria and their use in another experiment. The recovery of stained bacteria is an important option that was unrealistic with the staining protocol of Schaeffer and Fulton because, due the heating step, bacteria stick to the glass slide.

The Hochst 34580 dye was used, together with Nile Red and Fast Green, to observe spores into the cheese matrix. Spores were added to milk during cheese making and, after 1 month of ripening, the triple staining was performed on slices of cheese (Fig. 5.6). The staining procedure was successful in showing the protein/fat microstructure of the cheese (Ong et al. 2011) and most often spores were observed within the protein matrix.

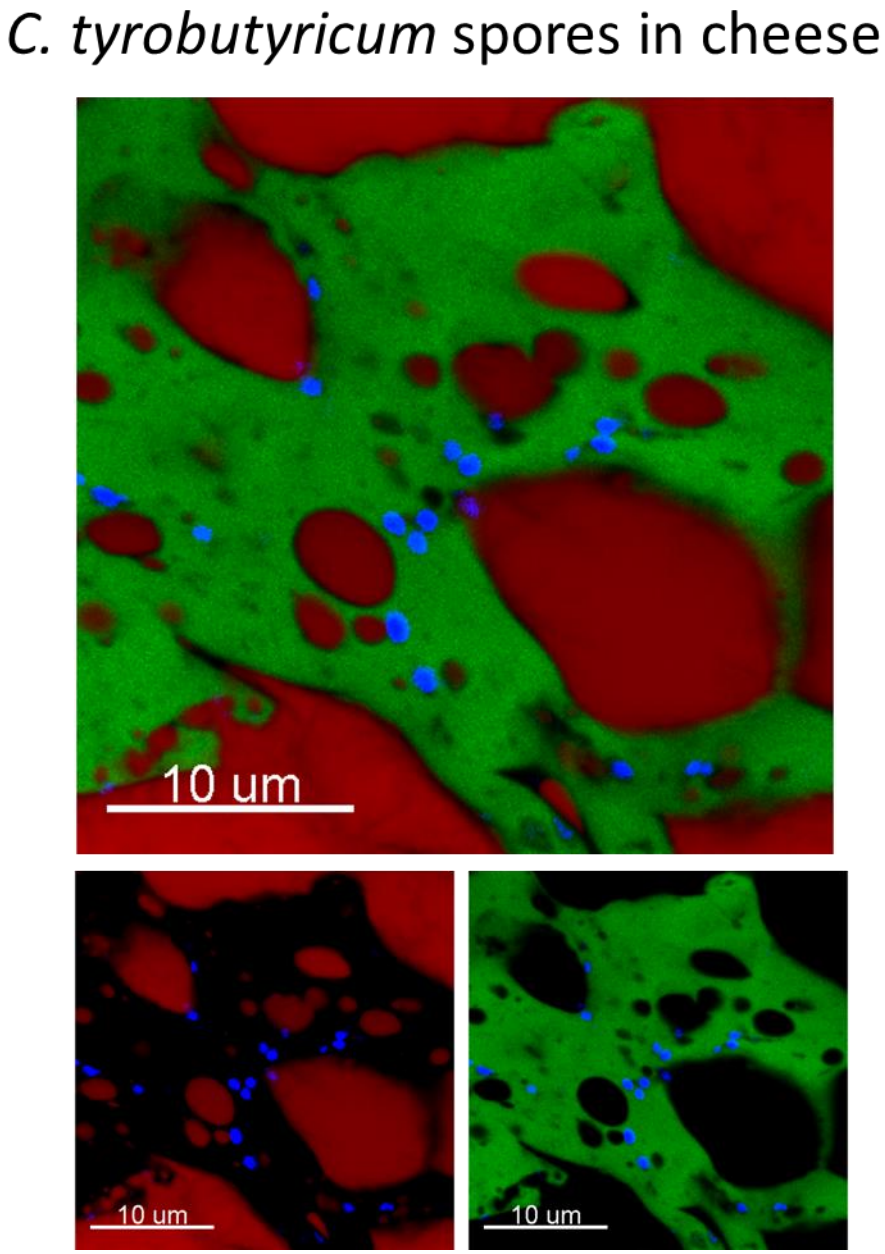

Figure 5.6. CLSM image of triple staining Hoechst 34580 / Nile red / Fast green of spores in cheese matrix. The fat appears red, the protein appears green and spores appear blue.

Further information on *C. tyrobutyricum* features came from the use of lectin WGA 488 combined with the double HO/PI staining. In fact, lectin WGA 488 allows staining of bacterial structures containing N-acetylglucosamine and N-acetyl neuraminic acid (sialic acid) residues. The main components of the bacterium were well distinguished when the three channels were split up (Fig. 5.7): the viable endospore (blue), the sugar-based layers (green) surrounding the endospore, and the dead mother cell (red). This last still contained the endospore. The lectin WGA 488 dye highlighted the different features of glycosylated layers. The layer surrounding the endospore was continuous

and thicker than that surrounding the mother cell (Fig. , WGA 488 panel), confirming the presence of more layers - exosporium, coat, and cortex – for spore protection.

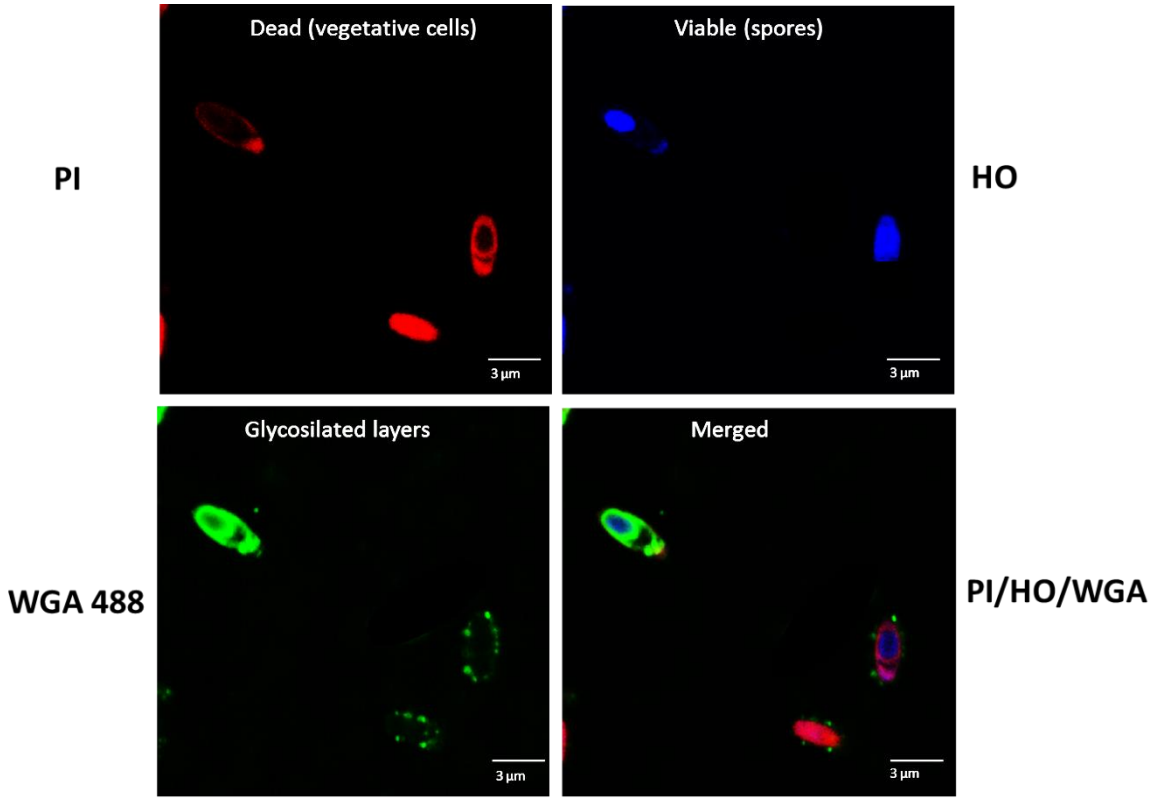

Figure 5.7. CLSM images of *C. tyrobutyricum* stained with Hoechst 34580, Propidium iodide and WGA 488. Images from three layers (PI/HO/WGA) are assembled together in the merged image.

As expected, the double staining HO/PI combined with WGA488 provided more detailed information when the sample was examined by the super resolution microscope. The 3D pictures showed bacterial DNA organized as helical structure inside the spore (Fig. 5.8). The fluorescence of Hoechst dye was very sensitive to DNA conformation and chromatin state in cells so that interesting details were reached.

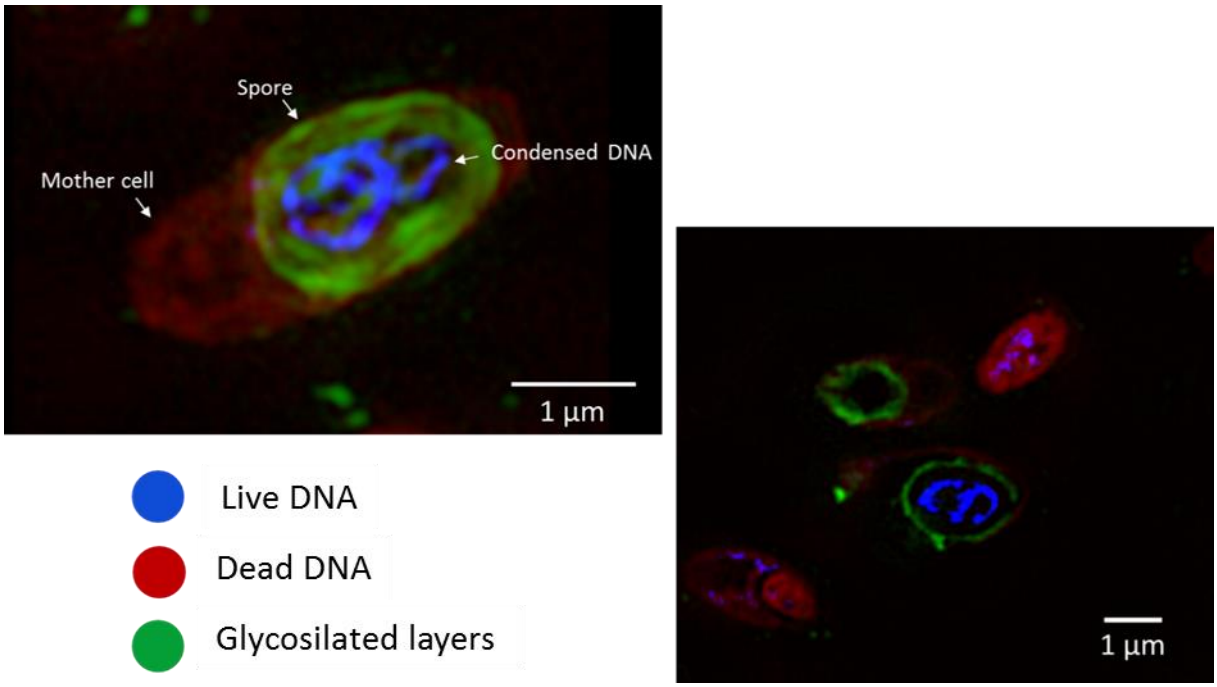

Figure 5.8. Super resolution images of sporulated *C. tyrobutyricum* cells.

5.4 CONCLUSION

A easy-to-apply and robust protocol has been developed for staining endospore-forming *Clostridia* responsible for the late blowing defect in cheese. We specifically focused on the vegetative cells under sporulation conditions induced by heat treatment. The simplicity of the HO/PI staining and the beautiful differentiation between cell and spore obtained with it make fluorescence microscopy a useful tool for studying endospore-forming bacteria.

6. Chapter 6: New insight on crystal and spot development in hard and extra hard cheeses: association of spots with incomplete aggregation of curd granules

6.1 INTRODUCTION

Hard and Extra-Hard are attributes used to define cheeses having a firm and brittle body texture (Codex Alimentarius, 1978). Hard and extra-hard cheeses share low moisture content, close structure, and a long ripening period. During ripening, many chemical, biochemical and microbiological phenomena take place. The biochemical changes are very important for the development of the flavour and texture of these cheeses and are characteristic of the different varieties. Proteolysis is the most relevant among the biochemical phenomena due to its complexity and final impact on the cheese taste. In fact, casein breakdown progressively brings to large and medium peptides, then to small peptides and free amino acids (FAA). Since FAA are rather stable, they tend to accumulate with the ripening time and may reach up to 20-24% on cheese protein basis in 10-12 months old extra-hard cheeses (Masotti et al., 2010). Proteinases and peptidases that catalyse proteolysis in cheese originate from different sources, namely milk, rennet, starter and non-starter lactic acid bacteria (LAB). LAB have complex enzyme patterns that release peptides and amino acids from the proteins into the cheese environment to satisfy their own nutritional requirements (Gatti et al., 2014). After vat processing, the loss of water, diffusion of salt, and formation of soluble molecules, such as FAA and lactate, are factors concurring to the increase of solute concentration and concomitant decrease of water activity (a_w) in cheese throughout the whole ripening period. Beside these main events, minor changes contribute to lower the water activity in cheese, like changes in water binding by new carboxylic and amino groups formed on protein hydrolysis (McSweeney, 2004). The moisture content and a_w are strongly correlated in cheese throughout ripening (Marcos, 1993).

The increasing solute (salt, ions, FAA) concentration in cheese water phase may give rise to aggregation and crystallization phenomena that result in different types of structures observed by some authors in the interior and on the surface of different cheese varieties (Bianchi et al., 1974; Agarwal et al., 2006; Tansman et al., 2015). Although earliest studies date back to the 1900s (Babcock et al., 1903; Tuckey et al., 1938), a clear and unambiguous characterization of these structures has not been achieved yet. Moreover, an univocal association between the terminology (e.g. crystals, specks, dots, granules, spots, pearls) and the appearance of these structures is still lacking.

In long ripened extra-hard cheeses, having a thick dry rind, these structures develop inside the cheese becoming visible when the wheel is cut. Typically, two different types of structures visible

to the naked eye can be observed, referred to as specks and spots in this article. Specks look bright white and firmer against the cheese matrix, and are usually smaller than 2-3 mm. Consumers (cheese lovers) appreciate the crispness of the specks while chewing the cheese and their contribution to the overall cheese taste. Previous studies about specks reported them to contain clusters of tyrosine, cysteine as well as other FAA, calcium lactate and magnesium (Shock et al. 1948) or tyrosine and phenylalanine (Giolitti and Mascherpa, 1970). More recently, Bottazzi et al., (1994) and Tansman et al., (2015) converged on identifying them as tyrosine crystals in extra hard cheeses.

Spots are spherical and paler than the cheese, and can grow up to 4-5 mm. They appear to be amorphous and firmer with respect to the surrounding cheese matrix, and become visible after 10-12 months of ripening. Spots can become so numerous and flashy that may influence the visual appeal of the cheese. Spots have been very little studied, moreover without achieving consistent results (Giolitti and Mascherpa, 1970; Bianchi et al., 1974; Tansman et al., 2015).

Besides specks and spots, extra-hard cheeses contain microscopic crystals, mostly investigated in Cheddar cheese. However, some authors generically referred to crystals, without distinguishing between the microscopic ones and those visible to the naked eye (Kalab, 1980; Bottazzi et al., 1982; Washam et al., 1985; Bottazzi et al., 1994).

The aim of the present work was to shed light on the nature and origin of specks, spots and microscopic crystals in extra-hard cheeses by a multidisciplinary approach. Due to the effectiveness in cheese structure studies (Ong et al., 2010; Schrader et al., 2012; D'Incecco et al., 2015), various microscopy techniques and different dyes (light and fluorescence, confocal, confocal micro Raman and transmission electron microscopy) were used in combination with chemical data to achieve an unambiguous characterization of these particles in cheese. Our ultimate goal was to formulate an hypothesis on the origin of these structures as they appear in hard and extra-hard cheeses. This knowledge will contribute useful information to understanding the bioavailability of selected minerals and nutrients in cheese. Furthermore, this knowledge could provide insights into the nature of these structures that might lead to new manufacturing strategies to control the formation of spots in commercial cheeses.

The work described in this chapter is already published as a research article (D'Incecco et al., 2016).

6.2 MATERIAL AND METHODS

6.2.1 Cheese samples and collection of specks and spots.

Eleven extra-hard cheeses, ripened for 18-20 months, were kindly provided by two dairies producing Grana Padano (7 cheeses) and Parmigiano-Reggiano (4 cheeses) respectively. Specks were harvested from the cheese using a pin, while spots were collected from the cheese using a spatula and then gently brushed to remove the cheese matrix on the surface. Specks and spots were separately collected from individual cheese samples in a sufficient amount (20-22 g) to conduct all the analyses. Equivalent cheese amount was taken from the portion (0.5-cm thick) immediately surrounding the single spot, as shown in Figure 6.1, as used as a term of reference. When necessary, a slice representative of the whole cheese was taken as well. Additional cheese portions were taken as required for microscopy investigations with various techniques. In particular, 20 spots of different size and taken from different cheeses were observed for their structural characterization.

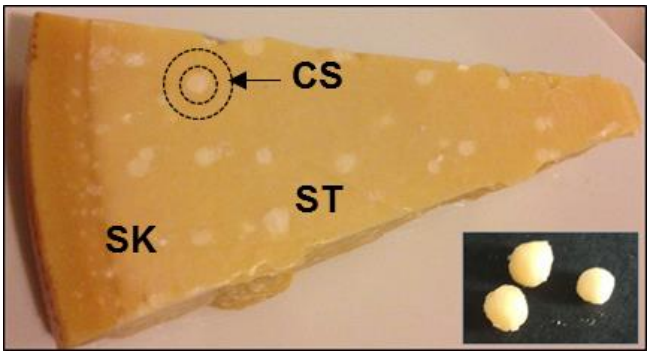

Figure 6.1. Photograph of extra hard cheese showing speaks (SK) and spots (ST). (CS) cheese portion surrounding a spot, sampling mode. Inset, isolated spots from the cheese.

6.2.2 Chemicals

Glutaraldehyde, paraformaldehyde, cacodylate buffer, and osmium tetroxide were purchased from Agar Scientific (Stansted, UK). Toluidine blue, rhodamine and single amino acids were purchased from Sigma Aldrich (Milan, Italy). Ninhydrin was purchased from Biochrom Ltd (Cambridge, UK). Water purified with Milli-Q system (Millipore Corp., Bedford, MA) was used.

6.2.3 Composition analyses

The ISO Standard methods for cheese were used to determine the content of protein (ISO 27871:2011), fat (ISO 1735:2004), ash (ISO 5545:2008) and moisture (ISO5534:2004), respectively. Content of calcium and phosphorus were determined by ICP-MS spectrometer (Agilent Technologies, Milan, Italy).

The pattern of FAA was determined on the various cheese portions (including pecks and spots) using the method described by Masotti et al. (2010). Briefly, the cheese portion was solubilized with sodium citrate, homogenized and deproteinized with sulphosalicilic acid. The extract was diluted (1:1) with lithium citrate buffer at pH 2.2, filtered and analysed by ion exchange chromatography. The chromatographic separation was carried out on a Biochrom 30+ (Biochrom Ltd, Cambridge, UK) amino acid analyser operated under the conditions provided by the manufacturer. These employ an eight-step elution program with lithium citrate buffers of increasing pH and ionic strength, post-column derivatisation with ninhydrin, and detection at 440 and 570 nm. The quantification was carried out using four-level calibration lines of the 21 amino acids in the range 0.75-22.5 mg/L and using norleucine (Sigma Aldrich) as an internal standard. Repeatability values of ISO Standard 13903:2005 were fulfilled.

6.2.4 Amino acid diffusion trial

To confirm the different diffusivity of individual FAA within the cheese, 0.3 mL of an aqueous FAA solution having three times the concentration of the cheese water phase was injected into the core of a spot-free cheese portion (a disk of 10 g) using a microsyringe. The cheese portion was kept in a forced-ventilation thermostatic oven at 18 °C for 18 days and then sampled as described in the Results. The FAA pattern and the moisture content were determined in each sampled portion.

6.2.5 Light and Confocal Microscopy

Specimens for light and fluorescence microscopy observations were thin sections obtained from resin-embedded cheese samples prepared as below described for transmission electron microscopy (TEM). Thin sections (4-5 per sample) were directly dried on the microscope slide, stained and subsequently washed. Two different staining were performed, (i) toluidine blue (1% in water, w/v) for 5 min at room temperature, to visualize the overall protein structure by light microscopy, and (ii) rhodamine B (0.5% in water, w/v) for 5 min at room temperature. In the latter case, the sample was examined by a Hg lamp, with the following filters: excitation wavelength = 570 nm, emission wavelength = 590 nm. In addition a 5-cm cube of cheese was immersed in ninhydrin solution for 1 h and then cut with a blade until a thin section containing a spot was obtained. All samples were

examined with an Olympus BX optical microscope (Tokyo, Japan) equipped with Nomarski interference contrast and QImaging Retiga camera (Surrey, BC, Canada). Specimens for confocal microscopy observations were cryo-sectioned by a CM1950 cryostat (Leica, Germany) and stained directly onto the microscope slide with fast green (0.1 % in water, w/v). Sections were examined with a Video confocal microscope, Nikon Vico (Tokyo, Japan).

6.2.6 Transmission Electron Microscopy

Cubes of cheese (1 mm edge length) were fixed in a mixture (w/v) of glutaraldehyde 3% and paraformaldehyde 2% in cacodylate buffer for 2 h at 4 °C, then washed with cacodylate buffer for 1 h and post-fixed in osmium tetroxide (1% in water, w/v) for 2 h. After the dehydration in an ethanol series, the samples were embedded in London Resin White ™ resin and cured at 60 °C for 24 h. Ultrathin sections (50 to 60 nm thick) were stained with uranyl acetate and lead citrate and examined with a Philips E208 transmission electron microscope (Aachen, Germany).

6.2.7 Confocal Micro Raman

The Raman spectral data were collected in the range from 3200 to 200/cm Raman shift using a confocal DXR Raman Microscope (Thermo Scientific, Waltham, MA, USA). An Olympus 50X objective (numerical aperture 0.75) with a 50 µm confocal pinhole was used to collect the Raman signal directly from a flat area of the sample (cut using a sharp knife) with a spatial resolution lower than 1 µm, without any preparation of the sample. A laser with an excitation wavelength of 780 nm with a low energy power (5-10 mW) to avoid overheating and a 400 lines/mm grating was used to record Raman spectra over the focalized area. A photobleaching time equal to 1 min was set up. For the specks, spectra were collected individually while for the microcrystals a selected area was analysed collecting around 70 spectra over the entire surface, using 10 µm as the interval between positions. In particular, each sample was placed on an automated x,y mapping stage and Raman spectra were obtained at different points of the selected surface, by moving it under the microscope objective. Autofocus at each map point was applied. Omnic Atlµs software (Thermo Fisher Scientific, Madison, WI, USA) was used to obtain Raman spectra, perform spectrometer operations and process data. All spectra were corrected for background contributions and an automated subtraction of cosmic ray peaks was employed.

6.2.8 Statistical analysis

Statistical treatment of data was performed by means of SPSS Win 12.0 program (SPSS Inc., Chicago, IL, USA). Data were analysed by Student's t-test and one way Anova. A $P<0.05$ was assumed as significance limit.

6.3 RESULTS

6.3.1 Speck characterization

Attempts to obtain a section of specks or to embed them in resin failed because they were too hard and packed. In contrast, specks *in toto* could be directly observed by light microscopy after isolation by cheese and showed the characteristic structure of crystalline tyrosine (Figure 6.2). The FAA pattern (Figure 6.2) indicated that specks were indeed tyrosine crystals of > 95% purity. The peak of ammonia in the chromatogram derived from the elution buffers and thus was ignored in purity calculation. The Raman spectrum also confirmed the nature of the specks: the doublet Raman bands at 828 and 848/cm due to the Fermi resonance between ring fundamental and overtone were strongly evident, as was the ring-O stretching vibration located at 1263/cm (Culka et al., 2010). Also the highly resolved bands found in the finger print region (1614-250/cm) were associated to the signals collected for the solid and pure (98-99%) crystalline form of L-tyrosine (spectrum not shown).

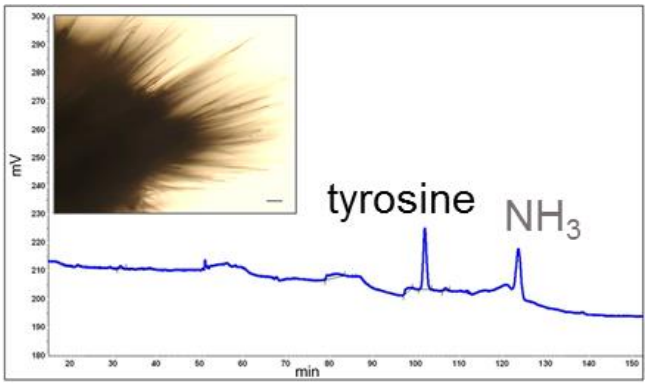

Figure 6.2. Free amino acid analysis and (inset) light microscopy of a speck isolated from cheese. Bar=200 µm.

6.3.2 Spot characterization

Spot structure was firstly examined by light microscopy. A cheese portion was immersed in the protein-staining solution (ninhydrin) and then sectioned up to reveal a spot inside which appeared surrounded by an highly dense layer (Figure 6.3, arrowhead) that impaired staining permeation inside. However, some stain could permeate through preferential micro pathways (junctions, indicated by arrows in Figure 6.3), making the structure visible.

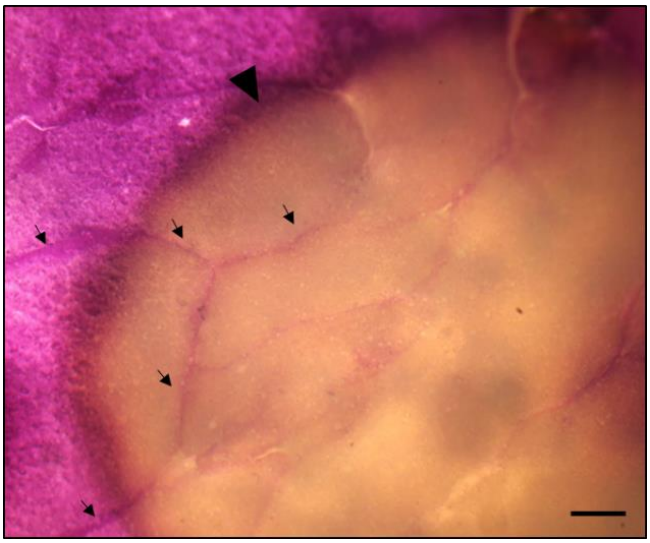

Figure 6.3. Hand-made section of Grana Padano cheese including a spot: light microscopy after ninhydrin staining revealed a dense layer limiting the spot (arrowhead) and the junctions among curd granules (arrows). Bar=200 µm.

Thin sections of resin-embedded spots, stained with toluidine blue, gave more insight of the inner structure (Figure 6.4a). The spot appeared as made of several curd particles having clean-cut irregular shapes and size up to 0.5 mm. The darker lines, corresponding to the junctions among curd particles, were richer in protein than the particle body. Several openings, including a large hole collecting the junctions, were visible in the section (Figure 6.4b). Although the cheese around the spot showed the same composite structure (not shown), large cavities were observed only inside spots. With respect to the curd particles, the junctions appeared as thick protein strings almost free of fat (Figure 6.4c) and rich in microcrystals (arrows). Microcrystals were also observed in the cheese matrix outside the spot, as further discussed.

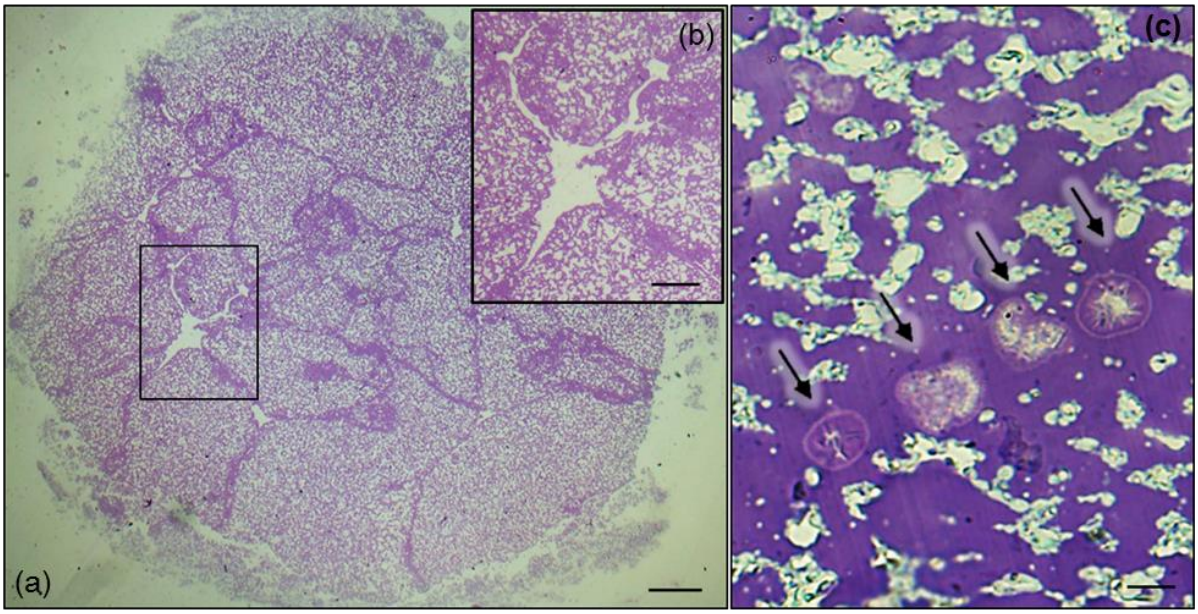

Figure 6.4. Light microscopy of spot semi-thin section (2-5µm) stained with toluidine blue. (a) the curd junctions are visible as darker lines; bar=200 µm. (b): Detail of the large hole in which junctions converge; bar=50 µm. (c) Microcrystals (arrows) along a curd junction; bar=10 µm.

The ultrastructure of the spot, examined by TEM, proved to be remarkably different compared to that of the surrounding cheese (Figure 6.5). In particular, the interface between protein (Figure 6.5, in grey) and fat (in white) was more irregular and fringed by crystal-like particles (Figure 6.5 a) in respect with the cheese surrounding the spot (Figure 6.5 b).

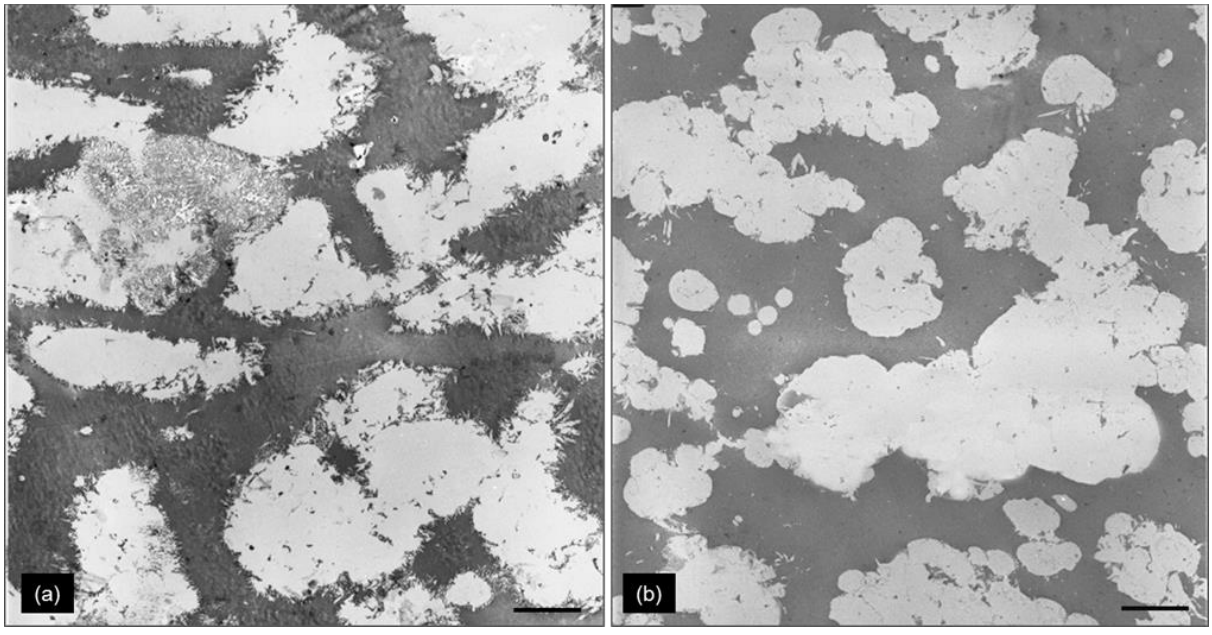

Figure 6.5. Ultrathin section of spot ultrastructure (a) in comparison with the surrounding cheese (b): the network of electron dense (grey) proteins shows a more irregular profile in the spot, particularly at the interface with the electron transparent (white) fat matrix; bar=1 µm.

The chemical composition of the spots was compared to that of the cheese portion just around them and to that of the whole cheese. Five different cheeses were individually analysed (Table 6.1). Spots proved to be significantly richer in protein ($p<0.00$) and poorer in moisture ($p<0.00$) and ash ($p<0.00$) with respect to the surrounding cheese portion, which did not differ from the whole cheese. Fat content was not different ($p<0.17$). The contents of both calcium and phosphorus were 10% lower in the spot than in the cheese, with a Ca/P molar ratio of 1 in both zones (not shown).

Table 6.1. **Chemical composition of spot, cheese portion around it and whole cheese.***

	MOISTURE	FAT	PROTEIN	ASH
SPOT	$24.2^{a} \pm 1.2$	$27.5^{a} \pm 2.6$	$37.6^{a} \pm 1.3$	$3.9^{a} \pm 0.1$
CHEESE AROUND THE SPOT	$29.5^{b} \pm 1.0$	$29.6^{a} \pm 1.2$	$33.5^{b} \pm 0.6$	$4.4^{b} \pm 0.3$
WHOLE CHEESE	$29.8^{b} \pm 1.0$	$29.9^{a} \pm 1.1$	$33.5^{b} \pm 0.2$	$4.4^{b} \pm 0.2$

* Data were mean ± standard deviation based on duplicate analyses of five cheeses.
[a, b] Means in the same column with different letters are significantly different ($p= 0.05$).

The protein fraction was characterized by capillary zone electrophoresis as described in our previous work (Masotti et al., 2010). No difference could be evidenced, neither in casein nor in peptide patterns, between the spots and the rest of the cheese (not shown), indicating that the primary proteolysis had proceeded to the same extent within and outside the spot. On the contrary, significant differences were found in the FAA patterns of the two zones.

In order to compare data of cheese portions (i.e. spots and surrounding cheese) having different moisture contents, and considering that FAA are soluble molecules, values were expressed on the respective moisture content. Furthermore, data from both Grana Padano and Parmigiano-Reggiano were pooled to increase statistical significance. In particular, spots contained significantly higher amounts (from 4 to 12 times) of six FAA, i.e. valine ($p<0.00$), methionine ($p<0.00$), isoleucine ($p<0.00$), leucine ($p<0.00$), tyrosine ($p<0.00$) and phenylalanine ($p<0.00$) (Figure 6.6).

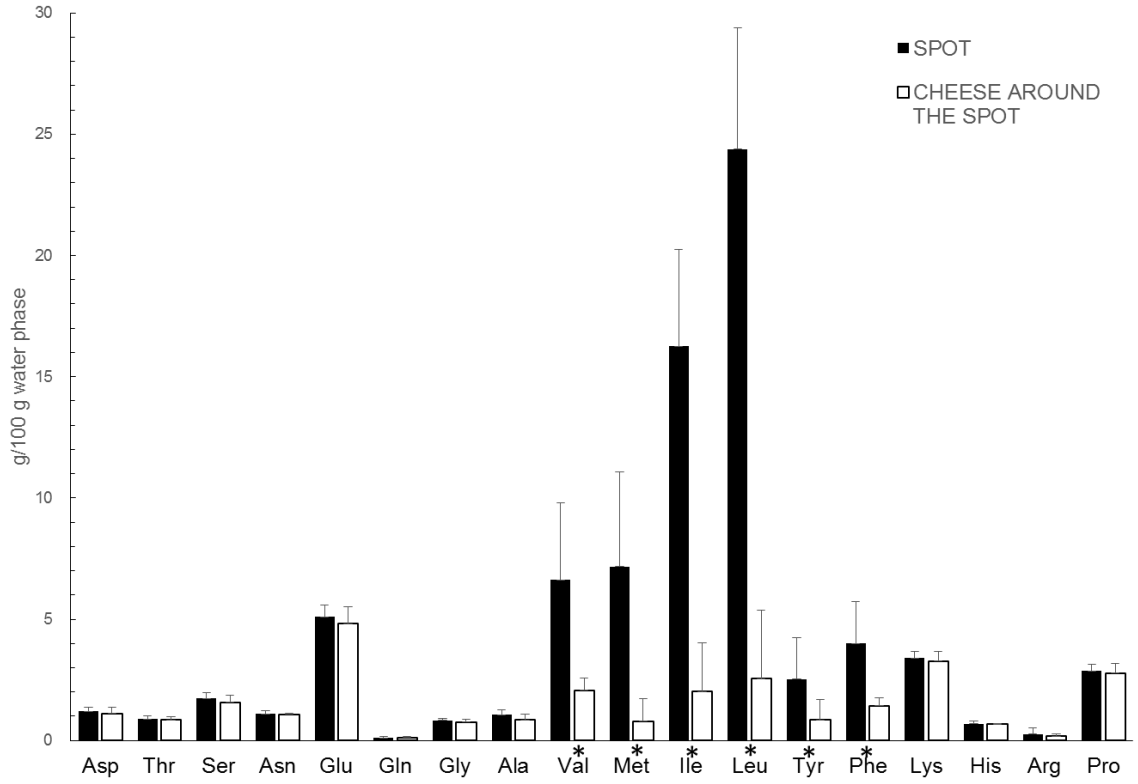

Figure 6.6. Free amino acid content of the spot and the cheese portion around it. Data were mean of duplicate analyses of eleven cheeses. (*) Values statistically different ($p<0.05$).

It is worthy of remark that the content of the other FAA was the same as in the cheese portion around the spot. Nevertheless, this last portion had the usual FAA pattern we observed for the two target cheeses in previous studies (Cattaneo et al., 2008; Masotti et al., 2010). To achieve direct confirmation of such a different composition in individual FAA within the cheese, a simple experiment was carried out. A water solution having the approximate concentration of FAA in cheese water phase was injected into a spot-free cheese slice. After a resting time suitable to allow diffusion of the solution, the cheese was sampled taking three distinct portions: one circular, corresponding to the injection point (mimicking the spot), and two concentric rings around it, as shown in Figure 6.7 (inset). Despite of the approximate experimental conditions and sampling procedure, the obtained data confirmed that the same six FAA were retained in the zone where the mixture was injected, while the others diffused to the surrounding portions largely reaching an equilibrium (Figure 6.7).

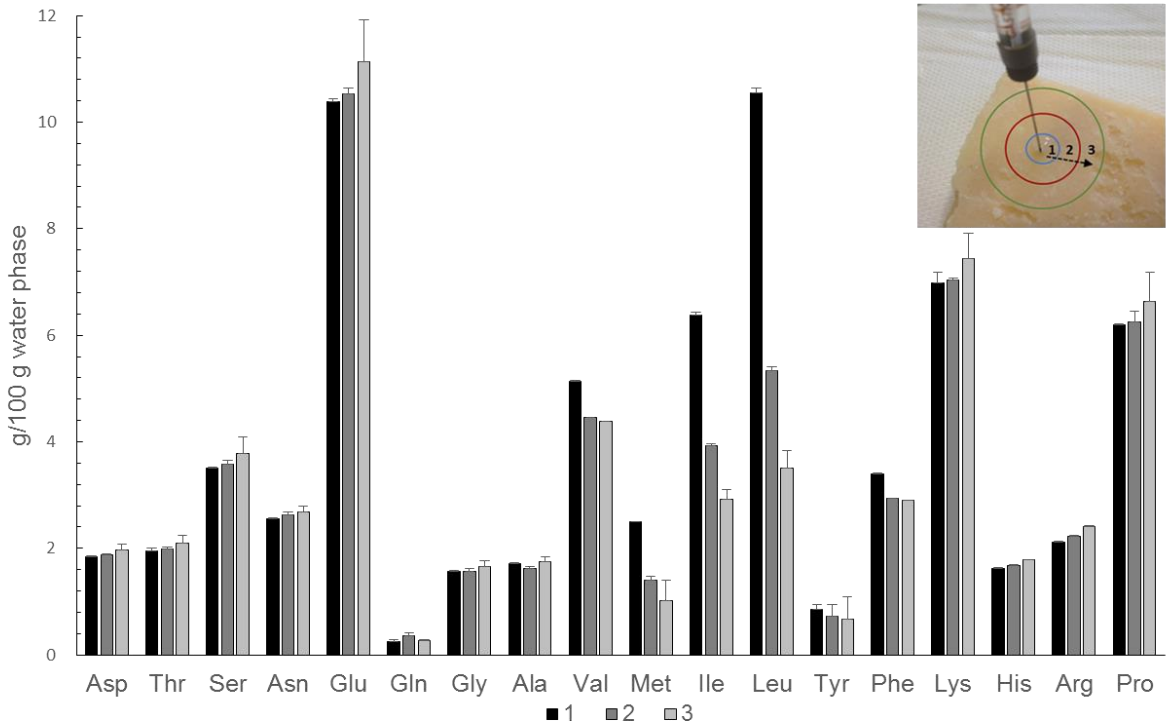

Figure 6.7. Free amino acid content of the portions 1-3 taken from cheese after the diffusion of 0.3 mL aqueous amino acid solution injected in 1 (inset). Data were mean of duplicate analyses.

6.3.3 Microscopic crystals

Microscopic crystals were investigated through various microscopy techniques. Observations by fluorescence microscopy of cheese semi-thin sections, after resin embedding and staining with rhodamine B, allowed to see a huge number of microscopic crystals in bright red (Figure 6.8 a). Confocal microscopy showed that crystals had different shapes, i.e. circular, oval or kidney-shaped, and their core was not fluorescent, indicating a different composition in respect to the peripheral zone (Figure 6.8 b). The number of crystals ranged from 30 to 100 crystals/mm^2 in 18-20 months ripened cheeses and apparently was not different between cheese and inside spots. Crystals with the same structure were detected in younger (three and six months of ripening) extra hard cheeses, although in a lower amount (not shown).

Microscopic crystals observed by TEM showed a complex ultrastructure (Figure 6.8 c). Three main zones could be outlined: (i) a central star-shaped crystal, (ii) an intermediate zone and (iii) a peripheral compact shell at the interface with the protein matrix. Figures 8d shows both the external shell and the intermediate zone to be constituted by fibrils with prismatic morphology, radially ordered and packed around the central crystal.

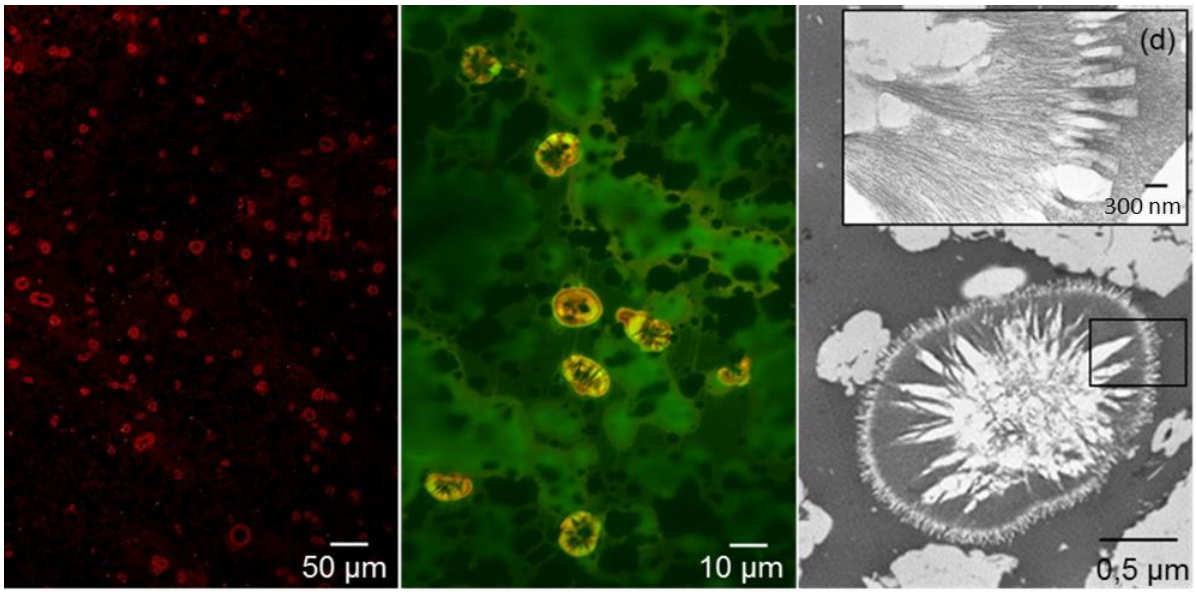

Figure 6.8. Calcium phosphate crystals in cheese. (a) Fluorescence microscopy of crystals stained with rodhamine B. (b) Video confocal microscopy of crystals stained with fast green and observed with TRITC and FITC filters, revealing a non-fluorescent core. (c) Ultrathin section of a crystal showing a star shaped zone in the center; at the interface with protein matrix, the fibrillar structure of the crystal is visible (d).

Confocal Raman microscopy was used to obtain information on the chemical composition since this technique does not require any sample preparation. Area maps of the crystals, detected both inside and outside the spot, confirmed the presence of distinct regions, as observed by TEM. Spectra of the central star shaped crystal matched the calcium phosphate spectrum, dominated by the very strong band at 986/cm and the medium band at 878/cm (Figure 6.9) that derived from the symmetric stretching mode of the phosphate group (Sauer et al., 1994). The band at 1081/cm corresponded to the stretching vibration (υ_3) of PO_4^{3-}, while the band at 588/cm to the P-O and O-P-O stretching and bending modes (υ_4) of the same group.

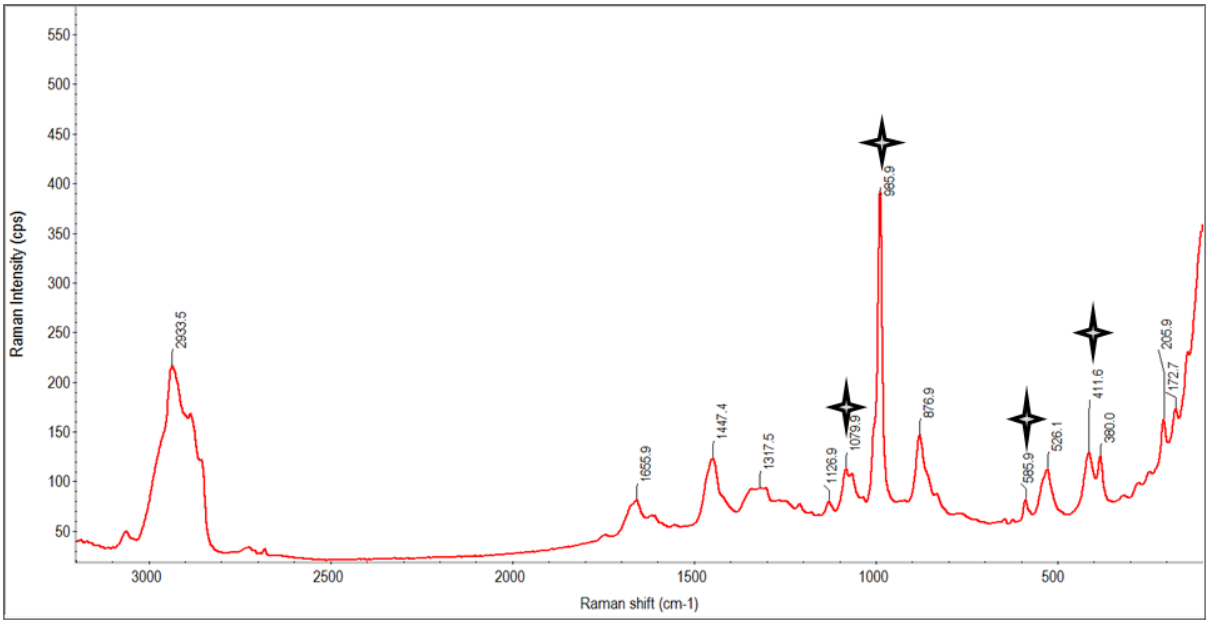

Figure 6.9. Raman spectrum of calcium phosphate crystal in cheese. Stars represent typical signals of the salt.

In calcium phosphate crystals, the minerals can be identified by the position and shape of the main bands. Raman shifts and assignment for some calcium phosphate minerals were studied by Koutsopoulos (2002). The Savitsky-Golay second derivative of the spectra highlighted the presence of other weak bands attributable to the dibasic calcium phosphate dehydrate form. No calcium phosphate was detected in other parts of the complex crystal structure. In fact, in the outer zone, appearing as a dark area in the optical magnification used for the Raman acquisition, spectra presented bands that arose from both free fatty acids and proteins (Figure 6.10 a). The spatial distribution of fatty acid/protein with respect the calcium phosphate within the crystal area is shown in Figure 6.10b (in blue). It is evident that the crystal is immersed in the cheese matrix. A deeper analysis of the spectra of this portion provided a major characterization of the protein structure contribution. Usually, the amide I and III peaks in a protein are less sharply resolved if compared with the signals of small peptides (Jenkins et al., 2005). In other words, Raman spectral signatures of the single amino acids are retained in the peptide or protein, being largely derived from their side chain or backbone. The higher the resolution and intensity of the bands in a complex spectrum, the more probable the contribution of amino acids and/or small peptides. Thus, in the original spectrum collected from the cheese matrix around the phosphate crystal, some peculiar bands of amino acids were evident. In particular, a spectral subtraction of an unsaturated free fatty acid spectrum (considered as a background) from the original spectrum of the external region returned the profile of leucine (match higher than 60% with the pure spectrum of L-leucine) and phenylalanine (match equal to 53% with the pure spectrum of L-phenylalanine). Leucine was mainly characterized by the

bands at 1237/cm due to the twisting of CH_2, and by the bands at 1187 and 1132/cm due to the rocking of NH_3^+, whilst phenylalanine showed a very intense band around 1000/cm. These results indicated that the protein component around the crystal was mainly due to these two amino acids, present in free form or in small peptides.

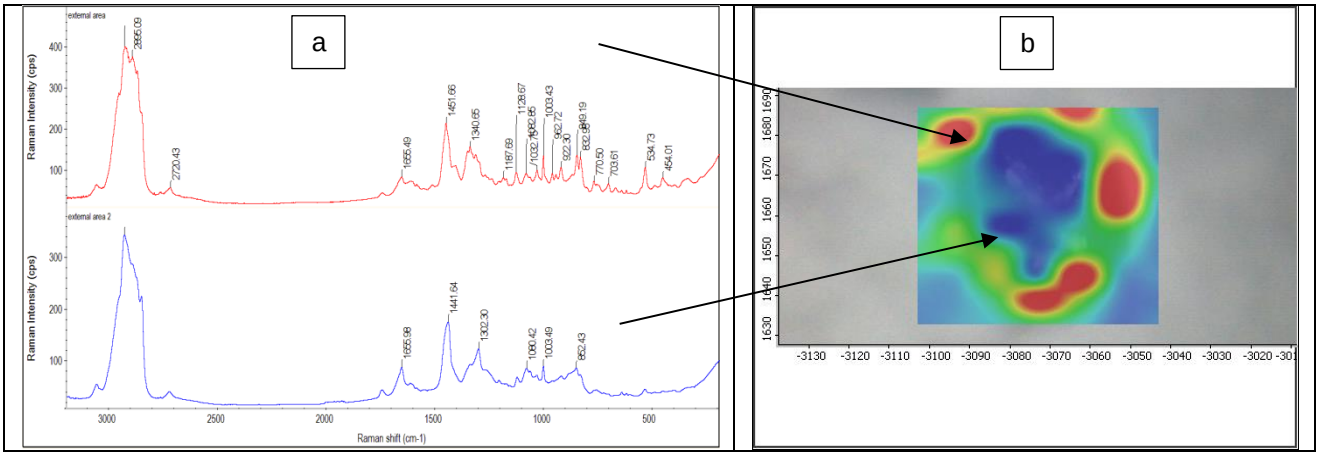

Figure 6.10. Raman spectra (a) and images (b) of spatial distribution of lipid/protein components around the crystal (central dark grey area).

Other crystalline structures were randomly detected within the cheese and analysed by means of micro Raman spectroscopy. Only calcium carbonate crystals were identified so far. They appeared spheroidal in shape and translucent: the peaks at 1083, 1410, 713 and 284/cm confirmed their nature (Tlili et al., 2001) (data not shown). The presence of calcium carbonate in cheese seems to be attributable to the microbial metabolism that produces CO_2 (Gaucheron et al. 1999).

6.4 DISCUSSION

6.4.1 Speck characterization

By evaluating the confocal micro Raman spectrum and FAA composition of specks we obtained a tyrosine purity >95% confirming previous reports indicating the presence of this amino acid in these structures (Bottazzi et al., 1994; Tansman et al., 2015). Free tyrosine concentration increases in the whole cheese throughout the ripening process, like for all other FAA (Pellegrino et al., 1997). In our samples of Grana Padano and Parmigiano-Reggiano, free tyrosine concentration was approximately 0.8 g / 100 g of water phase (Figure 6.6), i.e. about ten times higher than its water solubility at room temperature (Grosse Daldrup et al., 2010). Therefore, formation of crystals spread within the cheese would suggest that progress of proteolysis is not homogeneous in the matrix thus leading to FAA accumulation, including tyrosine, preferentially into micro openings until saturation. Furthermore, we have obtained by light microscopy further structural details of tyrosine crystals from cheese (Figure 6.2), showing that the former reported description (Tansman et al., 2015) is due to micro spike of the crystalized amino acid. When observed by atomic force microscopy in protein hydrolysates (McPherson et al., 2012), tyrosine crystals appeared to be covered by a stable layer of 3-nm particles, likely represented by micellar arrangement of small peptides present in the medium and able to prevent re-solubilisation of crystals once formed. Considered the remarkable content of peptides in ripened cheeses, this aspect would be worthy of investigation.

6.4.2 Spot characterization

Contrary to the hard specks, spots were easily resin embedded and cut into thin sections that allowed a deeper characterization by various microscopy techniques. Previous studies on spots in cheese did not investigate their structure and ultrastructure (Giolitti and Mascherpa, 1970; Bianchi et al. 1974; Tansman et al., 2015). Unexpectedly, when the cheese was directly stained with ninhydrin and observed by light microscopy, the original grains of curd were still visible. During cheese manufacturing, curd grains (20-50 mm), obtained by cutting the rennet gel, are let in hot whey for 50-60 min to settle and aggregate at the bottom of the vat. Further fusing and shrinking of curd grains are induced by the subsequent acidification of the cheese loaf when kept in mould for 48 hours. Since Grana Padano and Parmigiano-Reggiano loaves are not pressed, high temperature and low pH (5.2-5.3) play the major role in promoting whey draining (Pellegrino et al., 1997) and the tight aggregation of curd grains. However, as said above, these grains appeared as separate units even several months later. The junctions between contiguous grains are low in fat because many fat

globules escape the protein network at the surface of the grains before they stick together. For those grains having either irregular shape or different size their aggregation during settling forms an internal hole, connected with several openings and radial junctions. This pattern was frequently observed within the spots (Figure 6.3 b). In the young cheese, even before the spot formation, these hollow cavities likely represent preferential zones where whey stagnates and entrapped bacterial cells find substrates for growth (Le Boucher et al., 2016). Growth of bacterial colonies as affected by local concentration of substrates in cheese is receiving increasing attention (Silva et al., 2013; Jeanson et al., 2015). Although no intact bacterial cells were detected by TEM in cavities within the spot, as well as in the surrounding cheese, likely due to the prolonged ripening process, an indirect, preliminary confirmation of this hypothesis came out by measuring the amount of total DNA extracted from the spot and the surrounding cheese following the procedure of (Cremonesi et al., 2007). In fact, DNA amount was more than three times higher in the spots than in the surrounding cheese (72.94 µg *vs* 22.41 µg/mg).

Spots proved to be significantly more dry, with respect to the surrounding cheese portion, and to contain more protein and less ash (Table 6.1), confirming the data reported by Tansman et al. (2015). In addition, we showed the cheese portion just around the spot had the same chemical composition as the rest of the cheese, confirming that the spot is a fully isolated unit. The dense layer we observed around it by light microscopy is likely responsible for this (Figure 6.3, arrowhead). Overall, these findings point to a migration of whey, with consequent draining of solutes, occurring locally within the cheese where the spot would originate later.

Spots were also reported to have a different FAA composition compared to the whole cheese. Bianchi et al. (1974) found spots in 18- and 25-month ripened Grana Padano cheeses to contain (g/100 g): leucine (9.86), isoleucine (4.96), methionine (1.64), valine (1.52), glutamic acid (1.84), and asparagine (1.63), as dominant FAA. However, these authors did not notice that the last two FAA were equally abundant in the whole cheese. Recently, Tansman et al. (2015) detected only 1% of free leucine in spots from a 24-month old Parmigiano-Reggiano cheese but they did not give explanation for the discrepancy of this result with those of literature. We obtained FAA data similar to those of Bianchi et al. (1974), however we put forward a different interpretation. The key to understand the genesis of the spot relays in the chemical properties of the different FAA present in the spot and in the cheese regardless of their concentration. In fact, the six FAA we detected at much higher levels in the spot (i.e. leucine, isoleucine, methionine, valine, phenylalanine and tyrosine) (Figure 6.6) are all hydrophobic because of either the aromatic or branched chain structure, and thus insoluble in the water phase of cheese. This shared FAA characteristic leads us to hypothesise that local water movements are responsible for their different distribution and,

consequently, for the spot blowing in hard and extra hard cheeses. This hypothesis was confirmed by our experiment mimicking the migration of FAA within the cheese.

As already mentioned, in young cheese the cavities in which the residual whey stagnates could be the sites where bacterial colonies develop. During cheese ripening, the water phase in these sites becomes more concentrated in solutes due to lactic acid bacteria metabolism and, at a later stage, to cell lysis. Progressively, the water phase migrates through the curd grain junctions, dragging solutes including, preferentially, polar FAA over the hydrophobic ones. Consequently, less water soluble molecules concentrate in a restricted area, that evolves into a spot, from which water moves away radially (Figure 6.7) dragging away also salts. For this reason, many crystals were visible in the junctions (Figure 6.4 c).

6.4.3 Microscopic crystal characterization

Microcrystals appeared to be spread within the whole cheese. Among these crystals we have up to now identified calcium phosphate by micro Raman, directly on the cheese, without any sample preparation. The central star shaped crystals observed by TEM (Figure 8c) were clearly assigned to selected types of calcium phosphate. Gaucheron et al. (1999) demonstrated that the supersaturation of calcium phosphate salts increases strongly during cheese ripening due to the rise of pH, explaining the salt precipitation. Unfortunately, the few references that discuss crystals ultrastructure in cheese give no indication about the nature of the calcium phosphate. In our study, the micro Raman analysis produced sufficient information about their morphological features and complex ultrastructure. In fact, this technique allowed to evidence for the first time that the fibrillary layer surrounding the central crystal contains leucine and, to a lower amount, phenylalanine. These hydrophobic amino acids are reported to limit growth of calcium phosphate crystals due to their absorption on the crystal surface that blocks the active growth sites (Dalas et al., 2008). Although calcium lactate could form in cheese, due to lactic acid fermentation, the chelation of calcium by the phosphates should greatly prevail (Heertje et al., 1981), in agreement with the relevant number of calcium phosphate crystals we detected. Arkwall et al. (2006) reported that calcium lactate crystals only form when pH is higher than 5.1. We could not find calcium lactate crystals, although we cannot exclude their presence in extra hard cheeses, as different unidentified crystalline structures were observed by TEM. Some researcher detected calcium lactate crystals in cheeses other than Grana Padano and Parmigiano-Reggiano (Washam et al., 1982; Tansman et al., 2014), whereas only Bottazzi et al. (1982) detected them in 14-month ripened Grana cheese indicating their low incidence, i.e. 2-3 per square mm.

Presence of leucine crystals is likely within the spot where free leucine showed a concentration in the water phase ten times higher than in the cheese (Figure 6.6). Crystalline leucine was also detected by Tansman et al. (2015) in pearls collected from Parmigiano-Reggiano cheese.

6.5 CONCLUSIONS

In conclusion, combining the background knowledge about extra-hard cheese manufacturing and ripening with the new information about composition and structure of spots achieved in this study, we can hypothesize an incomplete aggregation of curd granules and a consequent local whey stagnation to be at the origin of spot development. Growth and lysis of bacterial cells entrapped in these micro cavities influence both metabolite availability and micro environmental conditions, that in turn regulate diffusion and crystallization of solutes locally. Therefore, all practices finalized to the syneresis improvement, such as fine-tuning of temperature control and curd grain size, would greatly reduce spot number and the occurrence of other confined phenomena.

REFERENCES

Abo-Elnaga, G., N. H. Metwally, and El-M. M. El-Mansy. 1981. The bacterial content of creamed milk. Archiv Lebensmittelhyg. 32:19-21.

Agarwal, S., J. R. Powers, B. G. Swanson, S. Chen, and S. Clark. 2006. Cheese pH, protein concentration, and formation of calcium lactate crystals. J. Dairy Sci. 89: 4144-4155.

Agarwal, S., K. Sharma, B. G. Swanson, G. U. Yüksel, and S. Clark. 2006. Nonstarter lactic acid bacteria biofilms and calcium lactate crystals in Cheddar cheese. J. Dairy Sci. 89: 1452–1466.

Ayyar, B. V., Arora, S., Murphy, C., & O'Kennedy, R. 2012. Affinity chromatography as a tool for antibody purification. *Methods*, *56*(2), 116-129.

Ávila, M., Gómez-Torres, N., Hernández, M., & Garde, S. 2014. Inhibitory activity of reuterin, nisin, lysozyme and nitrite against vegetative cells and spores of dairy-related Clostridium species. International Journal of Food Microbiology, 172, 70-75.

Ávila, M., Gómez-Torres, N., Delgado, D., Gaya, P., & Garde, S. 2016. Application of high pressure processing for controlling Clostridium tyrobutyricum and late blowing defect on semi-hard cheese. *Food Microbiology*, *60*, 165-173.

Barbiroli, A., Bonomi, F., Casiraghi, M. C., Iametti, S., Pagani, M. A., & Marti, A. 2013. Process conditions affect starch structure and its interactions with proteins in rice pasta. *Carbohydrate polymers*, *92*(2), 1865-1872.

Babcock, S. M. 1889. The constitution of milk, and some of the conditions which affect the separation of cream. University of Wisconsin Agricultural Experiment Station Bulletin 18: 3-35.

Babcock, S. M., L. H. Russel, A. Vivian, and U. S. Baer. 1903. Condition affecting the development of white specks in cold-curd cheese. Pages 180-183 in Wis. Agric. Expt. Sta. 19th Annu. Rep.

Bassi, D., F. Cappa, and P. S. Cocconcelli. 2009. A combination of a SEM technique and X-ray microanalysis for studying the spore germination process of *Clostridium tyrobutyricum*. Res. Microbiol. 160:322-329.

Bassi, D., Puglisi, E., & Cocconcelli, P. S. 2015. Understanding the bacterial communities of hard cheese with blowing defect. *Food microbiology*, *52*, 106-118.

Beam, A. L., Lombard, J. E., Kopral, C. A., Garber, L. P., Winter, A. L., Hicks, J. A., & Schlater, J. L. 2009. Prevalence of failure of passive transfer of immunity in newborn heifer calves and associated management practices on US dairy operations. *Journal of dairy science*, *92*(8), 3973-3980.

Bergère J. L., and Hermier J. 1970. Spore properties of Clostridia occurring in cheese. J. app. Bact. 33:167-179.

Bergère, J. L., and J. Lenoir. 2000. Ripening Defects. Pages 484-506 in Cheese manufacturing accidents and cheese defects. Cheesemaking/from science to quality assurance. Second Edition. André Eck and Jean-Claude Gillis, ed. Lavoisier Publishing, Paris, France.

Bermúdez, J., González, M. J., Olivera, J. A., Burgueño, J. A., Juliano, P., Fox, E. M., & Reginensi, S. M. 2016. Seasonal occurrence and molecular diversity of clostridia species spores along cheesemaking streams of 5 commercial dairy plants. Journal of Dairy Science, 99, 1-9.

Bester, B.H., Lombard, S.H., 1990. Influence of lysozyme on selected bacteria associated with Gouda cheese. J. Food Prot. 53, 306-311.

Bianchi, A.; G. Beretta, G. Caserio, and G. Giolitti. 1974. Amino acid composition of granules and spots in Grana Padano cheeses. J. Dairy Sci. 57: 1504–1508.

Bosi, F., G. Scolari, V. Bottazzi, and F. Dellaglio. 1984. Morfologia delle spore, DNA-DNA ibridizzazione e esami HCLP dei prodotti della fermentazione dei clostridi del formaggio grana. Sci. Tecn. Latt. Cas. 35:7-19.

Bottari, B., Santarelli, M., Neviani, E., Gatti, M., 2010. Natural whey starter for Parmigiano Reggiano: culture-independent approach. J. Appl. Microbiol. 108, 1676-1684.

Bottazzi V. 1971. Sui fenomeni di agglutinazione nella preparazione del latte nel formaggio grana. Sci. Tecn. Latt. Cas. 22:253-273.

Bottazzi, V., and F. Dellaglio. 1970. Sulla presenza di spore di clostridi nel latte di produzione invernale e sulla comparsa di colonie di clostridi nel formaggio grana. Sci. Tecn. Latt. Cas. 21:59-72.

Bottazzi, V., B. Battistotti, and F. Bianchi. 1982. The microscopic crystalline inclusions in Grana cheese and their x-ray microanalysis. Milchwissenschaft Milk Sci. Internat. 37: 577–580.

Bottazzi, V., F. Lucchini, A. Rebecchi, and G. L. Scolari. 1994. I cristalli del formaggio grana (Crystals present in Grana cheese). Sci. Tecn. Latt.-Cas. 45: 7–14.

Bottazzi V., F. Dellaglio and P. G. Sarra. 1972. Affioramento del grasso ed agglutinazione dei microrganismi. Sci. Tecn. Latt. Cas. 23:287-304.

Bottazzi V., and C. Zacconi. 1980. Isolamento e prima caratterizzazione del principio attivo nell'aggregazione dei globuli di grasso e dei batteri. Sci. Tecn. Latt. Cas. 31:379-394.

Bove, C.G., De Dea Lindner, J., Lazzi, C., Gatti, M., Neviani, E., 2011. Evaluation of genetic polymorphism among Lactobacillus rhamnosus non-starter Parmigiano Reggiano cheese strains. Int. J. Food Microbiol. 144, 569-572.

Bove, C.G., De Angelis, M., Gatti, M., Calasso, M., Neviani, E., Gobbetti, M., 2012. Metabolic and proteomic adaptation of Lactobacillus rhamnosus strains during growth under cheese-like environmental conditions compared to de Man, Rogosa, and Sharpe medium. Proteomics 12, 3206-3218.

Brandsma, J.B., van de Kraats, I., Abee, T., Zwietering, M.H., Meijer, W.C., 2012. Arginine metabolism in sugar deprived Lactococcus lactis enhances survival and cellular activity, while supporting flavour production. Food Microbiol. 29, 27-32.

Brandtzaeg, P.; and Johansen, F.E. IgA and intestinal homeostasis. In *Mucosal Immune Defense: Immunoglobulin A*; Kaetzel, C.S., Ed.; Springer: New York, NY, USA, 2007; pp. 221–268.

Brasca M., Hogenboom J., Morandi S., Rosi V., D'Incecco P., Silvetti t. Pellegrino L. 2016. Proteolytic Activity and Production of γ-Aminobutyric Acid by Streptococcus thermophilus Cultivated in Microfiltered Pasteurized Milk, Journal of Agricultural and Food Chemistry, 64, 8604-8614.

Brasca, M., Morandi, S., Silvetti, T., Rosi, V., Cattaneo, S., Pellegrino, L., 2013. Different analytical approaches in assessing antibacterial activity and the purity of commercial lysozyme preparations for dairy application. Molecules 18, 6008–6020.

Brunt, Jason, Kathryn L. Cross, and Michael W. Peck. 2015. "Apertures in the Clostridium sporogenes spore coat and exosporium align to facilitate emergence of the vegetative cell." Food microbiology 51: 45-50.

Buchheim, W. 1986. Membranes of milk fat globules – ultrastructural, biochemical and technological aspects. Kieler Milchwirtschaftliche Forschungsberichte. 38:227-246.

Butler, J. E. 1973. Synthesis and distribution of immunoglobulins. *Journal of the American veterinary medical association*.

Caplan, Z., C. Melilli, and D. M. Barbano. 2013. Gravity separation of fat, somatic cells, and bacteria in raw and pasteurized milks. J. Dairy Sci. 96:2011-2019.

Carini, S., Mucchetti, G., Neviani, E., 1985. Lysozyme: activity against Clostridia and use in cheese production - a review. Microbiol. Alim. Nutr. 3, 299-320.

Cattaneo, S., Hogenboom, J. A., Masotti, F., Rosi, V., Pellegrino, L., Resmini, P., 2008. Grated Grana Padano cheese: new hints on how to control quality and recognize imitations. Dairy Sci. Technol. 88, 595–605.

Cerf, O., Berge`re, J.L., Hermier, J. 1967. Termoresistence des spores de *Clostridium tyrobutyricum* et *Clostridium butyricum*. J. *Dairy Res.* 34, 221.

Christiansen, J.K., Hughes, J.E., Welker, D.L., Rodriguez, B.T., Steele, J.L., Broadbent, J.R., 2008. Phenotypic and genotypic analysis of amino acid auxotrophy in Lactobacillus helveticus CNRZ 32. Appl. Envir. Microbiol., 74, 416-423.

CLAL web site, 2016. http://www.clal.it

Cocolin, L., Innocente, N., Biasutti, M., & Comi, G. 2004. The late blowing in cheese: a new molecular approach based on PCR and DGGE to study the microbial ecology of the alteration process. *International Journal of Food Microbiology*, *90*(1), 83-91.

Codex General Standard for Cheese. Codex Standard 283-1978.

Cosentino, C., Paolino, R., Valentini, V., Musto, M., Ricciardi, A., Adduci, F., & Freschi, P. 2015. Effect of jenny milk addition on the inhibition of late blowing in semihard cheese. *Journal of dairy science*, *98*(8), 5133-5142.

Cremonesi, P., G. Perez, G. Pisoni, P. Moroni, S. Morandi, M. Luzzana, M. Brasca, and B. Castiglioni. 2007. Detection of enterotoxigenic Staphylococcus aureus isolates in raw milk cheese. Lett. Appl. Microbiol. 45: 586–591.

Cremonesi, P., L. Vanoni, T. Silvetti, S. Morandi, and M. Brasca. 2012. Identification of *Clostridium beijerinckii*, *Cl. butyricum*, *Cl. sporogenes*, *Cl. tyrobutyricum* isolated from silage, raw milk and hard cheese by a multiplex PCR assay. J. Dairy Res. 79:318-323.

Culka, A., J. Jehlicka, and H. G. M. Edwards. 2010. Acquisition of Raman spectra of amino acids using portable instruments: Outdoor measurements and comparison. Spectrochim. Acta A. 77: 978–983.

Dalas, E., P. Malkaj, Z. Vasileiou, and D. G. Kanellopoulou. 2008. The effect of Leucine on the crystal growth of calcium phosphate. J. Mater. Sci.: Mater. Med. 19: 277-282.

Dellagio, F., J. Stadhouders, and G. Hup. 1969. Distribution of bacteria between the bottom, middle, and cream layers of creamed raw milk. Neth. Milk Dairy J. 23:140-145.

Diana, M., Rafecas, M., Arco, C., Quilez, J., 2014. Free amino acid profile of Spanish artisanal cheeses: importance of gamma-aminobutyric acid (GABA) and ornithine content. J. Food Comp. Anal. 35, 94-100.

D'Incecco, P., Faoro, F., Silvetti, T., Schrader, K., & Pellegrino, L. 2015. Mechanisms of Clostridium tyrobutyricum removal through natural creaming of milk: A microscopy study. *Journal of dairy science*, *98*(8), 5164-5172.

D'Incecco, P., Gatti, M., Hogenboom, J. A., Bottari, B., Rosi, V., Neviani, E., & Pellegrino, L. 2016. Lysozyme affects the microbial catabolism of free arginine in raw-milk hard cheeses. Food microbiology, 57, 16-22.

El Kafsi, H., Binesse, J., Loux, V., Buratti, J., Boudebbouze, S., Dervyn, R., Kennedy, S., Gallerom, N., Quinquis, B., Batto, J., Moumen, B., Maguin, E., van de Guchte, M., 2014. BMC Genomics 15, 407-418.

El-Loly, M. M. 2007. Identification and quantification of whey immunoglobulins by reversed phase chromatography. *Int. J. Dairy Sci.*, *2*(3), 268-274.

Euber, J. R., and J. R. Brunner. 1984. Reexamination of fat globule clustering and creaming in cow milk. J. Dairy Sci. 67:2821-2832.

European Parliament and Council. 2012. Regulation (EU) No. 1151/2012 on quality schemes for agricultural products and foodstuffs. European Union Official Journal L343, 4.12.2012, pp.1-29. http://www.granapadano.it/assets/documenti/pdf/disciplinare.pdf

European Union Regulation, 2011a. Regulation nr. 584, EU OJ nr. 160/65, 18 Giugno 2011.

European Union Regulation, 2011b. Regulation nr. 794, EU OJ nr. 204/19, 9 August 2011.

European Union Regulation, 2012. Regulation nr. 1151, EU OJ nr. 343/1, 14 December 2012.

Evers, J. M. 2004. The milk fat globule membrane–compositional and structural changes post secretion by the mammary secretory cell. Int. Dairy J. 14:661-674.

Evers, J. M. 2008. Novel analytical techniques for studying the milk fat globule membrane. Ph.D Thesis. Massey University, Palmerston North, New Zealand.

Evers, J. M., R. G. Haverkamp, S. E. Holroyd, G. B. Jameson, D. D. S. Mackenzie & O. J. McCarthy. 2008. Heterogeneity of milk fat globule membrane structure and composition as observed using fluorescence microscopy techniques. *Int. Dairy J*. 18:1081-1089.

Elwell, M. W., & Barbano, D. M. 2006. Use of microfiltration to improve fluid milk quality. *Journal of dairy science*, *89*, E20-E30.

Farrel, H.M., Jr., Jimenez-Flores, R., Bleck, G.T., Brown, E.M., Butler, J.E., Creamer, L.K., Hicks, C.L., Hollar, C.M., Ng-Kwai-Hang, K.F., Swaisgood, H.E., 2004. Nomenclature of the proteins of cows' milk: sixth revision. J. Dairy Sci. 87, 1641-1674.

Ferranti, P., Barone, F., Chianese, L., Addeo, F., Scaloni, A., Pellegrino, L., Resmini, P., 1997. Phosphopeptides from Grana Padano cheese: Nature, origin and changes during ripening. J. Dairy Res. 64, 601–615.

Fortina, M.G., Nicastro, G., Carminati, D., Neviani, E., Manachini, P.L., 1998. *Lactobacillus helveticus* heterogeneity in natural cheese starters: The diversity in phenotypic characteristics. J. Appl. Microbiol. 84, 72–80.

Foster, S. J., & Johnstone, K. 1990. Pulling the trigger: the mechanism of bacterial spore germination. *Molecular microbiology*, *4*(1), 137-141.

Franciosi, E., De Sabbata, G., Gardini, F., Cavazza, A., & Poznanski, E. 2011. Changes in psychrotrophic microbial populations during milk creaming to produce Grana Trentino cheese. *Food microbiology*, *28*(1), 43-51.

Fredrick, E., Walstra, P., & Dewettinck, K. 2010. Factors governing partial coalescence in oil-in-water emulsions. *Advances in Colloid and Interface Science*, *153*(1), 30-42.

Frenyo, V. L., J. E. Butler, and A. J. Guidry. 1986. The association of extrinsic bovine IgG1, IgG2, SIgA and IgM with the major fractions and cells of milk. Vet. Immunol. Immunopathol. 13:239-254.

Fröhlich-Wyder, M-T., Bisig, W., Guggisberg, D., Irmler, S., Jakob, E., Wechsler, D., 2015. Influence of low pH on the metabolic activity of *Lactobacillus buchneri* and *Lactobacillus parabuchneri* strains in Tilsit-type model cheese. Dairy Sci. Technol. DOI: 10.1007/s13594-015-0238-1.

Galassi, L., E. Salimei, and M. Zanazzi. 2012. Impiego del latte di asina in sostituzione di lisozima da uovo nella produzione del formaggio duro italiano: Prime esperienze (Grana Padano cheese making with lysozyme from ass's milk: First results). J. Italian Dairy Sci. Assoc. 63:73–79. (AITeL).

Garde, S., Ávila, M., Gaya, P., Arias, R., & Nuñez, M. 2012. Sugars and organic acids in raw and pasteurized milk Manchego cheeses with different degrees of late blowing defect. *International Dairy Journal*, *25*(2), 87-91.

Gatti, M., Lindner, J.D.D., De Lorentiis, A., Bottari, B., Santarelli, M., Bernini, V., Neviani, E., 2008. Dynamics of whole and lysed bacterial cells during Parmigiano-Reggiano cheese production and ripening. Appl. Environ. Microbiol. 74, 6161-6167.

Gatti, M., Bottari, B., Lazzi, C., Neviani, E., Mucchetti, G., 2014. Invited review: Microbial evolution in raw-milk, long-ripened cheeses produced using undefined natural whey starters. J. Dairy Sci. 97, 573-591.

Gaucheron, F., Y. Le Graet, F. Michel, V. Briard and M. Piot. Evolution of various salt concentrations in the moisture and in the outer layer and centre of a model cheese during its brining and storage in ammoniacal atmosphere. Lait. 79: 553-566.

Geer, S. R., and D. M. Barbano. 2014a. Effect of colostrum on gravity separation of milk somatic cells in skim milk. J. Dairy Sci. 97:687-693.

Geer, S. R., and D. M. Barbano. 2014b. The effect of immunoglobulins and somatic cells on the gravity separation of fat, bacteria, and spores in pasteurized whole milk. J. Dairy Sci. 97:2027-2038.

Giolitti, G. and G. F. Mascherpa. 1970. La formazione di depositi di tirosina in formaggi a lunga stagionatura. Ind. Latte. 6: 83-85.

Gómez-Torres, N., Ávila, M., Gaya, P., & Garde, S. 2014. Prevention of late blowing defect by reuterin produced in cheese by a Lactobacillus reuteri adjunct. *Food microbiology*, *42*, 82-88.

Goudswaard, J., Virella, G., & Noordzij, A. 1979. Difference in hydrophobicity of human and animal IgA. *Comparative immunology, microbiology and infectious diseases*, *1*(3), 163-168.

Gould, G. W., & Sale, A. J. H. 1970. Initiation of germination of bacterial spores by hydrostatic pressure. *Microbiology*, *60*(3), 335-346.

Grosse Daldrup, J. B., C. Held, F. Ruether, G. Schembecker, and G. Sadowski. 2009. Measurement and modeling solubility of aqueous multisolute amino-acid solutions. Ind. Eng. Chem. 49: 1395–1401.

Heertje, I., M. J. Boskamp, F. Van Kleef, and F. H. Gortemaker. 1981. The microstructure of processed cheese. Neth. Milk Dairy J. 35, 177.

Honkanen-Buzalski T., and M. Sandhom. 1981. Trypsin-inhibitors in mastitic milk and colostrum: correlation between trypsin in inhibitor capacity, bovine serum albumin and somatic cell contents. J. Dairy Res. 48:213-223.

Hughey, V.L., Jonhson E.A., 1987. Antimicrobial activity of lysozyme against bacteria involved in food spoilage and food-borne disease. Appl. Environ. Microbiol. 53, 2165–2170.

Hunziker, W.; Kraehenbuhl, J.-P. 1998. Epithelial transcytosis of immunoglobulins. *J. Mammary Gland Biol. Neoplasia*, *3*, 287–302.

Hurley, W. L., & Theil, P. K. (2011). Perspectives on immunoglobulins in colostrum and milk. *Nutrients*, *3*(4), 442-474.

Jeanson, S., J. Floury, V. Gagnaire, S. Lortal, and A. Thierry. 2015. Bacterial colonies in solid media and foods: a review on their growth and interactions with the micro-environment. Front. Microbiol. 6: 1284.

Jenkins, A. L., R. A. Larsen, and T. B. Williams. 2005. Characterization of amino acids using Raman spectroscopy. Spectrochim. Acta A. 61: 1585–1594.

Jiménez-Saiz, R., Gordon, M. E., Carrillo, W., 2013. Hen egg white lysozyme: antimicrobial activity and allergenicity. In: X. G. Maang and W. F. Cheung (ed.), Lysozymes: sources, functions and role in disease. Nova Science Publishers, New York. pp. 215–226.

Jonsson, A., 1991. Growth of Clostridium tyrobutyricum during fermentation and aerobic deterioration of grass silage. J. Sci. Food Agric. 54:557–568.

Kaláb, M., J. Yun, and S. H. Yiu. 1987. Textural properties and microstructure of process cheese food rework. Food Microbiol. 6: 181-192.

Kanno, C., Emmons, D. B., Harwalkar, V. R., & Elliott, J. A. 1976. Purification and characterization of the agglutinating factor for lactic streptococci from bovine milk: IgM-immunoglobulin. *Journal of Dairy Science*, *59*(12), 2036-2045.

Keynan, A., & Evenchick, Z. 1969. Activation, p 359–396. *The bacterial spore. Academic Press, New York, NY*.

Koutsopoulos, S. 2002. Synthesis and characterization of hydroxyapatite crystals: a review study on the analytical methods. J. Biomed. Mater. Res., 62: 600-612.

Larson, B. L. 1979. Biosynthesis and secretion of milk proteins: a review. *J. Dairy Res, 46,* 161-174.

Larson, B. L., & Fox, P. F. 1992. Immunoglobulins of the mammary secretions. *Advanced dairy chemistry-1: Proteins.*, (Ed. 2), 231-254.

Le Bourhis, A. G., J. Doré, J. P. Carlier, J. F. Chamba, M. R. Popoff, and J. L. Tholozan. 2007. Contribution of *Cl. beijerinckii* and *Cl. sporogenes* in association with *Cl. tyrobutyricum* to the butyric fermentation in Emmental type cheese. Int. J. Food. Microbiol. 113:154-163.

Laht, T., Kask, S., Elias, P., Adamberg, K., Paalme, T., 2002. Role of arginine in the development of secondary microflora in Swiss-type cheese. Int. Dairy J., 12,831-840.

Lazzi, C., Rossetti, L., Zago, M., Neviani, E., Giraffa, G., 2004. Evaluation of bacterial communities belonging to natural whey starters for Grana Padano cheese by length heterogeneity-PCR. J Appl Microbiol. 96, 481-90.

Le Boucher, C., V. Gagnaire, V. Briard-Bion, J. Jardin, M. B. Maillard, G. Dervilly-Pinel, B. Le Bizec, S. Lortal, S. Jeanson, and A. Thierry. 2016. Spatial distribution of Lactococcus lactis colonies modulates the production of major metabolites during the ripening of a model cheese. Appl. Environ Microbiol. 82: 202–210.

Li, H., Cao, Y., 2010. Lactic acid bacterial cell factories for gamma-aminobutyric acid. Amino Acids 39, 1107-1116.

Lilius, E. M., & Marnila, P. (2001). The role of colostral antibodies in prevention of microbial infections. *Current opinion in infectious diseases*, *14*(3), 295-300.

Liu, S.Q., Holland, R., Crow, V.L., 2003. The potential of dairy lactic acid bacteria to metabolise amino acids via non-transaminating reactions and endogenous transamination. Int. J. Food Microbiol. 86, 257– 269.

Lodi, R. 1990. The use of lysozyme to control butyric acid fermentation. Bulletin of the International Dairy Federation. 251:51-54.

Loimaranta, V., Carlén, A., Olsson, J., Tenovuo, J., Syväoja, E. L., & Korhonen, H. (1998). Concentrated bovine colostral whey proteins from Streptococcus mutans/Strep. sobrinus immunized cows inhibit the adherence of Strep. mutans and promote the aggregation of mutans streptococci. *Journal of Dairy Research*, *65*(04), 599-607.

Lopez, C., V. Briard-Bion, O. Ménard, E. Beaucher, F. Rousseau, J. Fauquant, N. Leconte and B. Robert. 2011. Fat globules selected from whole milk according to their size: Different compositions and structure of the biomembrane, revealing sphingomyelin-rich domains. Food Chem. 125:355-368.

Lopez, C., M. N. Madec & R. Jimenez-Flores. 2010. Lipid rafts in the bovine milk fat globule membrane revealed by the lateral segregation of phospholipids and heterogeneous distribution of glycoproteins. Food Chem. 120:22-33.

Ma, Y., and D. M. Barbano. 2000. Gravity separation of raw bovine milk: fat globule size distribution and fat content of milk fractions. J. Dairy Sci. 83(8):1719-1727.

Marcos, A. 1993. Water activity in cheese in relation to composition, stability and safety. Pages 439-469 in Cheese: Chemistry, Physics and Microbiology, Vol. 1, ed.; Fox. P. F.; Chapman & Hall, London.

Martínez-Cuesta, M. C., Bengoechea, J., Bustos, I., Rodríguez, B., Requena, T., & Peláez, C. 2010. Control of late blowing in cheese by adding lacticin 3147-producing Lactococcus lactis IFPL 3593 to the starter. International Dairy Journal, 20 (1), 18-24.

Masotti, F., Hogenboom, J.A., Rosi, V., De Noni, I., Pellegrino, L., 2010. Proteolysis indices related to cheese ripening and typicalness in PDO Grana Padano cheese. Int. Dairy J. 20, 352–359.

McFadden, T. B., Besser, T. E., & Barrington, G. M. 1997. Regulation of immunoglobulin transfer into mammary secretions of ruminants. In *Milk Composition, Production and Biotechnology*, pp. 133-152. Wallingford UK: CAB International.

McPherson, A., S. B. Larson, and Y. G. Kuznetsov. 2012. Tyrosine Microcrystals Produced by Digestion of Proteins with Pancreatic Enzymes. Crystal Growth & Design. 12: 3594-3602.

McSweeney, P. L. H. 2004. Biochemistry of cheese ripening. Int. J. Dairy Technol. 57:127–144.

Mix, E., Goertsches, R., 2006. Zettl, U.K. Immunoglobulins—basic considerations. *J. Neurol., 253*, V/9–V/17.

Moir, A., Corfe, B. M., & Behravan, J. 2002. Spore germination. *Cellular and Molecular Life Sciences CMLS*, *59*(3), 403-409.

Morandi, S., Cremonesi, P., Silvetti, T., Castiglioni, B., & Brasca, M. 2015. Development of a triplex real-time PCR assay for the simultaneous detection of Clostridium beijerinckii, Clostridium sporogenes and Clostridium tyrobutyricum in milk. *Anaerobe*, *34*, 44-49.

Mostov, K., & Kaetzel, C. S. 1999. Immunoglobulin transport and the polymeric immunoglobulin receptor. In *Mucosal Immunology*, 2nd ed.; Ogra, P.L., Mestecky, J., Lamm, M.E., Strober, W., Bienenstock, J., McGhee, J.R., Eds.; Academic Press: New York, NY, USA, 1999; pp. 181–211.

Nagalakshmi, D. 2009. Colostrum management and feeding in neonatal calves. *Intas Polivet*, *10*(2), 142-152.

Neviani, E., Carminati, D., Veaux, M., Hermier, J., Giraffa, G., 1991. Characterization of Lactobacillus helveticus strains resistant to lysozyme. Lait 71, 65-73.

Neviani, E., Carminati, D., Giraffa, G., 1992. Selection of some bacteriophage and lysozyme-resistant variants of Lactobacillus helveticus CNRZ 892. J. Dairy Sci. 75, 905-913.

Nicoloff, H., Hubert, J.-C., Bringel, F., 2001. Carbamoyl-phosphate synthetases (CPS) in lactic acid bacteria and other Gram-positive bacteria. Lait 81, 151-159.

Ong, L., Dagastine, R. R., Kentish, S. E., & Gras, S. L. 2011. Microstructure of milk gel and cheese curd observed using cryo scanning electron microscopy and confocal microscopy. *LWT-Food Science and Technology*, *44*(5), 1291-1302.

Ong, L., R. R. Dagastine, S. E. Kentish, and S. L. Gras. 2010. Transmission electron microscopy imaging of the microstructure of milk in cheddar cheese production under different processing conditions. J. Food Sci. 75: 135–145.

Parham, P. 2009. The Immune System. 3rd ed. Pages 57-122. Garland Science, New York, NY.

Pellegrino, L., Battelli, G., & Resmini, P. 1997. Andamento centripeto della maturazione nei formaggi Grana Padano e Parmigiano-Reggiano. *Sci. Tecn. Latt.-Cas*, *48*, 73-82.

Pellegrino L., Battelli G., Resmini P., Ferranti P., Barone F., Addeo F., 1997. Effects of heat load gradient occurring in molding on characterization and ripening of Grana Padano. Lait 77, 217–228.

Pellegrino L., Resmini P., 2001. Cheesemaking conditions and compositive characteristics supporting the safety of the raw milk cheese Italian Grana, Sci. Tecn. Latt.-Cas. 52, 105–114.

Pellegrino L., Rosi V., D'Incecco P., Hogenboom J., Stroppa A. 2015. Changes in the soluble nitrogen fraction of milk throughout PDO Grana Padano cheese-making. Int. Dairy J., 47, 128-135.

Phalipon, A., Cardona, A., Kraehenbuhl, J. P., Edelman, L., Sansonetti, P. J., & Corthésy, B. 2002. Secretory component: a new role in secretory IgA-mediated immune exclusion in vivo. *Immunity*, *17*(1), 107-115.

Price, C.E., Zeynieyev, A., Kuipers, O.P., Kok, J., 2012. From meadows to milk to mucosa – adaptation of Streptococcus and Lactococcus species to their nutritional environments. FEMS Microbiol. Rev. 36, 949-971.

Pogacic, T., Mancini, A., Santarelli, M., Bottari, B., Lazzi, C., Neviani, E., Gatti, M., 2013. Diversity and dynamic of lactic acid bacteria strains during aging of a long ripened hard cheese produced from raw milk and undefined natural starter. Food Microbiol. 36, 207-215.

Raducan, G. 2013. The dynamic of immunoglobulin IgG, IgA and IgM type concentration in milk colostrum. *Scientific Papers Animal Science and Biotechnologies*, *46*(1), 309-311.

Recio, I., Olieman, C., 1996. Determination of denatured serum proteins in the casein fraction of heat-treated milk by capillary zone electrophoresis. Electrophoresis 17, 1228–1233.

Resmini, P., M. A. Pagani and F. Prati. 1984. L'Ultrafiltrazione del latte nella tecnologia del Mascarpone. Sci. Tecn. Latt. Cas. 35:213-230.

Robenek, H., O. Hofnagel, I. Buers, S. Lorkowski, M. Schnoor, M. J. Robenek, et al. 2006. Butyrophilin controls milk fat globule secretion. Proc. Natl. Acad. Sci. USA. 103:10385-10390.

Rossi, J. 1964. Sul processo di caseificazione del formaggio grana. Il Latte 38:301-305.

Ruusunen M., Surakka A., Korkeala H., Lindström M. 2012. Clostridium tyrobutyricum strains show wide variation in growth at different NaCl, pH, and temperature conditions. J Food Prot.75(10):1791-5.

Santarelli, M., Bottari, B., Lazzi, C., Neviani, E., Gatti, M., 2013. Survey on the community and dynamics of lactic acid bacteria in Grana Padano cheese. System. Appl. Microbiol. 36, 593-600.

Sando, L., R. Pearson, C. Gray, P. Parker, R. Hawken, P. Thomson, J. Meadows, K. Kongsuwan, S. Smith, R. L. Tellam. 2009. Bovine Muc1: a polymorphic gene encoding a highly glycosylated mucin that protects epithelial cells from bacterial attachment. J. Dairy Sci. 92:5276-5291.

Sauer, G. R., W. B. Zunic, J. R. Durig, and R. E. Wuthier. 1994. Fourier transform Raman spectroscopy of synthetic and biological calcium phosphates. Calcif. Tissue Int. 54: 414-420.

Schaeffer, A. B., and M. Fulton. 1933. A simplified method of staining endospores. Science. 77:194.

Scheuble, T. L., Kondo, J. K., & Salih, M. A. 1989. Agglutination behavior of lactic streptococci. *Journal of dairy science*, *72*(5), 1103-1111.

Schmidt, D. G. and W. Buchheim. 1992. The application of electron microscopy in dairy research. J. Microsc. 167:105-121.

Schrader, K. 2012. Structural analysis of milk and milk products. Strukturanalyse von Milch und Milchprodukten. 133: 30-34.

Setlow, P. 2003. "Spore germination." *Current opinion in microbiology* 6.6: 550-556.

Setlow, P. (2006). Spores of Bacillus subtilis: their resistance to and killing by radiation, heat and chemicals. *Journal of applied microbiology*, *101*(3), 514-525.

Sgarbi, E., Bottari, B., Gatti, M., Neviani, E., 2014 Investigation of the ability of dairy nonstarter lactic acid bacteria to grow using cell lysates of other lactic acid bacteria as the exclusive source of nutrients. Int. J. Dairy Tech. 67, 1-6.

Shock, A. A., W. J. Harper, A. M. Swanson, and H. H. Sommer. 1948. What's in those "white specks" on Cheddar. Wisconsin Agric. Experiment. Station. Bull. 474: 31–32.

Silva, J. V. C., D. Legland, C. Cauty, I. Kolotuev and J. Floury. 2015. Characterization of the microstructure of dairy systems using automated image analysis. Food Hydrocolloid. 44:360-371.

Silva, J. V. C., P. D. S. Peixoto, S. Lortal, and J. Floury. 2013. Transport phenomena in a model cheese: the influence of the charge and shape of solutes on diffusion. J. Dairy Sci. 96: 6186–6198.

Solieri, L., Bianchi, A., Mottolese, G., Lemmetti, F., Giudici, P., 2014. Tailoring the probiotic potential of non-starter Lactobacillus strains from ripened Parmigiano Reggiano cheese by in vitro screening and principal component analysis. Food Microbiol. 38, 240-249.

Stadhouders, J. 1990a. Prevention of butyric acid fermentation by the use of nitrate. Bulletin of the IDF 251, 40-46.

Stadhouders, J. 1990b. Alternative methods of controlling butyric acid fermentation in cheese. Bulletin of IDF 251, 55-98.

Stadhouders, J., and G. Hup. 1970. Complexity and specificity of euglobulin in relation to inhibition of bacteria and to cream rising. Neth. Milk Dairy J. 24:79-95.

Stephan, W., Dichtelmüller, H., & Lissner, R. 1990. Antibodies from colostrum in oral immunotherapy. *Journal of clinical chemistry and clinical biochemistry. Zeitschrift für klinische Chemie und klinische Biochemie*, *28*(1), 19.

Storari, M., Kulli, S., Wüthrich, D., Bruggmann, R., Berthoud, H., & Arias-Roth, E. 2016. Genomic approach to studying nutritional requirements of Clostridium tyrobutyricum and other Clostridia causing late blowing defects. *Food Microbiology*.

Tansman, G., P. S. Kindstedt, and J. M. Hughes. 2014. Powder x-ray diffraction can differentiate between enantiomeric variants of calcium lactate pentahydrate crystal in cheese. J. Dairy Sci. 97: 7354–7362.

Tansman, G., P. S. Kindstedt, and J. M. Hughes. 2015. Crystal fingerprinting: elucidating the crystals of Cheddar, Parmigiano-Reggiano, Gouda, and soft washed-rind cheeses using powder x-ray diffractometry. Dairy Sci. Technol. 95: 651–664.

Tlili, M. M., M. Ben Amor, C. Gabrielli, S. Joiret, G. Maurin, and P. Rousseau. 2001. Characterization of CaCO3 hydrates by micro-Raman Spectroscopy. J. Raman Spectrosc. 33. 10–16.

Tsioulpas, A., Grandison, A. S., & Lewis, M. J. 2007. Changes in physical properties of bovine milk from the colostrum period to early lactation. *Journal of dairy science*, *90*(11), 5012-5017.

Tuckey, S. L., H. A. Ruehe, and G. L. Clark. 1938. X-ray diffraction analysis of white specks in Cheddar cheese. J. Dairy Sci. 21: 161.

Ueno, H. Enzymatic and structural aspects of glutamate decarboxylase. J. Mol. Catal. B. Enzym. 2000, 10, 67-79.

Ugarte, M.B., Guglielmotti, D.M., Giraffa, G., Reinheimer, J., Hynes, E., 2006. Nonstarter lactobacilli isolated from soft and semihard Argentinean cheeses: Genetic characterization and resistance to biological barriers. J. Food Protection, 69, 2983-2991.

Van den Berg, G., W. C. Meijer, E. M. Düsterhöft, and G. Smit. 2004. Gouda and Related Cheeses, In: Fox, P. F., McSweeney, P. L. H., Cogan, T. M., Guinee, T. P. (Eds.), Cheese: Chemistry, Physics and Microbiology, Vol. 2: Major Cheese Groups, 3rd ed. Elsevier Academic Press, London, pp. 103-140.

Van de Gukte, M., Serror, P., Chervaux, C., Smokvina, T., Ehrlich, S.D., Maguin, E., 2002. Stress responses in lactic acid bacteria. Antonie van Leeuwenhoek 82, 187–216.

Vinderola, G., Briggiler Marcò, M., Guglielmotti, D.M., Perdigon, G., Giraffa, G., Reinheimer, J., Quiberon, A., 2007. Phage-resistant mutants of Lactobacillus delbrueckii may have functional properties that differ from those of parent strains. Int. J. Food Microbiol. 116, 96-102.

Vissers, M.M., Driehuis, F., Te Giffel, M.C., De Jong, P., Lankveld, J.M.G., 2006. Improving farm management by modeling the contamination of farm tank milk with butyric acid bacteria. J. Dairy Sci. 89, 850–858.

Vrancken, G., Rimaux, T., Weckx, S., De Vuyst, L., Leroy, F., 2009a. Environmental pH determines citrulline and ornithine release through the arginine deiminase pathway in

Lactobacillus fermentum IMDO 130101. Int. J. Food Microbiol. 135, 216-222.

Vrancken, G., Rimaux, T., Wouters, D., Leroy, F., De Vuyst, L., 2009b. The arginine deiminase pathway of Lactobacillus fermentum IMDO 130101 responds to growth under stress conditions of both temperature and salt. Food Microbiol. 26, 720-727.

Washam, C. J., T. J. Kerr, V. J. Hurst, and W. E. Rigsby. 1985. A scanning electron microscopy study of crystalline structures on commercial cheese. Dev. Ind. Microbiol. 26: 749–761.

Weaver, D. M., Tyler, J. W., VanMetre, D. C., Hostetler, D. E., & Barrington, G. M. 2000. Passive transfer of colostral immunoglobulins in calves. *Journal of Veterinary Internal Medicine*, *14*(6), 569-577.

Woof, J.M. 2007. The structure of IgA. In *Mucosal Immune Defense: Immunoglobulin A*; Kaetzel, C.S., Ed.; Springer: New York, NY, USA. Chapter 1, pp. 1–24.

Zacconi C., and Bottazzi V. 1982. Anticorpi ed aggregazione dei globuli di grasso del latte. Sci. Tecn. Latt. Cas. 33:1-14.

Zamora, A., V. Ferragut, B. Guamis and A. J. Trujillo. 2012. Changes in the surface protein of the fat globules during ultra-high pressure homogenisation and conventional treatments of milk. Food Hydrocolloid. 29:135-142.

Zúñiga, M., Pérez, G., & González-Candelas, F. 2002. Evolution of arginine deiminase (ADI) pathway genes. *Molecular phylogenetics and evolution*, *25*(3), 429-444.

PRODUCTS

Articles with Impact Factor:

1) D'Incecco, P., Faoro, F., Silvetti, T., Schrader, K., & Pellegrino, L. (2015). Mechanisms of Clostridium tyrobutyricum removal through natural creaming of milk: A microscopy study. *Journal of dairy science*, *98* (8), 5164-5172. http://dx.doi.org/10.3168/jds.2015-9526.

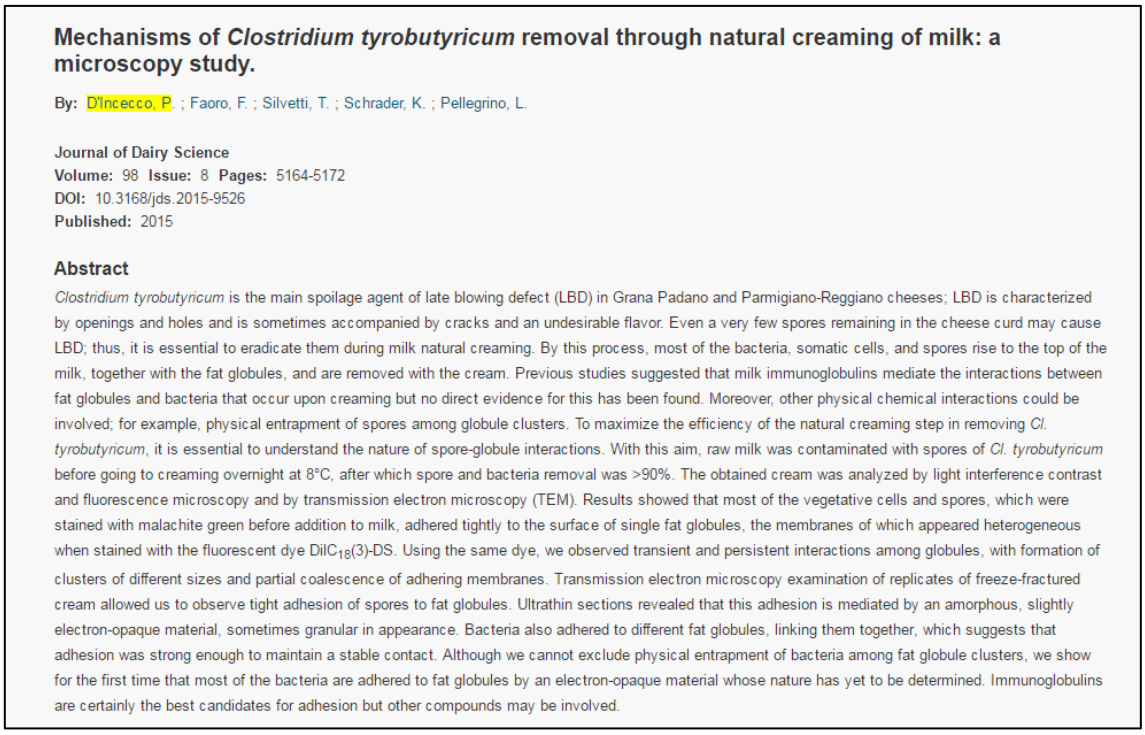

Mechanisms of *Clostridium tyrobutyricum* removal through natural creaming of milk: a microscopy study.

By: D'Incecco, P. ; Faoro, F. ; Silvetti, T. ; Schrader, K. ; Pellegrino, L.

Journal of Dairy Science
Volume: 98 **Issue:** 8 **Pages:** 5164-5172
DOI: 10.3168/jds.2015-9526
Published: 2015

Abstract

Clostridium tyrobutyricum is the main spoilage agent of late blowing defect (LBD) in Grana Padano and Parmigiano-Reggiano cheeses; LBD is characterized by openings and holes and is sometimes accompanied by cracks and an undesirable flavor. Even a very few spores remaining in the cheese curd may cause LBD; thus, it is essential to eradicate them during milk natural creaming. By this process, most of the bacteria, somatic cells, and spores rise to the top of the milk, together with the fat globules, and are removed with the cream. Previous studies suggested that milk immunoglobulins mediate the interactions between fat globules and bacteria that occur upon creaming but no direct evidence for this has been found. Moreover, other physical chemical interactions could be involved; for example, physical entrapment of spores among globule clusters. To maximize the efficiency of the natural creaming step in removing *Cl. tyrobutyricum*, it is essential to understand the nature of spore-globule interactions. With this aim, raw milk was contaminated with spores of *Cl. tyrobutyricum* before going to creaming overnight at 8°C, after which spore and bacteria removal was >90%. The obtained cream was analyzed by light interference contrast and fluorescence microscopy and by transmission electron microscopy (TEM). Results showed that most of the vegetative cells and spores, which were stained with malachite green before addition to milk, adhered tightly to the surface of single fat globules, the membranes of which appeared heterogeneous when stained with the fluorescent dye $DiIC_{18}(3)$-DS. Using the same dye, we observed transient and persistent interactions among globules, with formation of clusters of different sizes and partial coalescence of adhering membranes. Transmission electron microscopy examination of replicates of freeze-fractured cream allowed us to observe tight adhesion of spores to fat globules. Ultrathin sections revealed that this adhesion is mediated by an amorphous, slightly electron-opaque material, sometimes granular in appearance. Bacteria also adhered to different fat globules, linking them together, which suggests that adhesion was strong enough to maintain a stable contact. Although we cannot exclude physical entrapment of bacteria among fat globule clusters, we show for the first time that most of the bacteria are adhered to fat globules by an electron-opaque material whose nature has yet to be determined. Immunoglobulins are certainly the best candidates for adhesion but other compounds may be involved.

2) D'Incecco, P., Gatti, M., Hogenboom, J. A., Bottari, B., Rosi, V., Neviani, E., & Pellegrino, L. (2016). Lysozyme affects the microbial catabolism of free arginine in raw-milk hard cheeses. *Food microbiology*, *57*, 16-22. http://dx.doi.org/10.1016/j.fm.2015.11.020.

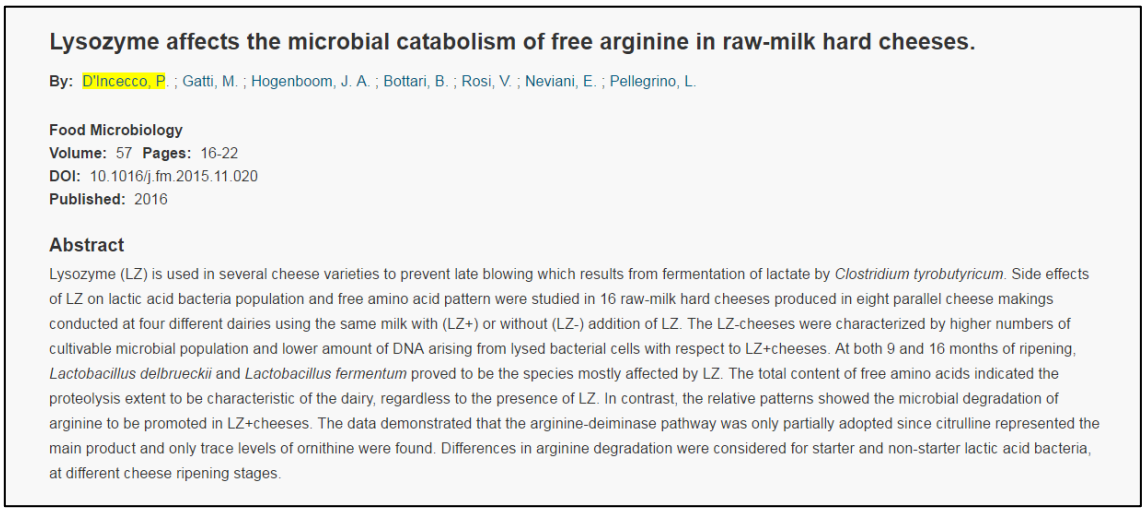

Lysozyme affects the microbial catabolism of free arginine in raw-milk hard cheeses.

By: D'Incecco, P. ; Gatti, M. ; Hogenboom, J. A. ; Bottari, B. ; Rosi, V. ; Neviani, E. ; Pellegrino, L.

Food Microbiology
Volume: 57 **Pages:** 16-22
DOI: 10.1016/j.fm.2015.11.020
Published: 2016

Abstract

Lysozyme (LZ) is used in several cheese varieties to prevent late blowing which results from fermentation of lactate by *Clostridium tyrobutyricum*. Side effects of LZ on lactic acid bacteria population and free amino acid pattern were studied in 16 raw-milk hard cheeses produced in eight parallel cheese makings conducted at four different dairies using the same milk with (LZ+) or without (LZ-) addition of LZ. The LZ-cheeses were characterized by higher numbers of cultivable microbial population and lower amount of DNA arising from lysed bacterial cells with respect to LZ+cheeses. At both 9 and 16 months of ripening, *Lactobacillus delbrueckii* and *Lactobacillus fermentum* proved to be the species mostly affected by LZ. The total content of free amino acids indicated the proteolysis extent to be characteristic of the dairy, regardless to the presence of LZ. In contrast, the relative patterns showed the microbial degradation of arginine to be promoted in LZ+cheeses. The data demonstrated that the arginine-deiminase pathway was only partially adopted since citrulline represented the main product and only trace levels of ornithine were found. Differences in arginine degradation were considered for starter and non-starter lactic acid bacteria, at different cheese ripening stages.

3) D'Incecco, P., Limbo, S., Faoro, F., Hogenboom, J., Rosi, V., Morandi, S., & Pellegrino, L. (2016). New insight on crystal and spot development in hard and extra-hard cheeses: Association of spots with incomplete aggregation of curd granules. *Journal of dairy science*. http://dx.doi.org/10.3168/jds.2016-11050.

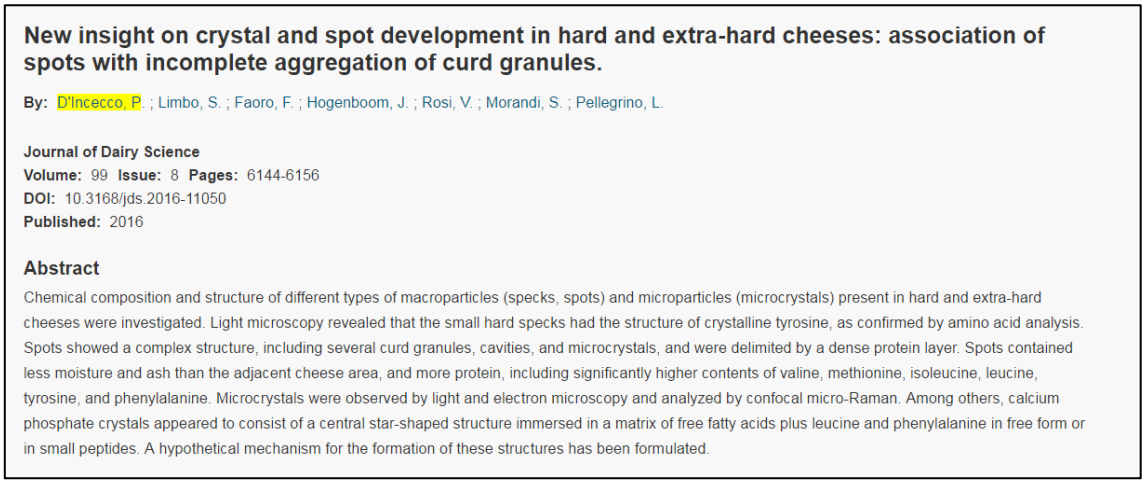

New insight on crystal and spot development in hard and extra-hard cheeses: association of spots with incomplete aggregation of curd granules.

By: D'Incecco, P. ; Limbo, S. ; Faoro, F. ; Hogenboom, J. ; Rosi, V. ; Morandi, S. ; Pellegrino, L.

Journal of Dairy Science
Volume: 99 **Issue:** 8 **Pages:** 6144-6156
DOI: 10.3168/jds.2016-11050
Published: 2016

Abstract

Chemical composition and structure of different types of macroparticles (specks, spots) and microparticles (microcrystals) present in hard and extra-hard cheeses were investigated. Light microscopy revealed that the small hard specks had the structure of crystalline tyrosine, as confirmed by amino acid analysis. Spots showed a complex structure, including several curd granules, cavities, and microcrystals, and were delimited by a dense protein layer. Spots contained less moisture and ash than the adjacent cheese area, and more protein, including significantly higher contents of valine, methionine, isoleucine, leucine, tyrosine, and phenylalanine. Microcrystals were observed by light and electron microscopy and analyzed by confocal micro-Raman. Among others, calcium phosphate crystals appeared to consist of a central star-shaped structure immersed in a matrix of free fatty acids plus leucine and phenylalanine in free form or in small peptides. A hypothetical mechanism for the formation of these structures has been formulated.

4) Pellegrino, L., Rosi, V., **D'Incecco, P**., Stroppa, A., & Hogenboom, J. A. (2015). Changes in the soluble nitrogen fraction of milk throughout PDO Grana Padano cheese-making. *International Dairy Journal*, *47*, 128-135. http://dx.doi.org/10.1016/j.idairyj.2015.03.002.

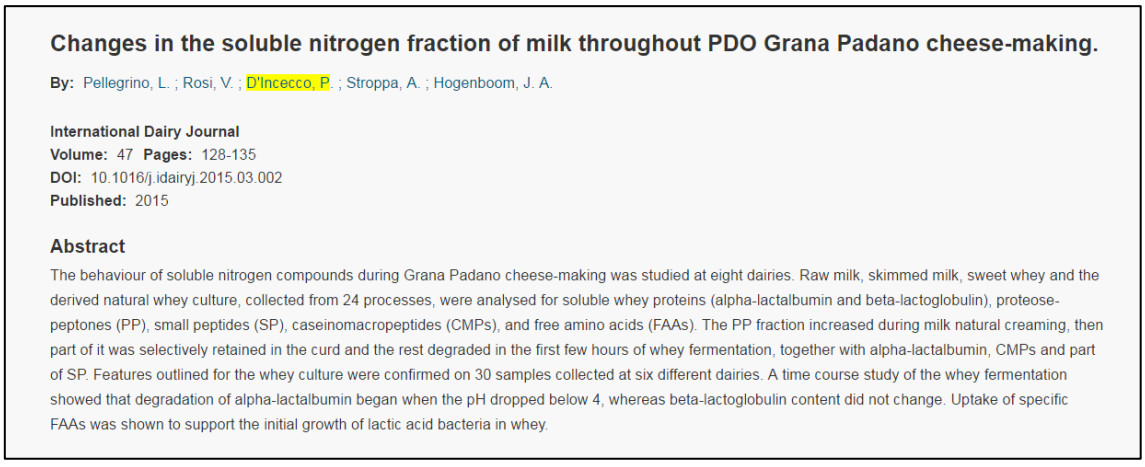

Changes in the soluble nitrogen fraction of milk throughout PDO Grana Padano cheese-making.

By: Pellegrino, L. ; Rosi, V. ; D'Incecco, P. ; Stroppa, A. ; Hogenboom, J. A.

International Dairy Journal
Volume: 47 **Pages:** 128-135
DOI: 10.1016/j.idairyj.2015.03.002
Published: 2015

Abstract

The behaviour of soluble nitrogen compounds during Grana Padano cheese-making was studied at eight dairies. Raw milk, skimmed milk, sweet whey and the derived natural whey culture, collected from 24 processes, were analysed for soluble whey proteins (alpha-lactalbumin and beta-lactoglobulin), proteose-peptones (PP), small peptides (SP), caseinomacropeptides (CMPs), and free amino acids (FAAs). The PP fraction increased during milk natural creaming, then part of it was selectively retained in the curd and the rest degraded in the first few hours of whey fermentation, together with alpha-lactalbumin, CMPs and part of SP. Features outlined for the whey culture were confirmed on 30 samples collected at six different dairies. A time course study of the whey fermentation showed that degradation of alpha-lactalbumin began when the pH dropped below 4, whereas beta-lactoglobulin content did not change. Uptake of specific FAAs was shown to support the initial growth of lactic acid bacteria in whey.

5) Brasca, M., Hogenboom, J. A., Morandi, S., Rosi, V., **D'Incecco, P.,** Silvetti, T., & Pellegrino, L. (2016). Proteolytic Activity and Production of γ-Aminobutyric Acid by Streptococcus thermophilus Cultivated in Microfiltered Pasteurized Milk. *Journal of Agricultural and Food Chemistry*, *64*(45), 8604-8614. **DOI:** 10.1021/acs.jafc.6b03403.

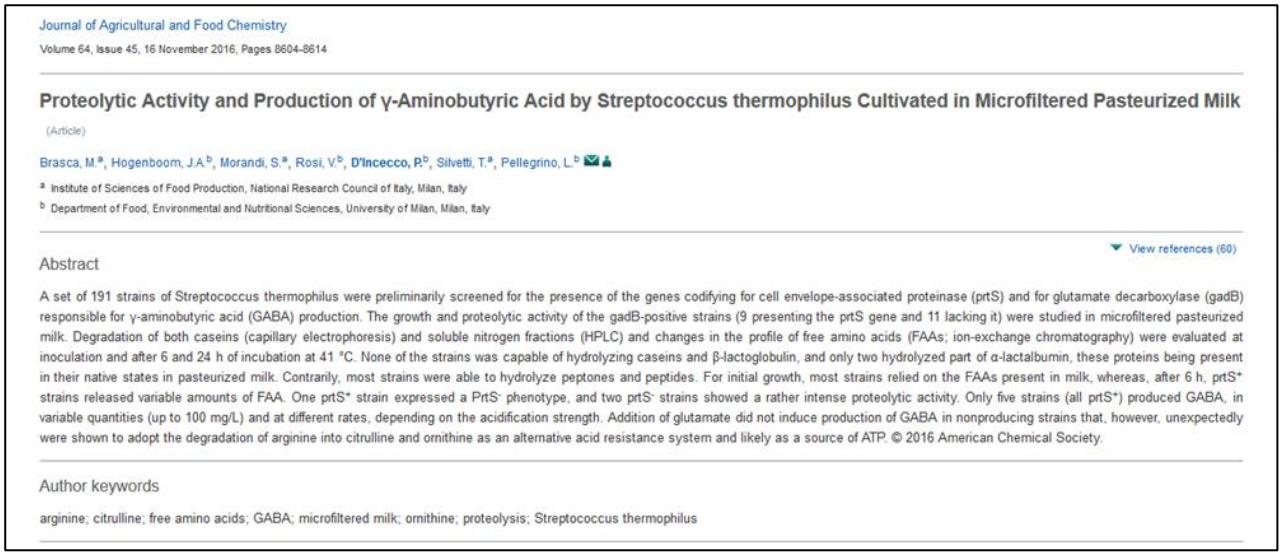

Journal of Agricultural and Food Chemistry

Volume 64, Issue 45, 16 November 2016, Pages 8604-8614

Proteolytic Activity and Production of γ-Aminobutyric Acid by Streptococcus thermophilus Cultivated in Microfiltered Pasteurized Milk

(Article)

Brasca, M.[a], Hogenboom, J.A.[b], Morandi, S.[a], Rosi, V.[b], **D'Incecco, P.**[b], Silvetti, T.[a], Pellegrino, L.[b]

[a] Institute of Sciences of Food Production, National Research Council of Italy, Milan, Italy

[b] Department of Food, Environmental and Nutritional Sciences, University of Milan, Milan, Italy

View references (60)

Abstract

A set of 191 strains of Streptococcus thermophilus were preliminarily screened for the presence of the genes codifying for cell envelope-associated proteinase (prtS) and for glutamate decarboxylase (gadB) responsible for γ-aminobutyric acid (GABA) production. The growth and proteolytic activity of the gadB-positive strains (9 presenting the prtS gene and 11 lacking it) were studied in microfiltered pasteurized milk. Degradation of both caseins (capillary electrophoresis) and soluble nitrogen fractions (HPLC) and changes in the profile of free amino acids (FAAs; ion-exchange chromatography) were evaluated at inoculation and after 6 and 24 h of incubation at 41 °C. None of the strains was capable of hydrolyzing caseins and β-lactoglobulin, and only two hydrolyzed part of α-lactalbumin, these proteins being present in their native states in pasteurized milk. Contrarily, most strains were able to hydrolyze peptones and peptides. For initial growth, most strains relied on the FAAs present in milk, whereas, after 6 h, prtS$^+$ strains released variable amounts of FAA. One prtS$^+$ strain expressed a PrtS$^-$ phenotype, and two prtS$^-$ strains showed a rather intense proteolytic activity. Only five strains (all prtS$^+$) produced GABA, in variable quantities (up to 100 mg/L) and at different rates, depending on the acidification strength. Addition of glutamate did not induce production of GABA in nonproducing strains that, however, unexpectedly were shown to adopt the degradation of arginine into citrulline and ornithine as an alternative acid resistance system and likely as a source of ATP. © 2016 American Chemical Society.

Author keywords

arginine; citrulline; free amino acids; GABA; microfiltered milk; ornithine; proteolysis; Streptococcus thermophilus

Oral presentation at International Congress

1) "Shedding light on crystals and white spots in cheese" - **P. D'Incecco, S**. Limbo, F. Faoro, J. Hogenboom, V. Rosi, L. Pellegrino. 3th International Multidisciplinary Microscopy and Microanalysis Congress – InterM - Oludeniz, 2015.

Abstract

Microscopy is a powerful research tool in food science, although a number of difficulties in sample preparation may discourage its use. Investigation at structure and ultrastructure level helps to understand changes and interactions the raw material components undergo when processed into food. We have adopted various microscopy techniques to study the nature and origin of different types of crystals and spots originating in hard cheeses during ripening. Although not directly affecting the flavor, in this type of cheese they are considered a desired attribute. Compositional, biochemical and microbiological data were obtained on the same samples to support the microscopy study.

In hard cheeses upon ripening, protein is progressively degraded into free amino acids. After 10-12 month ripening, free amino acids represent more than 20% of the cheese protein. This fact largely contributes to increase the concentration of solutes in cheese water phase, where sodium chloride, calcium, phosphates, lactate and other soluble molecules are already present. Crystals of tyrosine, calcium lactate and calcium phosphate are already reported to occur in some cheese varieties, such as Cheddar, Gouda, Emmental, Grana Padano and Parmigiano-Reggiano, due to the decreased solubility as the cheese water content decreases. In addition, non-crystalline spherical spots are reported to occur in the last two cheeses, sometimes named as "pearls" and whose origin is not yet understood. We have focused our attention on those pearls and investigated their structure and ultrastructure for the first time. The matrix, as observed by both optical and confocal microscopy after suitable staining procedures, appeared to be rather homogeneous but more compact with respect to the surrounding cheese portion from which the pearl is clearly distinguishable, with several crystals embedded. By TEM of the resin embedded material, the crystals showed a star-shaped core surrounded by a thick layer of dense material. The nature of the different components of the crystals was further investigated by confocal microscopy, confocal Raman microscopy and compositional data, and a possible role of some free amino acids as seeding components was hypothesized.

2) "Lysozyme side effects in Grana Padano PDO cheese: new perspective after 30 years using" - **P. D'Incecco**, M. Gatti, J.A. Hogenboom, E. Neviani, V. Rosi, M. Santarelli, L. Pellegrino. 9th Cheese Symposium, International Dairy Federation. Cork (IR), 2014.

Abstract

Since thirty years, hen's egg white lysozyme is in use as an anti-clostridial agent in Grana Padano PDO cheese manufacturing in order to avoid the cheese blowing defect. However, as the EU legislation includes egg among allergens, Grana Padano falls into the category of food products containing allergens. In view of discontinuing this situation, this work aimed to investigate the effects of abandoning lysozyme use on cheese characteristics.

Nine manufacturing processes, conducted with and without lysozyme, were monitored from milk to ripened cheese at four different dairies. Both the lactic acid bacteria microbiota (LAB) and chemical parameters related to cheese maturation were evaluated.

The presence of the enzyme seems to affect the capacity of some LAB species and biotypes to grow in cheese during ripening. Accordingly, primary proteolysis was not affected, whereas differences were found in amino acids release that could be traced back to the lysozyme-dependent LAB growth.

3) "The late blowing defect in Grana Padano PDO cheese: effects of milk natural creaming and cheese making conditions"- **P. D'Incecco**. Dairy Innovation Hub Workshop - University of Queensland – Brisbane – 29 June 2016.

Oral presentation at National Congress

1) "Formazioni cristalline in formaggi extra duri: ruolo della tecnologia". **Paolo D'Incecco**. Universo Latte: Giovani Ricercatori e Imprese a Confronto. Piacenza, 17 – 18 marzo 2016.

Abstract

La presenza di formazioni cristalline in formaggi duri ed extra duri è stata osservata da tempo. Tuttavia i pochi, precedenti ricercatori non hanno individuato una nomenclatura comune per tali formazioni e, allo stesso modo, ne mancano in letteratura una caratterizzazione chimica univoca e un'indagine ultrastrutturale. Nel presente lavoro abbiamo studiato cristalli e "spot", visibili ad occhio nudo, e micro cristalli con lo scopo di fare chiarezza sulla loro natura e sulla loro genesi attraverso uno studio interdisciplinare. Le informazioni ottenute possono essere di supporto alle imprese nella prospettiva di un controllo della formazione di cristalli, spot e micro cristalli nei formaggi duri ed extra duri. Cristalli e spot di Grana Padano e Parmigiano-Reggiano sono stati caratterizzati chimicamente e la loro struttura ed ultrastruttura sono state studiate con diverse tecniche di microscopia: ottica, a fluorescenza, confocale, raman ed elettronica. I cristalli visibili ad occhio nudo sono più bianchi e duri rispetto al formaggio. Sono grandi fino a 3 mm e hanno una struttura cristallina quando osservati al microscopio ottico. A seguito sia dell'analisi raman che

dell'analisi amminoacidica sono risultati essere cristalli di tirosina con una purezza > 95%. Gli spot sono visibili nei formaggi solo dopo un anno di stagionatura e più frequentemente dopo 16-18 mesi. Hanno una struttura sferica e un diametro compreso tra i 2 e i 5 mm. Sono bianchi, di materiale amorfo più compatto rispetto al formaggio nel quale sono immersi e per questo facilmente estraibili dallo stesso. Gli spot risultano più ricchi in proteine e più poveri in grasso, umidità e ceneri rispetto al formaggio prelevato attorno allo spot. La determinazione degli aminoacidi liberi mostra una differenza statisticamente significativa, tra lo spot e il formaggio circostante, per sei aminoacidi: valina, metionina, leucina, isoleucina, tirosina e fenilalanina. L'osservazione in campo chiaro di sezioni dello spot incluso in resina mostra una struttura complessa ma organizzata. Sono visibili i chicchi di cagliata che si generano a seguito della rottura della stessa e le linee di giunzione tra i chicchi. La microscopia elettronica rivela una differente ultrastruttura tra lo spot e il controllo. Nello spot, l'interfaccia tra la matrice proteica e la fase grassa è irregolare e sfrangiata, contrariamente alla stessa osservata nel controllo dove appare lineare ed omogenea. Il DNA totale di origine microbica negli spot risulta circa il triplo rispetto a quello trovato sia nel formaggio prelevato attorno allo spot sia nel campione di controllo. I risultati ottenuti, assieme alle conoscenze già esistenti in merito al processo di stagionatura, ci permetteranno di fornire una spiegazione alla formazione di cristalli, spot e micro cristalli in formaggi duri ed extra duri.

Posters at National Workshop

1) "Clostridium tyrobutyricum behaviour during Grana Padano cheese making". **D'Incecco P.** XX Workshop on the developments in the Italian PhD Research on Food Science Technology and Biotechnology. University of Perugia, Perugia, 23-25 September 2015.

2) "The late blowing defect in Grana Padano PDO cheese: effects of milk natural creaming and cheese making conditions". **D'Incecco P.** XIX Workshop on the developments in the Italian PhD Research on Food Science Technology and Biotechnology. University of Bari, Bari, 24-26 September 2014

ACKNOWLEDGEMENTS

This work was carried out between the years 2014-2016 at the Department of Food, Environmental and Nutritional Sciences (DeFENS) of the University of Milan, Italy, and financially supported by the Graduated School in Food Systems.

Some results showed in this thesis were achieved during abroad research activity conducted at both the Max Rubner Institute (MRI), Kiel, Germany and the Bio21-Institute, University of Melbourne, Parkville, Australia.

I would like to thank all the people that supervised me during my research activity: Prof. Luisa Pellegrino, Prof. Franco Faoro, Prof. Sally Gras, Dr. Lydia Ong and Dr. Katrin Schrader and also all the people that gave a great contribution to this thesis with their research activity: Prof. Monica Gatti, Prof. Francesco Bonomi, Prof. Limbo Sara, Prof. Pier Sandro Cocconcelli, Dr. Daniela Bassi, Dr. Angelo Stroppa, Dr. Milena Brasca, Dr. Stefano Morandi, Dr. Tiziana Silvetti, Dr. Dario Maffi, Dr. Marilù Decimo, Dr. John Hogenboom, Dr. Veronica Rosi, Dr. Alessandro Ranghetti and Dr. Aristodemo Carpen.